

THESIS

DETECTION AND ANALYSIS OF LOW LEVEL TRITIUM IN RAINWATER FOR A
PROPOSED ENVIRONMENTAL MONITORING PROGRAM

Submitted by

Jessica McDonnel Gillis

Department of Environmental and Radiological Health Sciences

In partial fulfillment of the requirements

For the Degree of Master of Science

Colorado State University

Fort Collins, Colorado

Summer 2014

Master's Committee:

Advisor: Alexander Brandl

Ward Whicker

Jeffrey Collett

Copyright by Jessica McDonnel Gillis

All Rights Reserved

ABSTRACT

DETECTION AND ANALYSIS OF LOW LEVEL TRITIUM IN RAINWATER FOR A PROPOSED ENVIRONMENTAL MONITORING PROGRAM

Radioactive tritium, an isotope of hydrogen, is present at low levels in the atmosphere and can be deposited by precipitation. Tritium is produced naturally by the interaction of cosmic rays with gaseous atoms in the atmosphere, but the primary contributors to atmospheric concentrations are residues from past nuclear weapons testing and releases of tritium produced at nuclear facilities. The National Atmospheric Deposition Program (NADP) is a nationwide program that manages and analyzes rain and snow samples from networks of precipitation monitoring stations. The NADP and Savannah River National Laboratory have jointly proposed a monitoring program for tritium in rainwater in order to demonstrate the use of existing sampling locations in the NADP's National Trends Network and characterize the deposition of radionuclides in the United States. This research investigates the feasibility of measuring tritium concentrations in rainwater samples given the proposed laboratory detection range of 0.6-1.2 Bq/L. Rainwater samples were analyzed using Colorado State University's liquid scintillation counter (LSC), and minimum detectable activity concentrations on the LSC were investigated based on background count rate, count duration, and detection efficiency. To achieve the analytical capabilities and throughput proposed, count times of several hours and comparison with tritium-depleted blanks were determined to be necessary. Detection efficiencies for tritium in rainwater were affected by quench in the samples, optimization of the counting window, and LSC vial type.

TABLE OF CONTENTS

ABSTRACT.....	ii
TABLE OF CONTENTS.....	iii
LIST OF TABLES.....	v
LIST OF FIGURES.....	vi
INTRODUCTION.....	1
Motivation.....	1
Tritium: General Overview & Health Effects.....	1
Overview of Rainwater Tritium Levels and Monitoring Programs.....	7
Rainwater Collection & Analysis.....	10
Using Liquid Scintillation Counting to Measure Tritium.....	12
Statistical Considerations of Low Level Counting.....	15
Limits of Tritium Detection.....	22
MATERIALS AND METHODS.....	23
Consideration of Project Goals and Steps.....	23
Annual NADP Scientific Symposium: 2-5 October 2012.....	24
CSU Lab Existing Equipment.....	26
Decision for Sample to Cocktail Ratio.....	28
Investigation of Colorado Background and FOM Optimization.....	29
Counting Rainwater Samples.....	31
Manipulation of Sample, Background, & Standard Data.....	33

RESULTS	35
Window Optimization and FOM Calculations	35
LSC Outputs.....	38
Counting Prepared Tritium Standards	42
TDCR Investigation & Comparisons.....	44
Statistical Considerations of Low Level Counting (Theoretical)	47
Statistical Considerations of Low Level Counting (Empirical).....	52
Quench Considerations with Rainwater Samples	56
Effectiveness of Counting Rainwater Samples for ³ H.....	57
Investigation of Concentration Methods.....	60
DISCUSSION.....	63
Characterization of Background or Near-Background Samples.....	63
Additional LSC Considerations	66
Viable NTN Program Requirements.....	68
Differentiation of Samples by Estimated Activity Level.....	70
Concentration of Samples of Tritium	73
Alternative Radionuclide Program Options.....	75
CONCLUSION.....	76
APPENDIX A: NTN SITE SAMPLE PREPARATIONS.....	86
APPENDIX B: T-TESTS COMPARING BACKGROUND AND SAMPLE COUNTS.....	87
APPENDIX C: TDCR COMPARISON – 2 HOUR COUNTS.....	89
APPENDIX D: TDCR COMPARISONS BY BOTTLE COLOR	90

LIST OF TABLES

Table 1: Radiological characteristics of tritium (^3H) [3]	2
Table 2: List of operating nuclear power reactors in the United States in 2014 [5]	4
Table 3: Rainwater collection samples received by CSU illustrating the spread of dates and locations	24
Table 4: Calibration standard specifications for Eckert & Ziegler tritium standard used at CSU	28
Table 5: Literature comparison of scintillation fluid to sample to determine most appropriate ratio	29
Table 6: Background blank preparations using deionized water and Ultima Gold TM LLT cocktail	29
Table 7: Counts of background blanks indicating number of samples run for each count duration	30
Table 8: Recorded information for rainwater samples allowing for a calculation of tritium activity.....	32
Table 9: Counts of cocktail-only sample in a plastic vial, ROI 15-185.....	35
Table 10: Results of 2 hr counts of deionized water blank in glass vial, 8:12 ratio, ROI 16-154	36
Table 11: Comparison of results for cocktail only background and three highest activity tritium standard spikes, ROI 15-185.....	37
Table 12: Average values for background counts of various durations, plastic vials, 8:12 sample to cocktail ratio, ROI 20-180	53
Table 13: Literature comparison of tritium concentration methods	61

LIST OF FIGURES

Figure 1: Map of operating nuclear power reactors in the United States [4] generated using Google maps 5

Figure 2: Department of Energy (DOE) nuclear facilities and sites [2] generated using Google maps 5

Figure 3: NADP NTN sites as of 31 July 2012 [52]..... 11

Figure 4: Illustration of the relationship between error types, LC, origin and sample mean for background and source distributions (assumes true activity is present in the sample)..... 19

Figure 5: Idealized diagram of the LSC spectrum illustrating the restriction of the window and resultant loss of integrated counts for both background and source distributions 21

Figure 6: Map of NTN sites, blue circles indicate sites from which samples were received, red circle indicates NTN site SC03 (Savannah River Site) 25

Figure 7: Map of NTN sites from which samples were received, generated using Google maps 25

Figure 8: Counting drawer on CSU's LSC offering 40 sample wells, image shows drawer loaded for plastic/glass comparisons, 3 March 2014..... 27

Figure 9: Activity concentration (Bq/L) of tritium standard solutions in deionized water based on calibration specifications 30

Figure 10: LSC spectra: double coincidence beta counts per channel forming spectra of eight background blanks (each color represents a sample). 8 mL deionized water in 12 mL scintillation cocktail run for 2 hours 38

Figure 11: LSC spectra: double coincidence beta counts per channel for ten selected NTN site rainwater samples (each color represents a sample). 8 mL sample to 12 mL cocktail run for 2 hours..... 39

Figure 12: Energy spectra of tritium standards in plastic vials: number of counts per energy bin versus energy (keV) for 8 mL standard solution and 12 mL scintillation, levels vary from background (water only) to 440 Bq/L.....	40
Figure 13: Energy spectra of standard solution in glass vial (green) and glass background samples (red): counts per channel versus channel number	40
Figure 14: Energy spectra of standard solution in glass vial (green) and glass background samples (red): counts per energy bin versus energy (keV).....	41
Figure 15: Energy spectra of standard solution in glass vial (green) and glass background samples: counts per energy bin (log) versus energy (keV).....	41
Figure 16: Energy spectra of standard solution in glass vial (green) and standard solutions in plastic vials: counts per energy bin (log) versus energy (keV),.....	41
Figure 17: Calculated net activity concentration of standard solutions plotted against actual activity concentration per the calibration certificate, plastic vials, 8:12 ratio, ROI 20-180	43
Figure 18: Paired comparison of measured and actual tritium activities for various count durations, plastic vials, 8:12 ratio, ROI 20-180	43
Figure 19: Counting efficiency estimated by TDCR for varying standard activity concentration, plastic vials, 8:12 ratio, ROI 20-180.....	44
Figure 20: Counting efficiency estimated by dividing net CPM _{opt} by DPM _{exp} for added standard activity concentrations between 1 Bq/L and 440 Bq/L, plastic vials, 8:12 ratio, ROI 20-180.....	45
Figure 21: Two methods of estimating counting efficiency for varying activity concentration, plastic vials, 8:12 ratio, ROI 20-180.....	46

Figure 22: Average efficiency as estimated by $TDCR_{opt}$ for plastic background, standard and sample runs and glass runs, plastic ROI 20-180, glass ROI 16-154..... 47

Figure 23: MDA concentration varying count time for constant background count rate (10.3 CPM) and efficiency (24.3%) [21] 48

Figure 24: MDA concentration varying background count rate (CPM) for a constant count duration (2 h) and efficiency (24.3%) [21] 48

Figure 25: MDA concentration varying counting efficiency for a constant background count rate (10.3 CPM) and count duration (2 h) [21] 49

Figure 26: LLD total counts varying sample count time for constant background count time (2 h), background count rate (10.3 CPM), and counting efficiency (24.3%) [23] 50

Figure 27: MDA concentration for varying sample count time with respect to a constant (2 h) background count time for background count rate of 10.3 CPM and efficiency of 24.3% 51

Figure 28: Net MDA concentration for varying background count time with a constant background count rate (10.3 CPM), efficiency (24.3%) and a constant (2 h) sample count time 51

Figure 29: Measurements of CPM_{opt} for background blanks over count durations of 10 m to 12 h (blue) and overall average CPM_{opt} (dashed red line)..... 52

Figure 30: Average MDA calculations for counts of various durations, plastic vials, 8:12 sample to cocktail ratio, Turner [21], Cember and Johnson [23], Knoll [18]. The graph illustrates similarity between the calculation and various simplifications. Note: the high MDA value calculated for 420 minutes reflects the high recorded count rate for the 2 blanks counted for that duration. 53

Figure 31: MDA concentration for equal count times of background and sample based on extrapolation of average background count rate (9.65 CPM) and NTN site sample efficiency (23.9%) from 2 hr counts, plastic, 8:12 ratio, ROI 20-180..... 54

Figure 32: MDA estimations based on individual background counts, average MDA estimations, and theoretical curve of MDA using overall average background of 10.5 CPM and 24.3% efficiency..... 55

Figure 33: Average MDA estimations and theoretical curve of MDA using overall average background of 10.5 CPM and 24.3% efficiency..... 56

Figure 34: Comparison of efficiency values for NTN site samples in plastic vials based on classification by storage bottle color..... 57

Figure 35: Decay corrected absolute activity concentration measured in NTN site samples (plastic, 2 hour counts, ROI 20-180) 58

Figure 36: Comparison of NTN site sample net activities and net MDA estimated using 2 hour average background count rate (9.65 CPM) and 2 hour average sample efficiency (23.9%), plastic vials, ROI 20-180 59

Figure 37: Comparison of NTN site sample net activities and net MDA estimated using 5 hour average background count rate (10.2 CPM) and 5 hour average sample efficiency (24.9%), plastic vials, ROI 20-180 59

Figure 38: Comparison of NTN site sample net activities and net MDA estimated using 2 hour average background count rate (18.6 CPM) and 2 hour average sample efficiency (17.9%), glass vials, ROI 16-154..... 60

Figure 39: MDA concentrations for varying count time based on a reduced background count rate of 1 CPM and the average NTN site sample TDCR_{opt} of 24.3% 65

Figure 40: MDA concentrations for varying count time based on a reduced background count rate of 0.25 CPM and the average NTN site sample $TDCR_{opt}$ of 24.3% 65

Figure 41: MDA concentrations for varying background count rate based on a count time of 2 hours and the average NTN site sample $TDCR_{opt}$ of 24.3% 66

Figure 42: Analytical capability of the lab based on background count rate for rainwater activity estimation based on a counting efficiency of 24.3% and a 30 minute count time..... 69

Figure 43: Composite map showing nuclear power reactors (red pins), DOE nuclear sites (blue squares), NTN sites below the MDA (red diamonds), and NTN sites that recorded an absolute activity level above 96 Bq/L in a 2 hour count (question marks), generated using Google maps 71

Figure 44: Composite map showing nuclear power reactors (red pins), DOE nuclear sites (blue squares), and NTN sites (orange diamonds), generated using Google maps..... 73

INTRODUCTION

Motivation

The National Atmospheric Deposition Program (NADP)'s National Trends Network (NTN) is a broad network of environmental sampling locations used to monitor rainwater in the United States for chemical substances of interest to environmental and human health. The motivation for this project is the potential expansion of the NTN's functionality to include monitoring for radioactive materials. Tritium (^3H) has been proposed as a pilot radionuclide for this expansion, which would require that a laboratory be able to accurately measure levels of tritium in rainwater with a high throughput of samples per week. Tritium is present in the environment at very low levels, and its radioactive decay results in a low energy emission that can be difficult to detect. These characteristics challenge the ability of the program to generate results on a regular basis in a manner that is both technically and financially feasible.

Tritium: General Overview & Health Effects

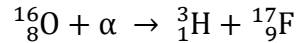
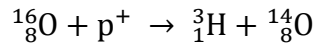
Tritium is the radioactive isotope of the element hydrogen, with a nucleus composed of one proton and two neutrons. This nuclide decays by the emission of a beta particle with a maximum energy of 18 keV, an average energy of approximately 6 keV, and a half-life of 12.3 years. Because it behaves chemically like all isotopes of hydrogen, tritium exchange in chemical, biological, and environmental compartments is nearly 100%, and the atom moves freely between its three primary forms: organically bound tritium (OBT), tritiated hydrogen gas (HT), and tritiated water (HTO) [1]. Table 1 summarizes the relevant radiological characteristics of tritium. Activity concentrations are reported in this paper in Bq/L, but tritium has also been measured in

the non-SI units of pCi/L (1 Bq/L = 27 pCi/L) or tritium units (TU), which correspond to an atomic ratio of one tritium atom per 10^{18} protium (normal hydrogen) atoms [2].

Table 1: Radiological characteristics of tritium (^3H) [3]

Radionuclide	Mode of Decay	Decay Energy	Half-life	Λ (Decay Constant)	Activity Unit Conversion
H-3 (tritium)	β^- to He-3 (100%)	β_{max} 18.59 keV (β_{avg} 5.69 keV)	12.32 y 3.89×10^8 s	0.056 y^{-1} $1.78 \times 10^{-9} \text{ s}^{-1}$	1 Bq/L = 8.47 tritium units (TU) = 27 pCi/L = 1 Bq/kg

Tritium occurs naturally in the environment and is also produced by anthropogenic sources. Natural production occurs in the upper atmosphere as a consequence of cosmic ray interaction with gaseous atoms. A variety of interactions are possible, with some of them terminating in the formation of tritium atoms, as described below [2]:



The most significant interaction forming tritium is fast neutron absorption by ^{14}N , which produces ^3H and ^{12}C [1]. Magnetic effects on the charged cosmic particles cause deviation of these particles toward the poles [2]. The higher cosmic particle fluence at higher latitudes results in increased tritium production. Naturally formed tritium tends not to occur or accumulate to levels of concern for human health effects.

Anthropogenic sources of tritium primarily include deposition from remnants of atmospheric nuclear weapons testing and releases from facilities that conduct nuclear processes.

While releases from nuclear facilities are of predominant importance today, the effect of atmospheric nuclear weapons testing is of significant historical importance. In the detonation of a nuclear weapon, tritium makes up a small fraction of the thermal fission yield as a ternary fission product. Fusion-type weapons also produce significant yields of tritium and use ^3H as a component to increase the explosive yield. After detonation, thermal convection transports radioactive products and debris into the atmosphere, where they can subsequently be deposited via rainout or washout. Because of the circulative flow of global air currents, the radioactivity released in either hemisphere is likely to be deposited in the same hemisphere. Therefore, the majority of atmospherically deposited tritium from nuclear weapons testing occurred in the northern hemisphere, where the majority of the tests took place. It is estimated that tritium concentrations in precipitation due to atmospheric weapons testing were between a factor of 5 and 20 higher in the northern hemisphere compared to the southern hemisphere [2]. A total of 521 nuclear devices (both fission and fusion) were detonated between 1945 and 1981, with 346 of those tests occurring between 1945 and 1962. The estimated tritium activity produced in the first 346 tests was approximately 1.2×10^{20} Bq [2].

Due to the radioactive decay of tritium over time, atmospheric weapons testing has faded in relevance and represents a decreasing component of current environmental ^3H concentrations. Tritium's 12.3 year half-life means that all of the ^3H produced by 1970 has undergone at least 3.6 half-lives. Based on the radioactive decay equation (Equation 1), only about 8% of this activity remains in 2014. The contribution from atmospheric weapons testing can be considered negligible after a period of 10 half-lives, or by approximately the year 2090.

Equation 1: Radioactive decay of tritium produced in 1970 over 44 years to present (2014)

$$A(t) = A_0 e^{-\lambda t} = A_0 \left[e^{-\frac{\ln(2)}{T_R} \times t} \right] = A_0 \left[e^{-\frac{\ln(2)}{12.3 \text{ y}} \times 44 \text{ y}} \right] = 0.084(A_0)$$

Today, facilities which engage in nuclear processes are the primary anthropogenic source of tritium in rainwater. As of early 2014, there are 100 operating nuclear power reactors (see Table 2 and Figure 1) and 19 Department of Energy (DOE) nuclear sites (see Figure 2) [4] which are licensed to operate in the United States and may contribute to the atmospheric ³H inventory.

Table 2: List of operating nuclear power reactors in the United States in 2014 [5]

Operating Nuclear Power Reactors in the US			
Arkansas Nuclear 1	Dresden 2	Nine Mile Point 1	River Bend 1
Arkansas Nuclear 2	Dresden 3	Nine Mile Point 2	Robinson 2
Beaver Valley 1	Duane Arnold	North Anna 1	Saint Lucie 1
Beaver Valley 2	Farley 1	North Anna 2	Saint Lucie 2
Braidwood 1	Farley 2	Oconee 1	Salem 1
Braidwood 2	Fermi 2	Oconee 2	Salem 2
Browns Ferry 1	FitzPatrick	Oconee 3	Seabrook 1
Browns Ferry 2	Fort Calhoun	Oyster Creek	Sequoyah 1
Browns Ferry 3	Ginna	Palisades	Sequoyah 2
Brunswick 1	Grand Gulf 1	Palo Verde 1	South Texas 1
Brunswick 2	Harris 1	Palo Verde 2	South Texas 2
Byron 1	Hatch 1	Palo Verde 3	Summer
Byron 2	Hatch 2	Peach Bottom 2	Surry 1
Callaway	Hope Creek 1	Peach Bottom 3	Surry 2
Calvert Cliffs 1	Indian Point 2	Perry 1	Susquehanna 1
Calvert Cliffs 2	Indian Point 3	Pilgrim 1	Susquehanna 2
Catawba 1	La Salle 1	Point Beach 1	Three Mile Island 1
Catawba 2	La Salle 2	Point Beach 2	Turkey Point 3
Clinton	Limerick 1	Prairie Island 1	Turkey Point 4
Columbia Generating Station	Limerick 2	Prairie Island 2	Vermont Yankee
Comanche Peak 1	McGuire 1	Quad Cities 1	Vogtle 1
Comanche Peak 2	McGuire 2	Quad Cities 2	Vogtle 2
Cooper	Davis-Besse	Millstone 2	Waterford 3
D.C. Cook 1	Diablo Canyon 1	Millstone 3	Watts Bar 1
D.C. Cook 2	Diablo Canyon 2	Monticello	



Figure 1: Map of operating nuclear power reactors in the United States [4] generated using Google maps

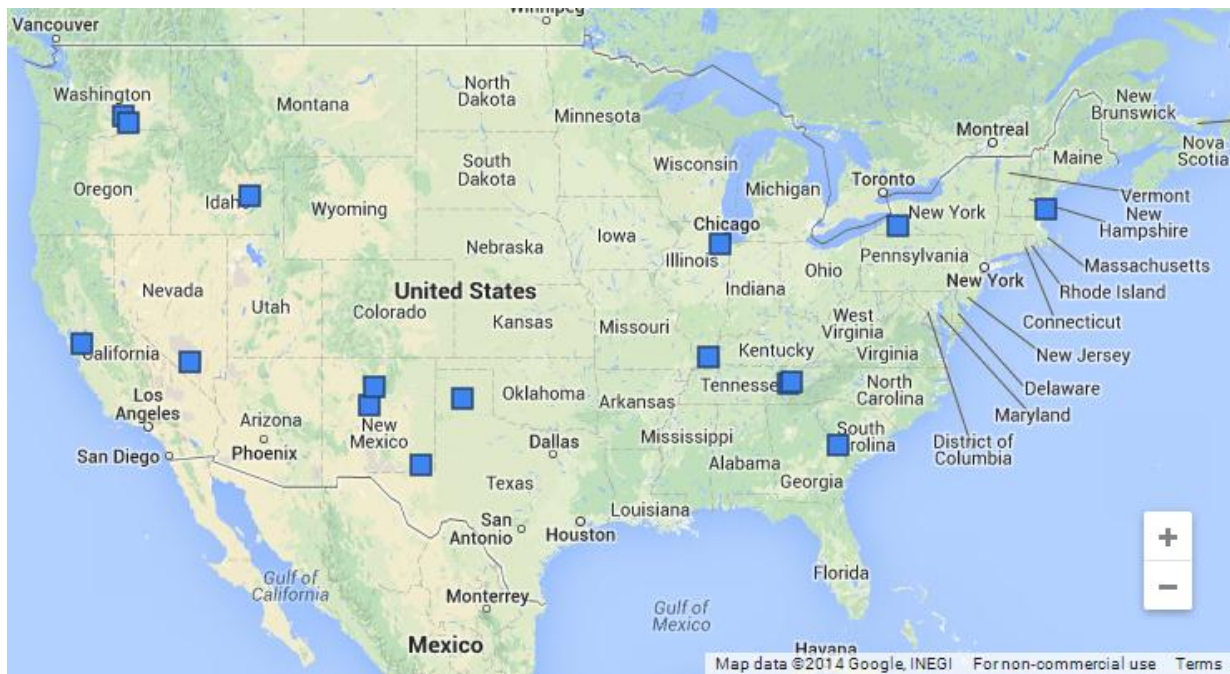


Figure 2: Department of Energy (DOE) nuclear facilities and sites [2] generated using Google maps

Relevant DOE licensed nuclear sites include the Hanford Site, the Pacific Northwest National Laboratory (PNNL), Idaho National Laboratory (INL), Los Alamos National Laboratory (LANL), the Nevada National Security Site (NNSS), Sandia National Laboratory (SNL), the Waste Isolation Pilot Plant (WIPP), the Pantex Plant, Argonne National Laboratory (ANL), the New Brunswick Laboratory (NBL), Paducah, the K-25 Plant (ETTP), Oak Ridge National Laboratory (ORNL), the Y-12 site, the Savannah River Site (SRS), the Portsmouth Gaseous Diffusion Plant, and the West Valley Demonstration Project (WVDP) [4].

Additionally, tritium has been released in the production of luminous watch dials, gun sights, and exit signs, and these trace contamination events can result in increased readings for tritium in specific situations.

When present in the atmosphere, tritium can be deposited in surface waters via rain or snow or deposited via dry deposition as a component of other hydrogen-containing air constituents. The health effects of tritium are not of particular concern, especially at the levels which occur commonly in the environment. Due to the low energy of the emitted β^- particles, tritium does not pose an external dose hazard, but may contribute to an individual's internal dose. Because tritium exchanges easily between chemical forms and can be incorporated in any molecule containing hydrogen, it rapidly distributes to all compartments within the human body. Therefore, any incorporated tritium will result in a whole body dose, but will also leave the body without concentrating in tissues. Tritium can be incorporated into the body via inhalation, ingestion, and absorption through the skin. The biological half-life of this nuclide (approximately 10 days [6]) is a parallel of body water turnover, and will therefore fluctuate between individuals and over time in the same individual.

The United States Environmental Protection Agency (EPA) sets legally enforceable standards in the national primary drinking water regulations to protect public health by limiting the levels of contaminants. Under the Safe Drinking Water Act, the EPA has specified a level of contamination in drinking water at which no adverse health effects are likely to occur considering costs, benefits, and the ability of treatment systems to remove contaminants. The maximum contaminant level (MCL) for tritium is an activity of 740 Bq/L (20,000 pCi/L) in drinking water, with a laboratory detection limit of 37 Bq/L [7]. Continuous exposure of a person to drinking water tritium at this level would result in a dose of 40 μ Sv per year (4 mrem per year) for an adult consuming 2L of water per day [8].

Overview of Rainwater Tritium Levels and Monitoring Programs

The natural background tritium concentration in precipitation around the globe has been estimated as approximately 0.6 Bq/L without the influence of anthropogenic sources [1] [8]. Additionally, the mean tritium concentration in precipitation in the northern hemisphere has been recorded to be between 0.6-1.2 Bq/L (5-10 TU) [9]. Tritium at these concentrations is difficult to measure because a concentration of 1 Bq/L corresponds to one radioactive decay resulting in one low energy β^- particle per second per liter of water. Some degree of enrichment can be required to obtain adequate net tritium count rates for most water samples [9].

Research and monitoring for atmospheric tritium were conducted beginning in the 1960s to characterize the atmospheric concentrations resulting from atmospheric thermonuclear bomb tests. Characterization of tritium levels during this time period recorded tritium concentrations due to anthropogenic sources of tens to hundreds of Bq/L (several thousand pCi/L) in the 1960s with consistent decreases since then [8]. A study in Australia found that the tritium activity in

rainwater for all Australian stations decreased after 1969, and that peak values for atmospheric concentrations in the southern hemisphere ranged between 6 and 12 Bq/L (50-100 TU) [2]. Because global air currents tend to restrict air movement between the northern and southern hemispheres, this lower concentration in Australia probably reflects the smaller fraction of nuclear weapons tests which occurred in the southern hemisphere. In the United States, one study found decreasing levels of tritium in New York City precipitation in the early 1970s, with average concentrations of 13 Bq/L, 7.8 Bq/L, and 7.4 Bq/L in 1971, 1972, and 1973, respectively [10]. Ranges in the northern hemisphere have been described as reaching a maximum of 118-236 Bq/L (1000-2000 TU) in 1962 and decreasing after that point to 1.2 Bq/L (10 TU) in 1996 [11].

The U.S. EPA's RadNet monitoring program has capabilities for monitoring for ^3H in air, water, precipitation, and milk (an animal metabolic byproduct). Routine precipitation monitoring includes sample collection after each measureable rainfall, and samples are sent to the EPA National Air and Radiation Environmental Laboratory (NAREL). Precipitation samples at 41 locations are composited into single monthly samples [12], and 27 locations sent in precipitation samples for tritium analysis in 2011 [13]. Each month that precipitation occurs, a monthly sample undergoes analysis for ^3H and gamma-emitting nuclides (overall beta analyses were eliminated in 2010). In their 2011 report, the NAREL reported a minimum detectable concentration for tritium in water of 5.6 Bq/L (150 pCi/L) [13]. An important consideration for this program is that RadNet does not report on precipitation depth, which means that values for wet deposition alone cannot be calculated. Instead, the collection systems used by RadNet for precipitation monitoring are continuously open before and after precipitation events, meaning that the collection method is only useful for bulk deposition (dry deposition as well as wet deposition) [14].

Worldwide networks of rain sampling stations have been used for tritium monitoring as well. The IAEA's Global Network for Isotopes in Precipitation (GNIP) monitors for radionuclides worldwide and has 78 stations in North America [4]. This monitoring program has looked at more than 420 meteorological stations in 49 countries and territories since 1961 and ^3H is one of the radionuclides of interest [15]. The IAEA Water Isotope System for Data Analysis, Visualization, and Electronic Retrieval generates samples that represented the integrated precipitation for a one-month period using a sampling system that collects water in a standard rain gauge which is emptied after precipitation events [16].

Facilities such as Savannah River National Laboratory (SRNL) release tritium as part of their normal processing and can be major contributors to tritium concentrations at and around their sites [8]. These facilities tend to maintain strict environmental monitoring programs for radionuclides. Typical rainwater tritium concentrations measured at the Savannah River Site (SRS) are well below the EPA drinking water standard (740 Bq/L) and range from approximately 4-400 Bq/L (between the orders of 10^2 and 10^4 pCi/L). These levels decrease with distance from the source and show a decreasing trend over time since the 1970s, a trend which is illustrative of the decay of atmospheric tritium released to the environment from weapons tests. Samples are taken onsite and at locations on radii of 10, 25, and 100 miles from the SRS. The highest recorded level from near SRNL was 1200 Bq/L (32,000 pCi/L) in November 1982, and a high of 137 Bq/L (3,700 pCi/L) was recorded in September 1995 for the period of 1995-1998 [8]. Today, the SRS Precipitation Monitoring Network records onsite highs around 111 Bq/L (3000 pCi/L) [4]. Oftentimes the SRS contribution to levels distant from the facility is indistinguishable from background due to fluctuations in releases from the facility. This incomplete characterization of offsite levels suggests the need for a larger, independent network

to monitor for radionuclides in the United States [4] which would record and have the capacity to map tritium concentrations at near-background levels of 0.6-1.2 Bq/L.

Rainwater Collection & Analysis

The National Atmospheric Deposition Program (NADP) monitors for a variety of chemical compounds in precipitation with a series of continent-scale networks. The National Trends Network (NTN) and Mercury Deposition Network (MDN) consisted of 244 and 104 sites, respectively, in 2011 [14]. The current NTN network is depicted in Figure 3. Overall, the NADP has been monitoring and producing annual reports of precipitation chemistry since 1978, and the recorded data have been used in colored maps to demonstrate spatial trends and animated maps to illustrate temporal variation. Samples from these networks are typically processed at the NADP's Central Analytical Laboratory (CAL).

At each site in the national trends network, an automated collection system is used to collect rainwater. The collection systems are sensitive to precipitation events, opening to allow for collection during periods of precipitation and closing to protect the contents from exterior influences during the remainder of the time. According to NADP protocols, samples from the NTN are decanted weekly into 1 L NalgeneTM bottles and shipped without preservation to the CAL. Preservation is not considered necessary for the samples because the tritium contained within them is present as a component of the water itself [7].

National Atmospheric Deposition Program National Trends Network

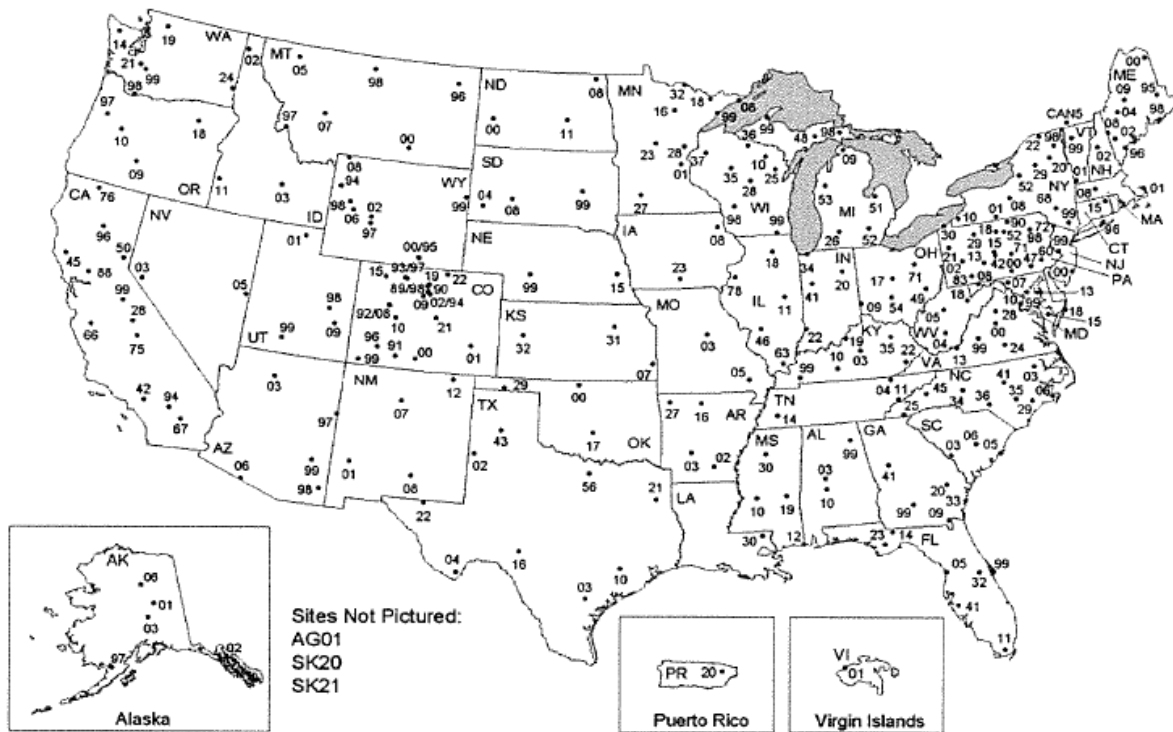


Figure 3: NADP NTN sites as of 31 July 2012 [52]

In 2011, shortly after the initial spread of contamination from the nuclear accident at the Fukushima Daiichi nuclear power station, the NADP coordinated with the U.S. Geological Survey (USGS) to measure precipitation samples for fission product isotopes using gamma spectrometry. The study found measurable levels of three gamma-emitting radionuclides (^{131}I , ^{134}Cs , and ^{137}Cs) in 21% of the 167 sampled sites, illustrating the usefulness of existing sample locations for measurement of radionuclides [14]. Additionally, the study found that the NADP had the capability to be a versatile cooperative partner to existing radionuclide monitoring programs. The nature and funding of the program allowed for rapid adaptation in order to

measure wet deposition of soluble and particle bound fission products and prioritize samples based on atmospheric transport models.

Using Liquid Scintillation Counting to Measure Tritium

Liquid scintillation counting (LSC) is frequently used for determination of activity of radionuclides with low energy beta emissions (such as tritium). This detection system converts incident radiation energy into fluorescence in an organic scintillator with a linear energy response, and has advantages due to its sensitivity and reproducibility [17]. Fluorescence is the prompt emission of visible light radiation from a substance after an excitation. In organic materials, the fluorescence arises from energy level transitions within individual molecules (so the crystalline lattice structure of an inorganic scintillator is not required.) In organic molecules with a π electron structure indicating symmetry properties, energy is absorbed by exciting the electron into an excited configuration. Nearly all molecules at room temperature are initially in the ground state. These molecules absorb kinetic energy from a charged particle passing nearby, which produces a number of molecules in the excited state. Each excited molecule promptly transitions back to the ground state, releasing a photon that is collected and magnified into a signal by a photomultiplier tube (PMT). Organic scintillators can be transparent to their own emission light because the fluorescence transitions (excited to ground) have lower energies than the absorption energies required for excitation (due to the presence of vibrational sub-states of the various energy levels) [18]. Organic scintillators are preferred for beta spectroscopy because of their hydrogen content, and liquid scintillators that allow for dissolution of the sample avoid typical counting problems associated with sample self-absorption, attenuation by detector windows, and backscattering.

Because LSC uses an organic scintillation fluid to convert energetic emissions from the sample to measurable light, there is a limit to the amount of sample material that can be incorporated into each measurement. The organic fluid has a limited ability to mix with aqueous samples, and turbidity in the mixture can cause quench (described in the next section) at certain mixing ratios [17]. Only purely organic samples can be mixed with a lipophilic cocktail. For aqueous samples such as rainwater, an emulsifying cocktail is required for adequate mixing [19]. Generally, as the ratio of sample to cocktail decreases, the number of counts per decay increases. One study investigated adjusting the ratio of scintillation cocktail to sample water for background, low, and high activities for ratios between 1.2 and 3.0, finding that the total counts increased up to a ratio of two parts cocktail to one part sample before leveling off [17]. A ratio of 8 mL sample to 12 mL cocktail is common practice in LSC measurement, and this ratio maximizes the amount of sample water for a 20 mL vial.

For measurement of high and low levels of tritium, studies offer conflicting recommendations on the use of plastic versus glass vials. For example, it has been found that glass vials allow higher counting rates than plastic vials [17], while plastic (polyethylene) vials have a lower optical clarity but are naturally lower in background radiation emitting nuclides. Plastic vials may be susceptible to static buildup, which would give incorrect results [7]. Glass is chemically inert, but K-40 and other background radionuclide effects have been shown to contribute to erroneous counts in glass vials. However, K-40 decays with a higher beta energy than tritium (maximum of 1312 keV and an average energy of 561 keV), and LSC vials are often made of borosilicate glass, which is lower in potassium content and will reduce background interference from K-40 [19]. Overall, research comparing plastic and glass scintillation vials found that performance in the ^3H energy region was significantly affected by residual

radioactivity and fluorescence in the glass [20], thus counting in plastic vials allows for better direct measurement of environmental tritium samples without enrichment. This project used primarily plastic vials, but measured duplicate samples in glass for comparison of counts and detection efficiencies.

Background counts on an LSC require a long count time to obtain lower statistical uncertainty due to their low count rate. The minimum detectable activity of tritium in a water sample is a function of the background count rate, the count duration, the detection efficiency, and whether or not the sample and background are counted for equal times. The statistical considerations of low level counting are described in more detail in a later section.

Quench

In LSC measurements, quench is a critical consideration. Quench refers to the sample emissions which transmit their energy to non-signal-producing endpoints, resulting in a lower count rate than radioactive emission rate and decreasing the scintillation efficiency [18]. The two types of quench which occur in LSC measurements are classified as chemical and optical quench. Both types of quench result from impurities in the sample, which limit the conversion of emissions to recorded signals. Chemical quench is an effect of impurities that absorb the energy in their chemical structure, while optical or color quench results from absorption of energetic radiations by molecules that release light at a different wavelength than the wavelength to which the detector is sensitive. The effect of quench induces a decrease in the recorded count rate and a shift of the energy spectrum toward lower energies [17]. Therefore, samples with higher quench are associated with lower detection efficiencies and have consequently higher minimum detectable activities.

Common correction methods for quench include internal standardization, sample channels ratio correction, and external standard ratio correction methods [17]. Some instruments, as a feature of their design, can calculate a triple to double coincidence ratio (TDCR) to measure quench, thereby estimating efficiency and producing a readout of the recorded measurements in units of activity. In a Hidex™ LSC such as the instrument used at Colorado State University, an array of three photomultiplier tubes arranged at 120 degree angles from one another allows for an estimation of quench via the TDCR. A single signal in one of three tubes is a good indicator of noise, two hits indicates a true signal with some quench, and lower quench will result in three hits. Rainwater samples may experience color quenching due to impurities present in the water, which will lower the efficiency.

Statistical Considerations of Low Level Counting

For low activity samples, statistical fluctuation is of primary concern. The uncertainties associated with low level tritium measurement are diverse and complex, and they present a constant challenge in counting rainwater samples. In these measurements, uncertainty can be introduced due to pipetting samples or variation in the sample collection method. After the sample has been collected, uncertainties are introduced due to storage and transport of the sample, which may include absorption of tritium by the sample containers. For the purpose of this investigation, tritium is always assumed to be evenly distributed in the sample and the contributions to uncertainty from the delay before counting, storage conditions, and age of the cocktail are ignored. Both the sample and background distributions are assumed to be normally distributed and are manipulated using Poisson statistics.

Comparison of the count rates and variances of counts is the first step in differentiating signal over background. For a set of counts, the standard deviation of a Poisson distribution is equal to the square root of the mean. Because of the requirements of combining multiple measurements and error propagation, the relationships described in Equation 2 come into play.

Equation 2

$$\sigma_{rate_{net}} = \sqrt{\sigma_{rate_g}^2 + \sigma_{rate_b}^2} = \sqrt{\frac{\sigma_g^2}{t_g} + \frac{\sigma_b^2}{t_b}} = \sqrt{\frac{n_g}{t_g^2} + \frac{n_b}{t_b^2}} = \sqrt{\frac{r_g}{t_g} + \frac{r_b}{t_b}}$$

Where: $\sigma_{rate_{net}}$ is the standard deviation of the net count rate, $\sigma_{rate_g}^2$ and $\sigma_{rate_b}^2$ are the variances of the gross and background count rates, σ_g^2 and σ_b^2 are the variances of the gross and background distributions, t_g and t_b are the gross and background count times, n_g and n_b are the numbers of gross and background counts, r_g and r_b are the gross and background count rates, respectively. These relationships are important in relating the information obtained from counts over different count times.

Equation 3 is obtained by manipulation of the sample variances and count times if the total allowable time for making both gross and background counts is fixed [21]. Thus, for a fixed total time for both counts (such as the number of hours in a week), the optimal gross count time (t_g) increases with the square root of the ratio between the gross count rate and the background count rate $\left(\sqrt{\frac{r_g}{r_b}}\right)$.

Equation 3

$$\frac{t_g}{t_b} = \sqrt{\frac{r_g}{r_b}} \quad \therefore \quad t_g = t_b \times \sqrt{\frac{r_g}{r_b}}$$

For low level counting, the activity of a radioactive source approaches background levels, the gross count rate (r_g) approaches the background count rate (r_b), and the square root in Equation 3 approaches 1. Consequently, equal allocation of time to the sample and background is the appropriate choice to minimize the uncertainty in the net counts when the source is weak compared with background [22]. However, this allocation is not always practical, especially for large numbers of samples.

The interpretation of counts of samples that may or may not contain excess activity is based on statistical analysis considering both type I (α) and type II (β) errors. Several statistical terms and definitions are included here for reference:

- Type I (α) – false positive – probability of detecting activity in the sample when none exists. This erroneous source detection would be due to statistical fluctuations in the background. To limit Type I error to 5% the decision threshold (L_C) is chosen at a net count rate greater than the net of the blank plus 1.65 standard deviations.
 - This type of error is also called False Alarm Probability (P_{FA}), and is equal to the area under the normal curve of background counts which is above the decision threshold L_C (see Figure 4).
- Type II (β) – false negative – probability of saying the sample is background when in fact there is activity present
 - This type of error is also called False Negative Probability (P_{FN}), and is equal to the area under the normal curve of gross counts which is below the decision threshold L_C .
 - The remaining area under the curve above the decision threshold L_C is called the detection probability (P_D) or the power of the test. The power of a statistical test is

a measure of the probability of rejecting the null hypothesis when the null hypothesis is false. Power is calculated as $1-\beta$.

- L_C – threshold of decision or alarm level. This value is chosen by the observer and represents the value at which the observer concludes that counts below L_C are background and counts above L_C are due to the presence of a radioactive source.

Typically, α and β errors are each set at 5%, and this decision is input into the equations necessary to derive a minimum detectable amount or activity. The minimum detectable activity (MDA) of a device is the source strength necessary to produce a mean value of net counts that maximizes the detection probability (true positive) and minimizes P_{FA} . In the context of radioactivity detection, the L_C is a number of counts during the count period which will indicate that a sample has more radioactivity present than the background. The sum of the average background counts and the L_C is the number of counts that the detector must record to determine that a radioactive source is present with the desired level of confidence that α and β errors will not occur. This sum is described as the lower limit of detection (LLD) of the device. The MDA is a function of the LLD incorporating information about the counting efficiency and a unit conversion to units of decays per second (Bq.)

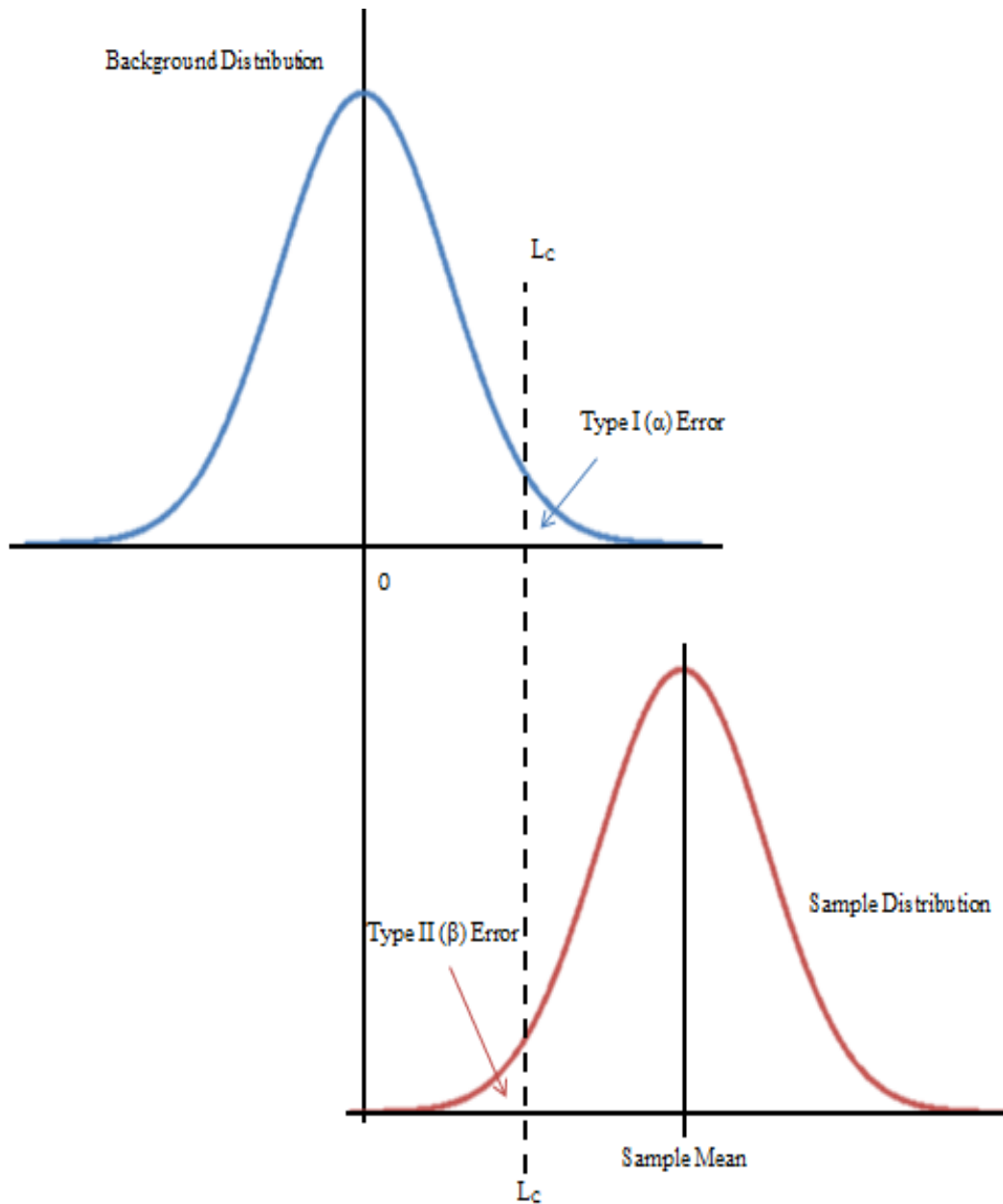


Figure 4: Illustration of the relationship between error types, LC, origin and sample mean for background and source distributions (assumes true activity is present in the sample)

Various equations are found in the literature which allow for a calculation of the LLD given a series of assumptions about uncertainty and count time [23] [21] [22]. Equation 4 is a simplified equation for the LLD for both types of errors set at 5% and different count times for background and gross counts. For those interested in changing the error levels, the textbook by

Turner [21] provides an expanded version of the calculation. Equation 5 is a simplification of this equation where values have been substituted to set both types of error at 5%. This equation relies only on the number of background counts (n_b).

Equation 4 [23]

$$LLD = 3.29 \sqrt{r_b t_g \left(1 + \frac{t_g}{t_b}\right)} + 3$$

Where r_b is measured in counts per minute (CPM) and both t_g and t_b are measured in minutes.

Equation 5 [21]

$$LLD = \sqrt{2n_b} \left[1.65 \left(\frac{1.65}{\sqrt{8n_b}} + \sqrt{1 + \frac{2.71}{8n_b}} \right) + 1.65 \sqrt{1 + \frac{2.71}{4n_b} + \frac{1.65}{\sqrt{2n_b}} \sqrt{1 + \frac{2.71}{8n_b}}} \right]$$

A valuable simplification of these equations can be derived if the sample and background counting times are equal. The literature provides several versions of this simplified equation for determining the minimum mean number of counts recorded by the detector from the radioactive source. The textbook by Cember and Johnson [23] estimates an LLD as given in Equation 6. Knoll [22] provides a similar equation, calling the simplification the “Currie equation” (Equation 7).

Equation 6 [23]

$$LLD = (4.66 \times \sigma_b) + 3$$

Equation 7 [22]

$$LLD = (4.65 \times \sigma_b) + 2.71 = 4.65 \times \sqrt{n_b} + 2.71$$

An additional statistical technique used in interpreting data is the t-test. This test is used to test the null hypothesis that there is no difference between two measurements or sets of measurements, and comes into play in the comparison of the count rates calculated for samples and backgrounds.

Finally, effective use of the LSC necessitates optimization of the energy window (called the region of interest or ROI) in order to maximize the ratio of signal over background. An “open” window indicates that the software analyzes counts in all energy channels recorded by the detector (5-1023 on CSU’s LSC). Variations of the ROI for detection will improve the overall statistical accuracy in the determination of the activity of the source. Increasing the ROI will give a higher counting efficiency but increase counts of a background signal [11]. Limiting the window will remove areas of source signal as well as areas of background signal, but proportionally more area will be removed from the background distribution than will be removed from the source distribution. This relationship is described in Figure 5.

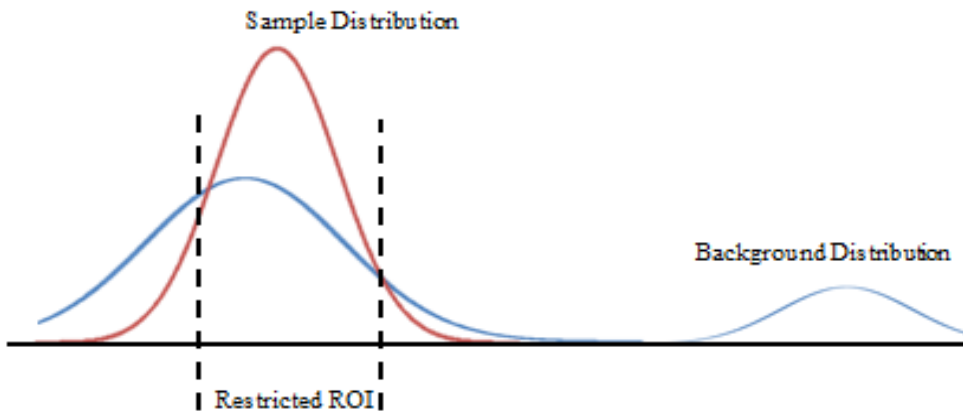


Figure 5: Idealized diagram of the LSC spectrum illustrating the restriction of the window and resultant loss of integrated counts for both background and source distributions

Limits of Tritium Detection

With samples which will frequently reflect background tritium levels, the true limit of detection is a critical consideration. For samples without enrichment, the sensitivity of detection depends on the counting efficiency, the background count rate, and the counting period. Additionally, for enriched samples, the sensitivity of detection depends on the initial volume of enriched water [11]. The IAEA has conducted several intercomparisons of laboratories measuring very low levels of tritium since 1985 [11]. The seventh intercomparison of tritium measurements from multiple laboratories based on standards prepared with a US National Institute of Standards and Technology (NIST) standard used six solutions prepared by the IAEA Isotope Hydrology Laboratory which varied from 0 Bq/L (virtually tritium-free water collected from an artesian well) to 119 Bq/L. The common approach of the compared laboratories was direct measurement without enrichment, and the study found that “the majority of laboratories show distinct deviations and bias in positive or in negative direction for all samples... [which] indicates problems with the calibration of measurements” [24].

Research has found that the results of tritium counting can be strongly affected by beta-emitting radon decay products [25] and variation in atmospheric tritium. Additionally, the multiple sources of uncertainty in measurements of tritium at very low levels have not been well characterized by most laboratories, and may be as high as 99% considering appropriate statistical propagation of all sources of uncertainty [26]. A study published in Accreditation and Quality Assurance suggested a strategy for improving the quality of the measurements by improving precision of sample and background measurements. Several techniques included increasing the counting time of sample and background and splitting the total measurement time into intervals to efficiently identify and eliminate outlying measurements [26].

MATERIALS AND METHODS

Consideration of Project Goals and Steps

The original scope of the project was an analysis of existing (low concentration) samples, collected at NTN sites and shipped out of the Central Analytical Laboratory (CAL), using existing methodology on CSU's LSC. This project would serve as a pilot demonstration of the potential to use the National Trends Network (NTN) to monitor radioactive tritium in precipitation in North America. CSU researchers received water samples from the NADP CAL using existing surplus sample amounts. The 42 rainwater samples were shipped in 1 L Nalgene™ bottles and contained approximately 500 mL of sample to allow for duplicate readings. Two of the initial/pilot samples came from NTN site SCO3, a region with traditionally elevated ^3H levels.

A more advanced project goal included investigation of concentration methods for measuring ^3H activity in precipitation and developing a standard operating procedure for the use of a selected concentration method. Because the activity in some rainwater samples was predicted to be of the order of tenths of a Bq/L (10 pCi/L), it was considered prudent to consider concentration of samples to practice large scale monitoring of ^3H activity in North American precipitation. Concentration procedures were evaluated to determine their efficacy, cost efficiency, and reproducibility. Should a sample concentration procedure prove to be effective, efficient, and reproducible in the laboratory, its potential for use in the field would be evaluated. Adsorption of ^3H onto silica gel was a proposed procedure to achieve the necessary concentration to count low level tritium samples efficiently.

In October 2012, the collaborators of this project met at the annual NADP scientific symposium in Portland, ME. During this conference, the capabilities of the NTN were reviewed and the sample collection techniques were investigated for feasibility in collecting rainwater samples for radioactivity analysis. The project collaborators communicated their interest in bringing a radionuclide monitoring program online if feasible. After the conference, CSU received 42 rainwater samples from 23 locations in the southern United States. Table 3, Figure 6, and Figure 7 illustrate the spatial and temporal spread of these samples.

Table 3: Rainwater collection samples received by CSU illustrating the spread of dates and locations

Site	Date of Sample Collection	
AL99	9/4/2012	9/18/2012
FL03	9/4/2012	9/11/2012
FL14		9/11/2012 9/18/2012
FL23	9/4/2012	9/11/2012 9/18/2012
GA09	9/4/2012	9/11/2012 9/18/2012
GA20	9/4/2012	
GA33		9/11/2012
GA41	9/4/2012	9/18/2012
GA99		9/11/2012
KY22		9/11/2012 9/18/2012
NC06	9/4/2012	9/11/2012
NC25	9/4/2012	9/18/2012
NC29	9/4/2012	9/11/2012
NC34		9/18/2012
NC35	9/4/2012	
NC41	9/4/2012	9/18/2012
NC45	9/4/2012	9/18/2012
SC03	9/4/2012	9/11/2012
SC05	9/4/2012	9/11/2012
SC06	9/4/2012	
TN04	9/4/2012	9/18/2012
TN11		9/11/2012 9/18/2012
VA13		9/11/2012 2/18/2012

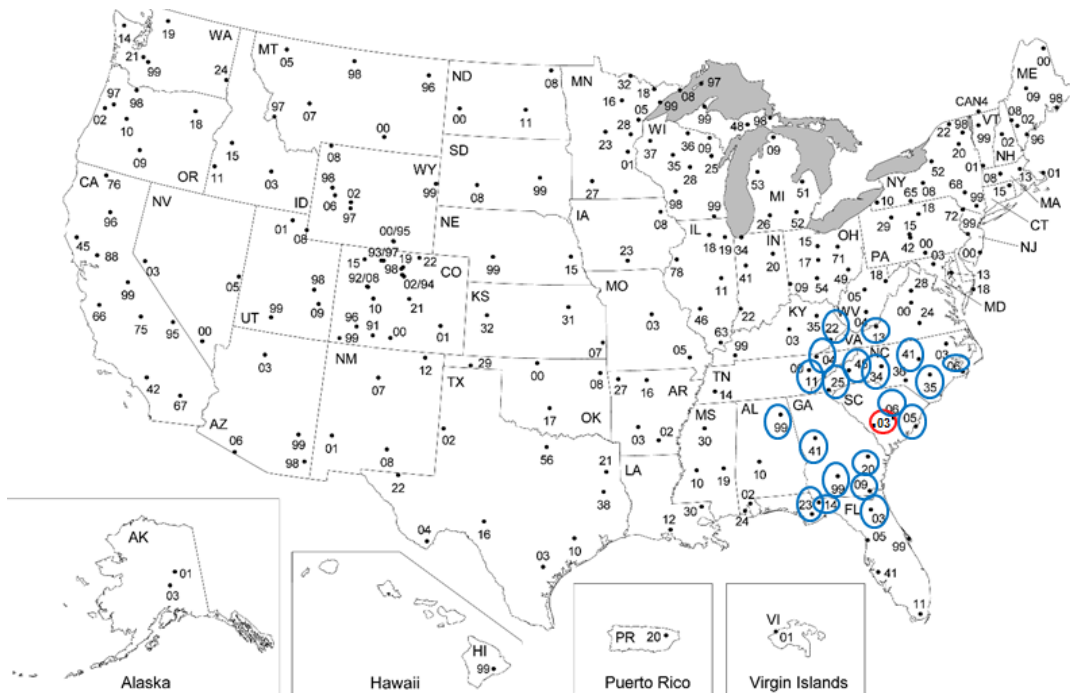


Figure 6: Map of NTN sites, blue circles indicate sites from which samples were received, red circle indicates NTN site SC03 (Savannah River Site)

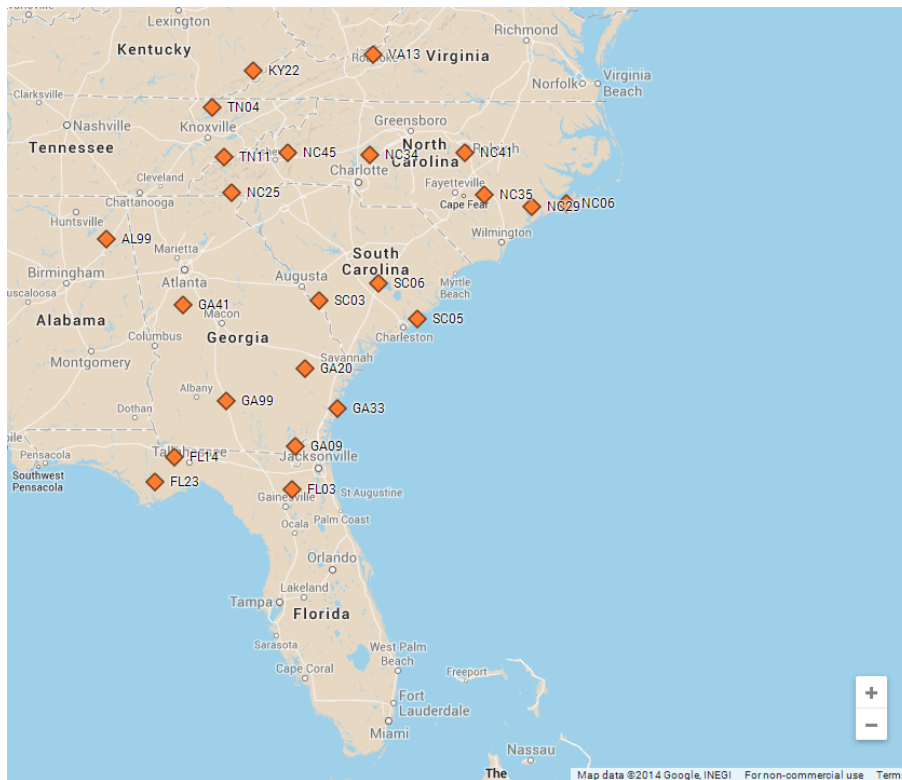


Figure 7: Map of NTN sites from which samples were received, generated using Google maps

CSU Lab Existing Equipment

CSU's counting laboratory uses a HidexTM Liquid Scintillation Counter. The LSC is programmed to record counts over a range of 5-1023 channels which correlate to a binning system for incident radiation energies. UV photons produced in the scintillation cocktail are collected by the photomultiplier tubes (PMTs) to record signals over the duration of the counting period. This machine is equipped with three PMTs arranged at 120 degree angles from one another around the detection location, which allows for an estimation of efficiency using the ratio of triple coincidence measurements of the scintillation photons to double coincidence measurements. This relationship is described by Equation 8.

Equation 8

$$\text{Efficiency} \approx \text{TDCR} \approx \frac{\text{counts incident upon three PMTs}}{\text{counts incident upon two PMTs}}$$

This triple to double coincidence ratio (TDCR) is the primary advantage of the CSU LSC. The TDCR allows for an accurate intrinsic estimate of efficiency based on the likelihood that increased quench in the sample will limit the collection of signal photons in the PMTs. While a radioactive source with no quenching would produce a signal in a 4π geometry, real (quenched) samples are more likely to cause coincident signals in two PMTs as opposed to three. The LSC output from the counting period will include a measure of total counts, counts per minute (CPM), the TDCR, and an estimate of nuclear disintegrations per minute in the sample (DPM) which is a direct relationship between the CPM and TDCR.

In the LSC, the scintillation cocktail used was Ultima GoldTM Low Level Tritium (LLT) Scintillation Cocktail by PerkinElmer. This cocktail is designed for environmental sampling of tritium in seawater, deionized, distilled, and rain water, and the manufacturer specifications

indicate a water capacity of up to 54% (12 mL sample to 10 mL cocktail) and tritium counting efficiencies of approximately 30%. For an 8 mL sample to 12 mL cocktail ratio, the cocktail has a listed efficiency of 24.6% for tritium detection and a minimum detectable activity (MDA) of 1.22 Bq/L when samples are counted for 500 minutes (8 h 20 m). The vials used were primarily Wheaton Scientific™ polyethylene anti-static LSC vials and also Research Products International™ glass LSC vials.

For analysis of the rainwater samples, the interface software used in CSU's laboratory is MikroWin™, which allows for specification of the counting parameters and output information. Adjustments were made within the software to specify a delay before count (dark adaptation time), count time, and specific wells (of the 40 available wells identified A01-E08). An image of the counting drawer is included in Figure 8. The output parameters of interest were imported and manipulated in an Excel spreadsheet with macros provided by the vendor. Some data analysis and graphs of the count per energy bin for each sample were available. Calculations of the figure of merit were prepared separately.



Figure 8: Counting drawer on CSU's LSC offering 40 sample wells, image shows drawer loaded for plastic/glass comparisons, 3 March 2014

A calibration standard tritium solution was used in the figure of merit calculation. This source was originally prepared by Eckert & Ziegler Analytics with the characteristics specified in Table 4. Dilutions of this standard solution were prepared in the lab over a range of low added activities between 1 Bq/L and 440 Bq.L.

Table 4: Calibration standard specifications for Eckert & Ziegler tritium standard used at CSU

H-3 Standard Specifications	
Original activity concentration	$\frac{9308 \text{ Bq}}{500.28 \text{ mL}} = 18.61 \frac{\text{Bq}}{\text{mL}}$ 18,610 Bq/L
Uncertainty associated with standard solution activity (per Eckert & Ziegler calibration info)	20%
Date of calibration	5 December 2011
Activity correction (Dec 2011 – Feb 2014 approximation)	$A_t = A_0 \times e^{-\frac{\ln(2)}{4500 \text{ days}} \times t[\text{days}]}$ $A_t = 0.88 A_0$
Decay corrected activity concentration	16,410 Bq/L

Decision for Sample to Cocktail Ratio

The primary sample to cocktail ratio used to measure the rainwater samples was 8 mL of sample water to 12 mL of cocktail (described later as a ratio of 8:12). A brief literature comparison of sample:cocktail decisions is described in Table 5. Due to the polar nature of the water samples and the nonpolar nature of the cocktail, some turbulence was observed upon mixing. Adequate mixing was ensured, and the dark adaptation time allowed for light and mixing interference to settle out of the samples.

Table 5: Literature comparison of scintillation fluid to sample to determine most appropriate ratio

Source	Instrument	Scintillation Cocktail	Sample:Cocktail Ratio
Theodorsson [11]	LSC (general)	(general)	Conventional sample is 10 mL enriched water to 10 mL cocktail, suggests that sensitivity is improved using a lower water/scintillator ratio
Garbarino et al [27]	Perkin Elmer Quantulus	Not listed	Counted in polyethylene with 2 g sample, 6 g ultrapure water and 12 g scintillation
Zhilin et al 2010 [17]	Perkin Elmer	Ultima Gold™ F cocktail (for dried filters and organics)	Varied from 1:3 to 5:6, found that 1:2 was best for maximizing the counts
Tjahaja & Sukmabuana [6]	Specific LSC system and cocktail used are not listed – 2 mL prepared sample is added to 13 mL scintillator in a 20 mL vial		
Colorado State University	Hidex™ LSC	Ultima Gold™ LLT cocktail for measuring low level tritium in multiple water types	8:12 ratio is not as extreme as the 12:10 ratio suggested by the manufacturers of the cocktail but allows for a relatively large water volume

Investigation of Colorado Background and FOM Optimization

Background blanks were prepared using deionized water with the Ultima Gold™ LLT scintillation cocktail. 7 different blanks were prepared in plastic vials with an 8:12 sample to cocktail ratio, 1 blank was prepared in a plastic vial with a 7:14 sample to cocktail ratio, 1 blank was prepared in a glass vial with an 8:12 ratio, and 1 vial was prepared with scintillation cocktail only (0:20 sample to cocktail ratio) to investigate the difference in counts from the deionized water addition versus counts from the scintillation cocktail alone. These blank samples and trials are summarized in Table 6 and Table 7.

Table 6: Background blank preparations using deionized water and Ultima Gold™ LLT cocktail

Type	Vial	# of Samples	Sample:Cocktail Ratio (mL)
Deionized water blank	Plastic	1	7:14
	Glass	2	8:12
	Plastic	7	8:12
Cocktail only	Plastic	1	0:20

Table 7: Counts of background blanks indicating number of samples run for each count duration

Type	Vial	Sample:Cocktail Ratio (mL)	# of Samples	Count Time (hours)
Deionized water blank	Plastic	7:14	1	2
	Plastic	8:12	7	0.17, 0.25, 0.5, 1, 2, 5
	Plastic	8:12	4	3
	Plastic	8:12	2	8
	Plastic	8:12	1	12
	Glass	8:12	1	2 (duplicate)
	Glass	8:12	2	2
Cocktail only	Plastic	0:20	1	2, 5, 8, 8 (duplicate)

In order to count measurable levels of tritium in water for comparison, eight plastic standard activity concentrations were prepared using dilutions with deionized water of the Eckert & Zeigler standard tritium solution (see Table 4). The prepared, decay-corrected activity concentrations are illustrated in Figure 9. An additional tritium standard solution was prepared without dilution in a glass vial. This vial contained 8 mL of the Eckert & Ziegler standard in 12 mL of scintillation cocktail for an added activity of 16,200 Bq/L.

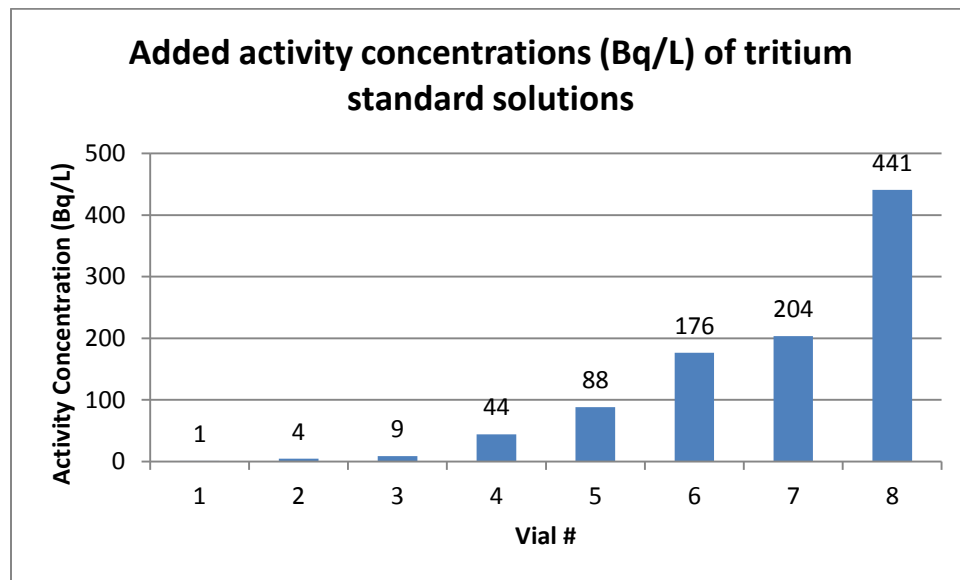


Figure 9: Activity concentration (Bq/L) of tritium standard solutions in deionized water based on calibration specifications

The standard spikes and background samples were initially run for 2 hours each to prepare an initial evaluation of the region of interest (ROI) necessary to optimize the figure of merit (FOM), which is a quantitative representation of the statistical quality of the data. To perform the FOM optimization, several extra columns were prepared in the output Excel document. Based on the counts within the ROI, a new CPM value for the optimization process (CPM_{opt}) was calculated by dividing the ROI beta double coincidence by the count time. Values were entered for the expected DPM for each of the standard spikes (DPM_{exp}). A counting efficiency for each spiked sample was estimated by dividing the CPM_{opt} by the DPM_{exp} of the spiked sample, which is the traditional method used to estimate detection efficiency in the absence of TDCR. This counting efficiency as a percentage is squared and divided by the average background counts to calculate an FOM according to Equation 9. An iterative procedure was used to narrow the ROI in order to maximize the FOM for each of the standard activities. The FOM optimization procedure was conducted three times: for plastic vials containing 8 mL deionized water and 12 mL scintillation cocktail, for glass vials containing 8 mL deionized water and 12 mL scintillation cocktail, and for the plastic vial containing scintillation cocktail only (20 mL).

Equation 9

$$\text{Figure of Merit} = \frac{\text{Efficiency (\%)}^2}{\text{Average Bkg CPM}}$$

Counting Rainwater Samples

The raw samples received from 23 NTN collection sites (42 unique samples) were prepared for counting without concentration. An aliquot of rainwater was added to an LSC vial and massed, and the scintillation cocktail was added to the vial via a volumetric dispensing

spout. The samples were inverted several times to achieve adequate mixing of sample water and LSC cocktail. Counts of the samples were taken with the Hidex™ LSC after allowing eight hours of dark adaptation time for each time that the drawer was opened. Outputs obtained from the LSC included total counts, count time, CPM, TDCR, and DPM calculations by the machine for the open window. These results were later restricted by setting the ROI in accordance with an optimized FOM, and the information described in Table 8 was recorded for each sample.

Table 8: Recorded information for rainwater samples allowing for a calculation of tritium activity

Sample results for optimized FOM (ROI _β channels restricted based on vial and sample:cocktail ratio)						
ROI _β Triple	ROI _β Double	TDCR _{opt}	CPM _{opt}	DPM _{opt}	DPM _{opt} /g	Activity Conc. (Bq/L)
Triple incidence counts	Double incidence counts	$\frac{\text{ROI}_{\beta} \text{ Triple}}{\text{ROI}_{\beta} \text{ Double}}$	$\frac{\text{ROI}_{\beta} \text{ Double}}{\text{Count time [m]}}$	$\frac{\text{CPM}_{\text{opt}}}{\text{TDCR}_{\text{opt}}}$	$\frac{\text{DPM}_{\text{opt}}}{\text{Sample mass [g]}}$	$\frac{\text{DPM}_{\text{opt}}}{\text{Sample mass [g]}} \times \frac{1 \text{ g}}{\text{mL}} \times \frac{1000 \text{ mL}}{\text{L}} \times \frac{\text{min}}{60 \text{ s}}$

A total of 36 samples were prepared in plastic vials with an 8:10 sample to cocktail ratio. 10 duplicates of NTN site samples were prepared in glass vials in order to visually evaluate the color of the samples and conduct comparisons with the plastic vial results. These prepared vials were counted on the LSC for varying times, with all 36 plastic samples counted for 2 hours, and a selection of 16 samples counted for 5 hours. Samples from the site SCO3, located onsite at SRNL, were treated with particular interest due to their expected higher levels of rainwater tritium concentration. These two samples in plastic vials were counted for 8 hours in addition to the 2 and 5 hour counts. Additionally, an initial selection of 6 rainwater samples was prepared in plastic vials with a 7:14 sample to cocktail ratio. These samples were counted for 2 hours.

Appendix A provides a list of which specific NTN site samples were included in each counting period.

Manipulation of Sample, Background, & Standard Data

After preparing the vials and performing multiple counts, the data were organized into a single spreadsheet. The LSC output could be used to graph individual count spectra, and to display the results of counting for the open window as well as within the region of interest. The total counts of background and sample water were compared using a t-test to check for the significance of differences between the data. Data from the spiked standard solutions were compared to the calculated added amount of tritium activity based on the calibration of the tritium source.

Because the variation in the minimum detectable activity is of critical importance to the motivation of this study, the MDA of the detector was investigated both theoretically and empirically. Using the observed average background count rate for samples in plastic vials, a curve was created illustrating the effect of varying count time on the minimum detectable activity concentration. Variations in vial type (glass or plastic) and sample to cocktail ratio were also investigated. Additionally, the total counts and detected activities were compared spatially and temporally for the NTN site samples with respect to the MDA. The TDCR (as a measure of counting efficiency) was investigated as it varied noticeably between the backgrounds, samples, and standard solutions.

Investigation of Feasibility of Various Concentration Methods

Tritium has an atomic mass of three times that of normal hydrogen, which gives it a lower vapor pressure and higher boiling point. Many studies have endeavored to quantify the

potential for isotopic separation of tritium from protium (^1H) and deuterium (^2H) for the purpose of sample concentration. Because of the increased number of counts achieved in counting concentrated samples, the potential for tritium concentration is of particular interest for rainwater samples, which can have a significant surplus amount available after analysis for its chemical constituents. However, sample concentration introduces significant sources of uncertainty that must be quantified and evaluated. A literature comparison of concentration methods was conducted, and the implications of such concentration efforts were explored specifically in the context of analyzing rainwater samples with a high throughput.

RESULTS

Window Optimization and FOM Calculations

Background counts were taken of blank vials prepared with 8 mL deionized water with 12 mL scintillation cocktail. This section describes the results of optimizing the window for plastic and glass vials and the cocktail-only plastic vial. The following example illustrates the effect of the open window on the result. For the seven background blanks prepared in plastic vials and counted over a 2 hour count time, the LSC recorded an open window average background of 38 CPM and found an average background of 51 DPM using individual sample TDCRs, which would be read as an average background activity of 0.86 Bq per sample and an average background activity concentration of 110 Bq/L H₂O. Due to the contribution from sources other than tritium and noise, these open window results do not accurately reflect the tritium content of the water.

Another critical consideration reflected in the remainder of the results was the effect of interference from background signals in addition to those present in the water samples. This effect was illustrated in the counts of the cocktail-only plastic vial. The results of these counts are summarized in Table 9. The “activity” recorded by the LSC for this vial likely contributed to the elevated tritium concentration readings in the rest of the results.

Table 9: Counts of cocktail-only sample in a plastic vial, ROI 15-185

Count Time (min)	TDCR _{opt}	CPM _{opt}	DPM _{opt}	“Activity” (Bq)
120	0.267	10.22	38.30	0.64
300	0.250	9.55	38.19	0.64
480	0.235	10.48	44.59	0.74
480	0.219	11.91	54.43	0.91

A window optimization was conducted using the 2 hour plastic vial background data to maximize the FOM for spiked tritium standards of three activities, also counted for 2 hours each. For 3.53 Bq (441 Bq/L), the FOM was at a maximum for an ROI of channels 20-179. For 1.63 Bq (204 Bq/L) the FOM was at a maximum for an ROI of 18-185. For 1.41 Bq (176 Bq/L), an ROI of 20-180 maximized the FOM. An optimized window of channels 20-180 was selected for uniformity in the subsequent analyses of samples with the same 8:12 sample to cocktail ratio in plastic vials. For the restricted ROI, new results were obtained for background levels based on the 2 hour counts. Within the ROI, a new TDCR was calculated by direct division of the ROI $_{\beta}$ triple counts to ROI $_{\beta}$ double counts. The detector saw an average of 9.7 CPM $_{opt}$ with an average TDCR $_{opt}$ of 0.260, and an average of 37.2 DPM $_{opt}$ was observed by averaging the individual DPM $_{opt}$ calculations. This DPM $_{opt}$ is equivalent to an average background tritium activity of 0.62 Bq in each sample or 77 Bq/L H₂O.

The second FOM optimization procedure was conducted for samples in glass vials with the same 8:12 sample to cocktail ratio. One background sample in a glass vial was read twice for 2 hours each and another glass background was run once for 2 hours, providing three background counts to average. A standard tritium solution was prepared in a glass vial with an activity concentration of 16,222 Bq/L (DPM $_{exp}$ = 7787) for the window optimization. For the three background samples in glass compared to the glass standard, the FOM was at a maximum at an ROI of channels 16-154. The window optimization for glass resulted in the data in Table 10.

Table 10: Results of 2 hr counts of deionized water blank in glass vial, 8:12 ratio, ROI 16-154

Count Time	# of samples	Avg. CPM $_{opt}$	Avg. TDCR $_{opt}$	Avg. DPM $_{opt}$	Avg. Activity (Bq)	Avg. Activity Conc. (Bq/L)
2 h	3	18.6	0.179	103.7	1.73	217

A third series of “blank” counts was conducted using scintillation cocktail-only in a plastic vial. Because the lack of sample water represents a significant change in the background preparation methodology, a separate window optimization procedure was conducted. Counts of the cocktail only vial were conducted over durations of 2 hrs, 5 hrs, and 8 hrs, and these values were compared to standard solution counts of 2 hours each. For 3.53 Bq (441 Bq/L), the FOM was at a maximum for an ROI of channels 16-179. For 1.63 Bq (204 Bq/L) the FOM was at a maximum for an ROI of 14-185. For 1.41 Bq (176 Bq/L), an ROI of 15-191 maximized the FOM. The average ROI channel for the cocktail only background would be channels 15-185.

For an ROI of 15-185, the results in Table 11 were obtained. A background “activity” for the cocktail-only sample averaged over the various count durations was calculated by averaging the DPM_{opt} for these counts and dividing by 60 seconds per minute. This value was subtracted from the activity seen by the detector for the three highest activity spiked samples, and the net activity concentration was compared to the added tritium concentration according to the calibration certificate. Each of the three counts varied from the expected activity by less than 10%.

Table 11: Comparison of results for cocktail only background and three highest activity tritium standard spikes, ROI 15-185

Count Time (h)	Sample	CPM _{opt}	TDCR _{opt}	DPM _{opt}	Sample Activity	Net Activity Concentration
2	Cocktail Only	10.22	0.267	38.30	Average Background DPM _{opt} /60 = 0.73 Bq	N/A
5	Cocktail Only	9.55	0.250	38.19		
8	Cocktail Only	10.48	0.235	44.59		
8	Cocktail Only (duplicate)	11.91	0.219	54.43		
2	176 Bq/L	39.32	0.328	119.91	2.00 Bq	159 Bq/L (9.7% off)
2	204 Bq/L	45.99	0.335	137.28	2.29 Bq	195 Bq/L (4.4% off)
2	441 Bq/L	83.50	0.350	238.84	3.98 Bq	406 Bq/L (7.9% off)

An optimized ROI was not calculated for samples prepared in 2012 with 7 mL of sample with 14 mL of scintillation cocktail, and the counts of these samples were not included in the MDA calculations below. However, because the changing ratio of sample water to scintillation cocktail would be likely to affect the counting efficiency, it would be advisable to adjust the window to obtain results for these counts.

LSC Outputs

Due to the large number of counts conducted and the similarity of most of these counts, individual spectra have not been generated. Figure 10 and Figure 11 offer illustrative graphs of the spectra obtained on the LSC for background counts and the majority of the NTN site sample counts, respectively. The general curve shape indicates contributions from low energy betas as well as higher energy contributions. The large variation due to noise is also evident in these low level spectra.

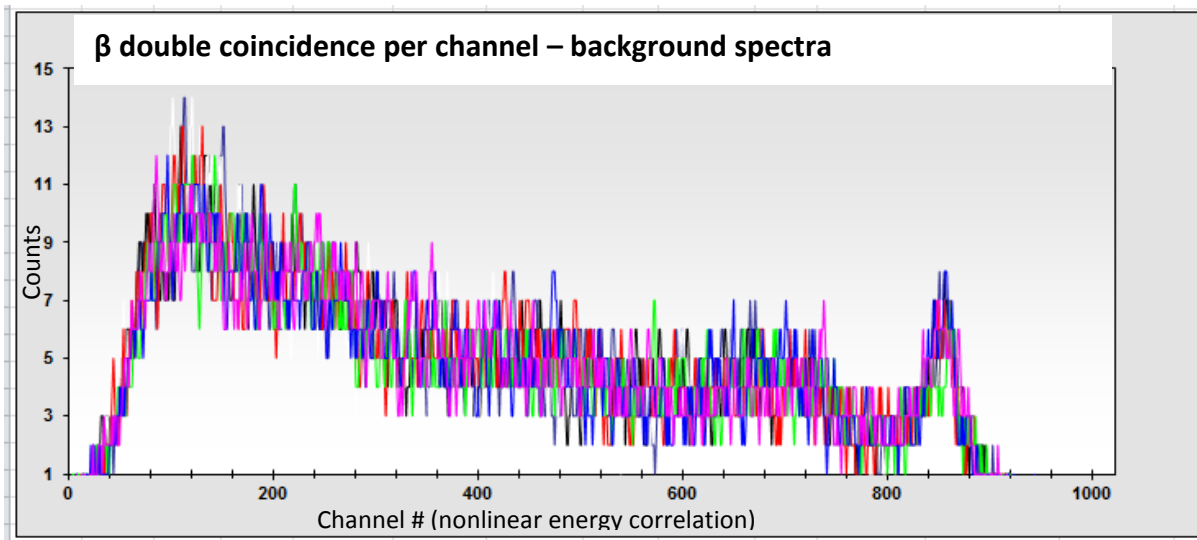


Figure 10: LSC spectra: double coincidence beta counts per channel forming spectra of eight background blanks (each color represents a sample). 8 mL deionized water in 12 mL scintillation cocktail run for 2 hours

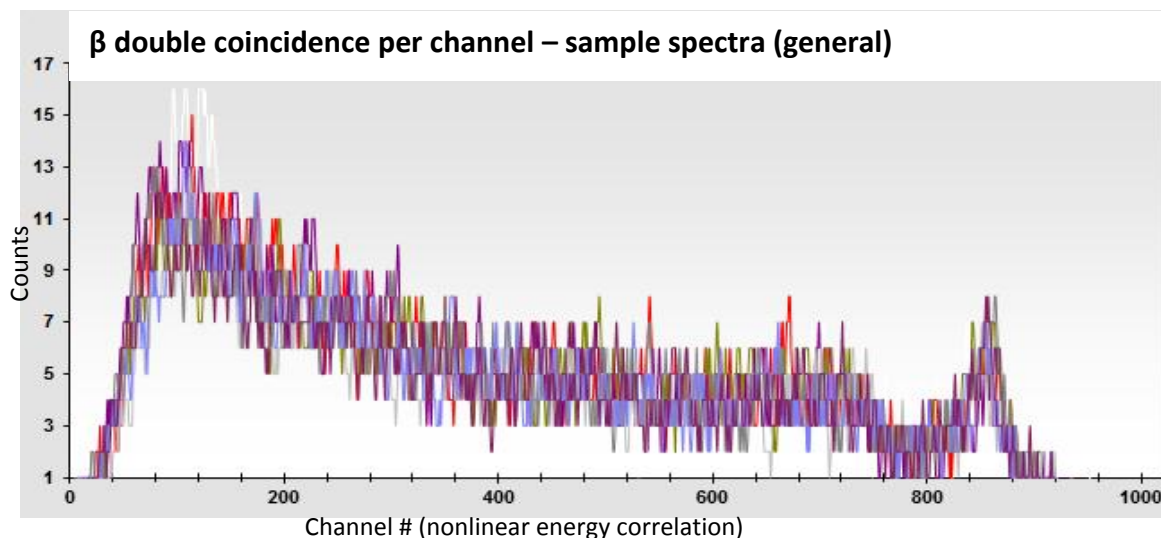


Figure 11: LSC spectra: double coincidence beta counts per channel for ten selected NTN site rainwater samples (each color represents a sample). 8 mL sample to 12 mL cocktail run for 2 hours

The total counts of background and sample water were compared using a t-test to check for the significance of differences between the data. For the 2 hour, 5 hour, and 8 hour counts, the calculated t statistic was greater than the t critical one-tail value, indicating that the difference between the means of the background counts and the means of the sample counts was statistically significant for all three counts. This result indicates that some positive tritium activity was present in at least some of the rainwater samples, raising the mean value for the rainwater above background. The p-value of these tests increased greatly as the number of samples run decreased, such that the 8 hour counts (two backgrounds and two samples) had limited confidence ($p = 0.31$). Full results of these statistical tests are included in Appendix B.

The spectra formed by counts of standards spiked with the tritium standard solution were more defined. Figure 12 illustrates the spectra generated by counts of the eight standard solutions with energy bins instead of channel numbers on the x-axis. The 8 mL tritium standard run in a glass vial was not diluted, so the peak was very clearly defined and the effects of background contributions were not apparent (see Figure 13). Figure 14 illustrates the change observed in the

glass standard spectrum when results are viewed with energy bins rather than channel numbers on the x-axis. Figure 15 and Figure 16 have the y-axis represented by a log scale to show the high activity peak and the contribution of noise at higher energies on the same graph, and the plastic standard solutions are included in Figure 16.

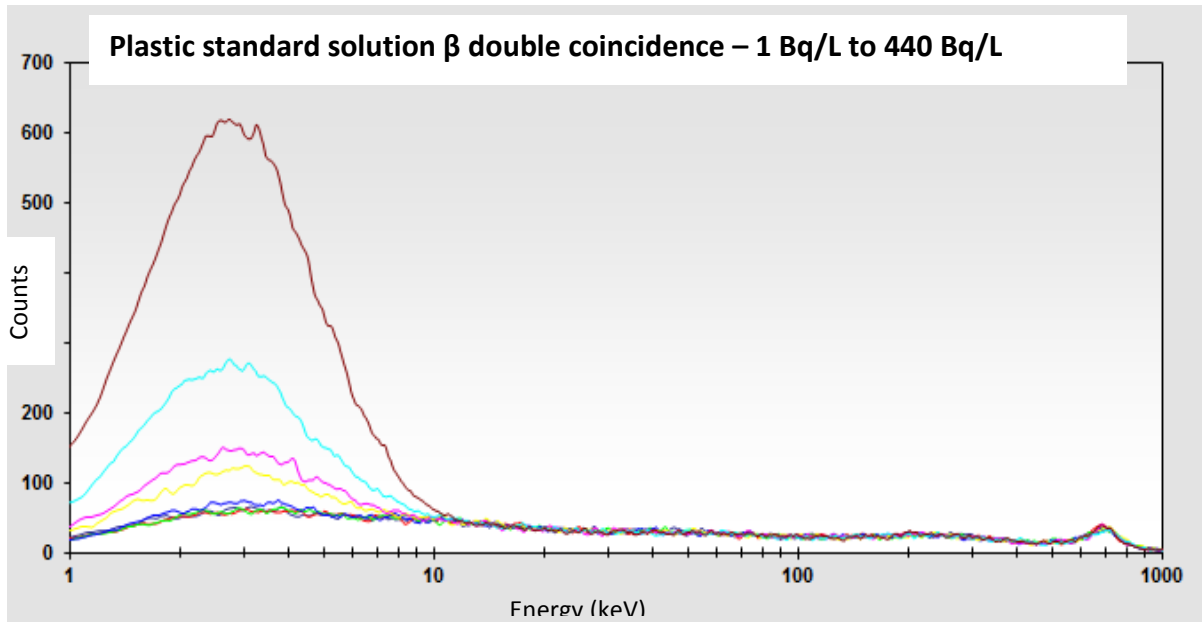


Figure 12: Energy spectra of tritium standards in plastic vials: number of counts per energy bin versus energy (keV) for 8 mL standard solution and 12 mL scintillation, levels vary from background (water only) to 440 Bq/L

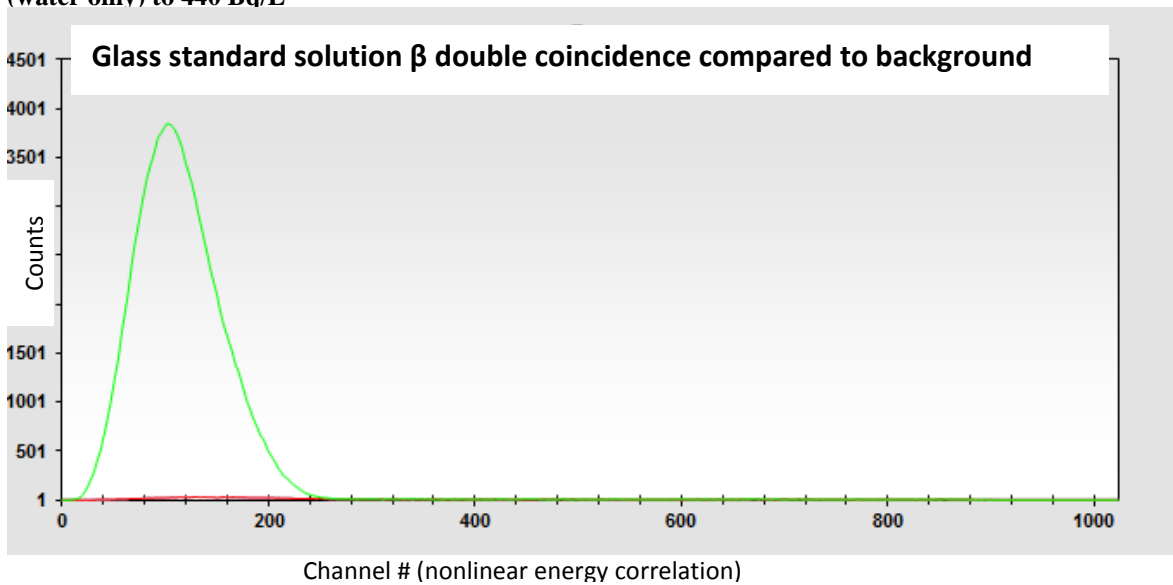


Figure 13: Energy spectra of standard solution in glass vial (green) and glass background samples (red): counts per channel versus channel number

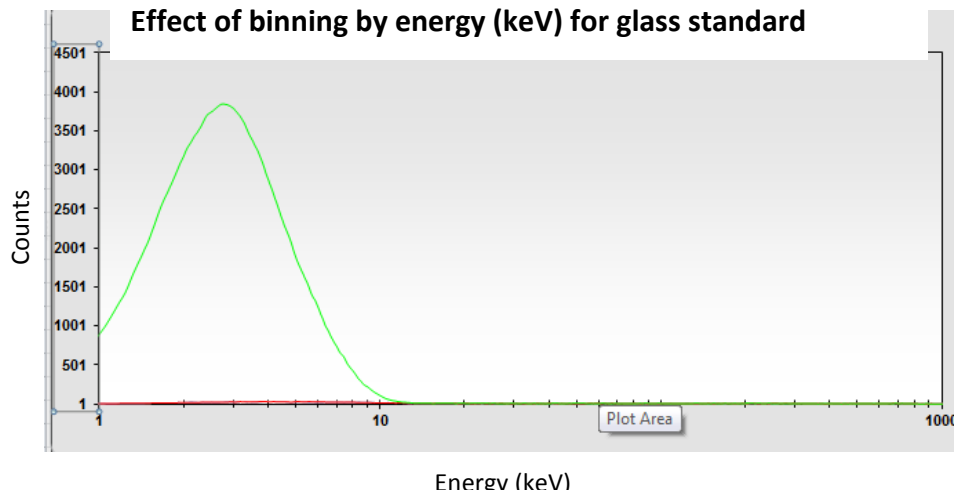


Figure 14: Energy spectra of standard solution in glass vial (green) and glass background samples (red): counts per energy bin versus energy (keV)

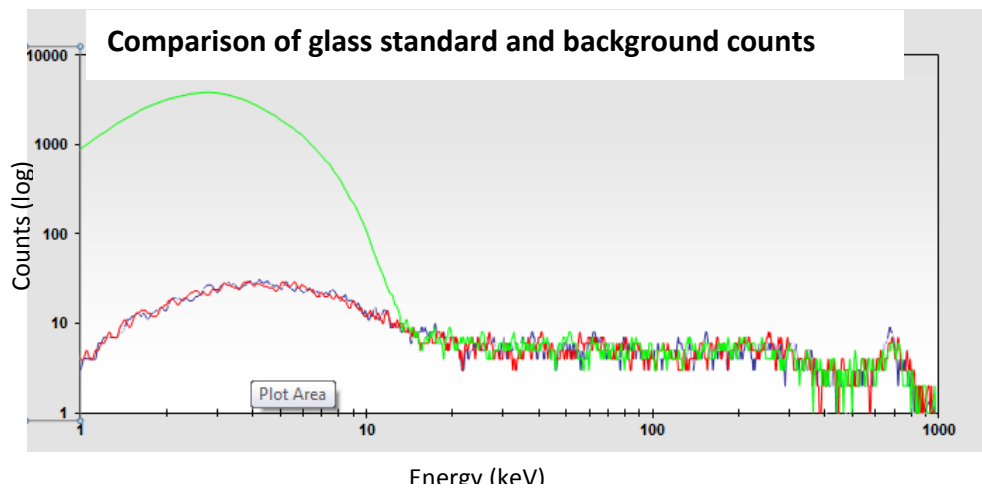


Figure 15: Energy spectra of standard solution in glass vial (green) and glass background samples: counts per energy bin (log) versus energy (keV)

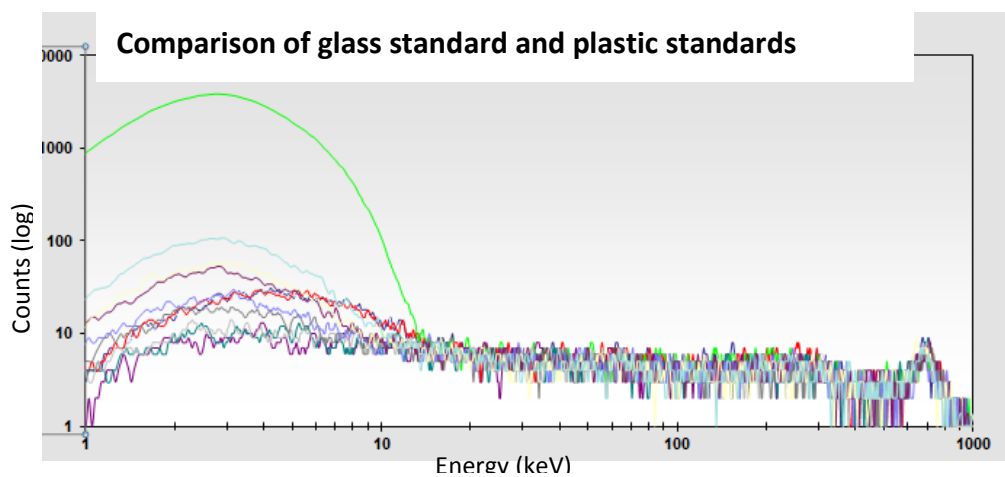


Figure 16: Energy spectra of standard solution in glass vial (green) and standard solutions in plastic vials: counts per energy bin (log) versus energy (keV),

Counting Prepared Tritium Standards

Standard samples were run with deionized water and spikes of tritium standard solution. The samples in plastic vials contained an aliquot of standard solution diluted into 8 mL of deionized water and 12 mL of scintillation cocktail, and the glass vial sample contained 8 mL of the tritium standard solution without dilution and 12 mL of scintillation cocktail.

Several observations were made with counts of the tritium standard solutions. Using an ROI of 20-180, the counts of the standard solutions were used to calculate a net activity concentration that the detector observed in each of the samples using the average background activity observed for each of the count durations. This calculated net activity concentration was plotted against the actual activity concentration of each standard solution (as described by the certificate of calibration) to investigate their correlation (see Figure 17). This plot exhibits a linear trend with a slope very close to one and a high R^2 value, indicating that the counts of the standard solutions are good estimators of the actual activity concentrations over the range of added activity concentrations. The negative y-intercept of this trend line indicates that the majority of the sample counts underestimate the true activity of the sample, or that the standard solution contains less activity than described by its calibration certificate. The difference could also be explained by uncertainty in the linear fit of the trendline.

A paired comparison of the data from the spiked standard solutions and the actual activity of the samples returned the results in Figure 18. The percent error by which the measured net activity differed from the calibration value decreased with increasing concentration, and was less than 40% for all samples greater than 44 Bq/L.

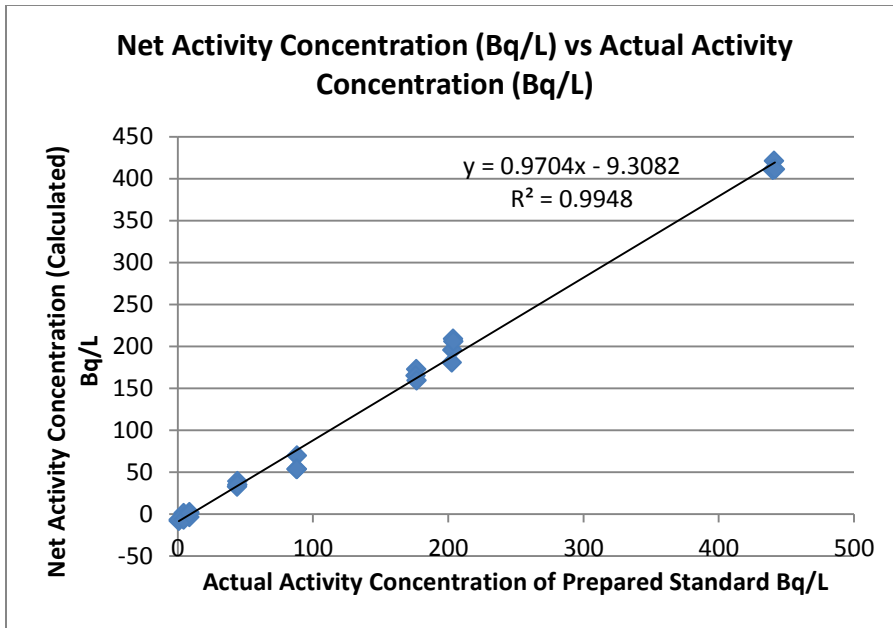


Figure 17: Calculated net activity concentration of standard solutions plotted against actual activity concentration per the calibration certificate, plastic vials, 8:12 ratio, ROI 20-180

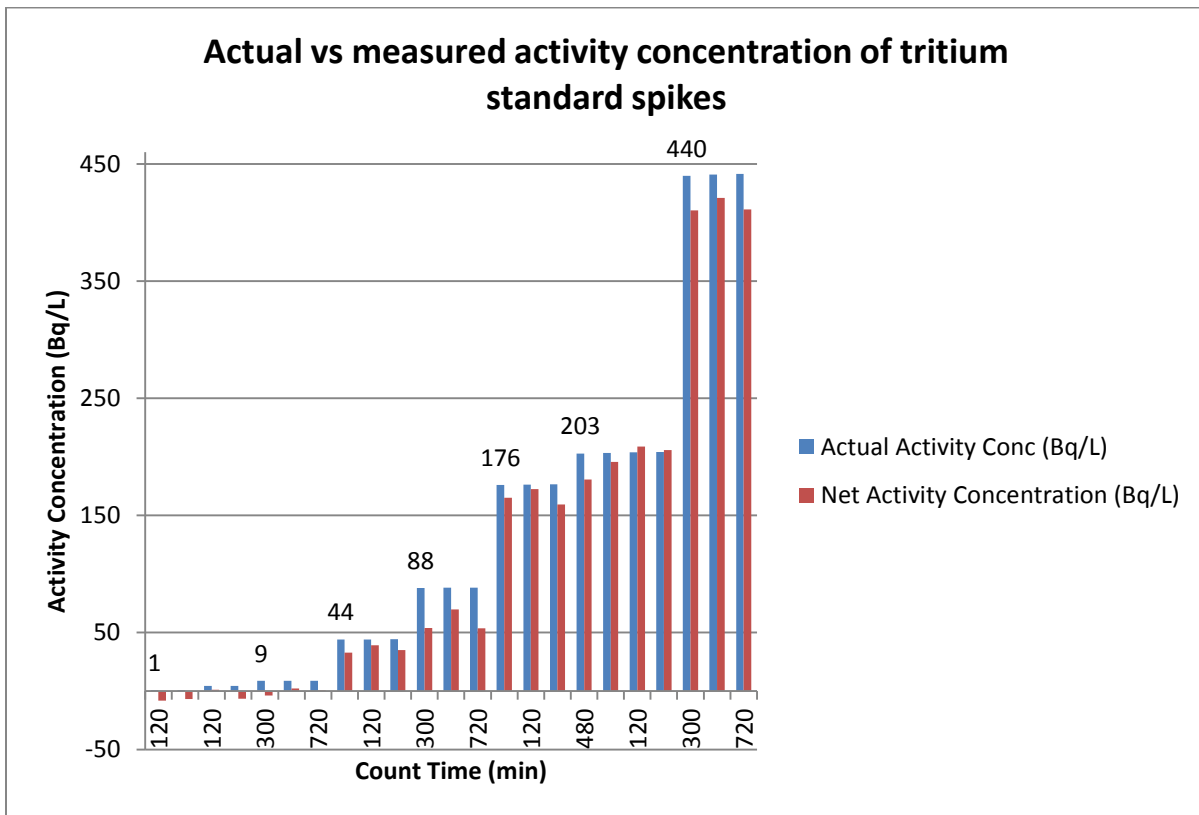


Figure 18: Paired comparison of measured and actual tritium activities for various count durations, plastic vials, 8:12 ratio, ROI 20-180

For the 2 hour count of the glass standard solution, the net measured activity concentration exceeded the actual activity concentration based on the calibration certificate. In this count, the net activity concentration measured for the glass standard was 17,858 Bq/L compared to the 16,222 Bq/L estimated to be in the standard sample, an overestimation by 10%.

TDCR Investigation & Comparisons

The TDCR (as a measure of counting efficiency) was investigated as it varied noticeably between the standard solutions, backgrounds, and NTN site samples.

For the standard solution preparations, two estimations of efficiency are possible: the traditional use of the $TDCR_{opt}$ and a direct division of the CPM_{opt} by the DPM_{exp} for each added activity concentration. Figure 19 illustrates the TDCR estimation of detection efficiency. The TDCR method produced results that could be fit with a power function trend line with a high R^2 value. The TDCR efficiency varies from 26% to 36% with an average of 31% for the standards.

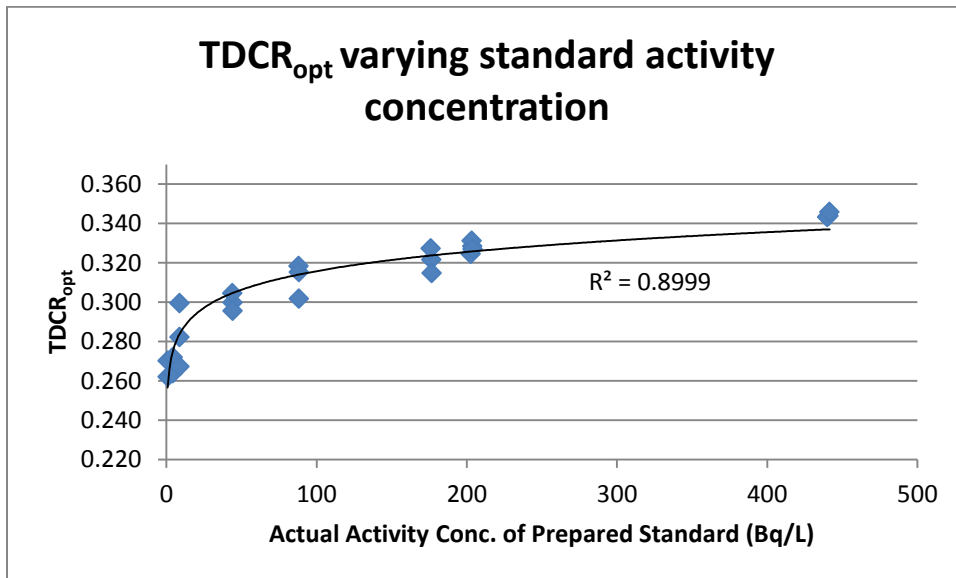


Figure 19: Counting efficiency estimated by TDCR for varying standard activity concentration, plastic vials, 8:12 ratio, ROI 20-180

Figure 20 was prepared by subtracting the overall average background count rate (ROI 20-180) of 10.5 CPM from the CPM_{opt} values recorded for the standards to obtain a new net CPM_{opt} . This net value was divided by the expected DPM for each standard activity concentration. The curve produced values for direct counting efficiency which vary between 25% and 36% for samples of activity concentrations greater than 44 Bq/L. Below activity concentrations of 44 Bq/L, the recorded count rate was very low or indistinguishable from the background count rate, resulting in negative calculated counting efficiencies.

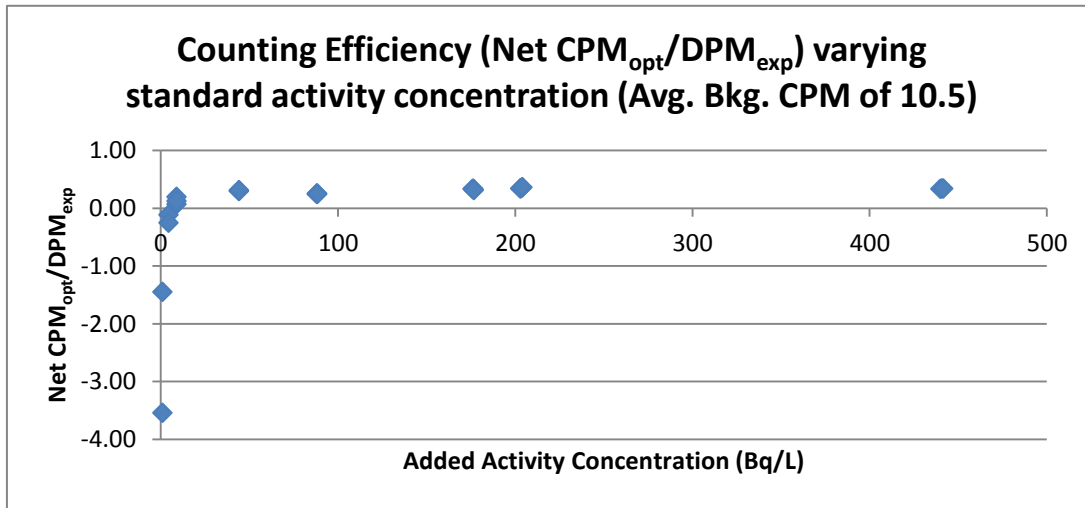


Figure 20: Counting efficiency estimated by dividing net CPM_{opt} by DPM_{exp} for added standard activity concentrations between 1 Bq/L and 440 Bq/L, plastic vials, 8:12 ratio, ROI 20-180

A plot of the curves for TDCR and direct counting efficiency on the same axes was generated for visual comparison in Figure 21. For the low added activity standards (< 44 Bq/L), the values for counting efficiency were considered to poorly reflect the actual counting efficiency of the LSC based on the elevated background count level and difficulty distinguishing low levels of added activity statistically. This inaccuracy reflects a minimum detectable activity of the device, which is investigated in a later section.

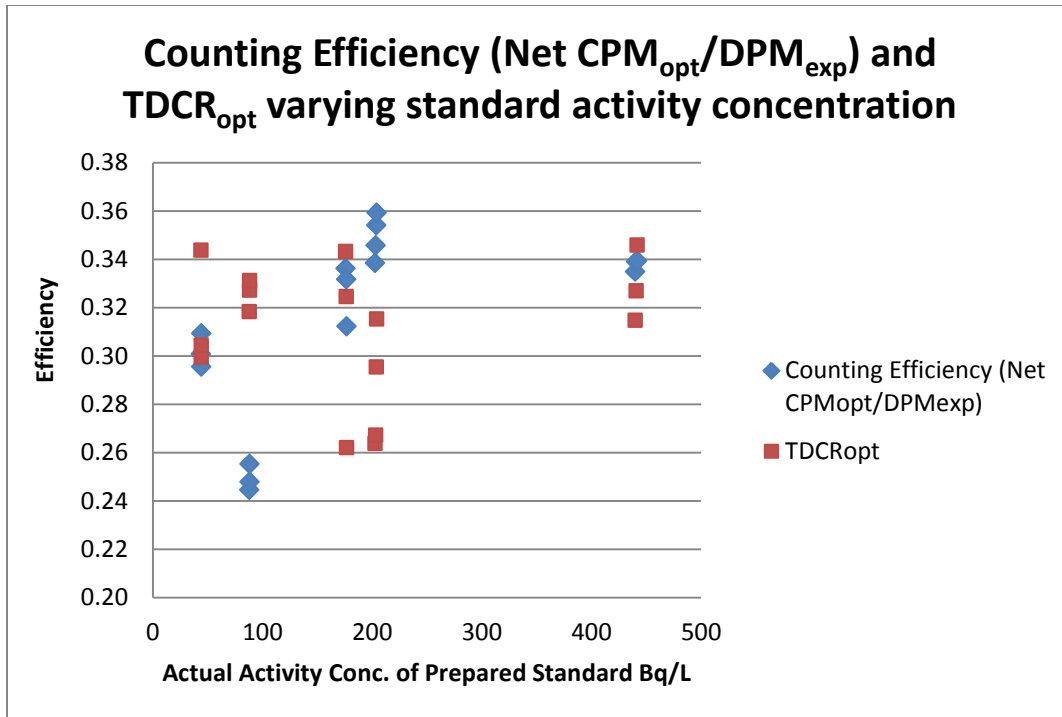


Figure 21: Two methods of estimating counting efficiency for varying activity concentration, plastic vials, 8:12 ratio, ROI 20-180

Of particular interest for the TDCR comparison was the difference between NTN site sample counts and background counts. For example, the TDCR values for 2 hour counts of plastic vials containing an 8:12 sample to cocktail ratio were compared (36 counts of NTN site samples were compared to 7 background blanks.) An F-test to compare the sample variances found an F statistic greater than the F critical value ($P = 0.007$), indicating that the variances of the two populations were unequal. Then, a t-test assuming unequal variances was conducted, and the t statistic was more extreme than the t-critical value ($P = 0.004$ two-tail), indicating that the means of the two populations were unequal. The full text of these analyses is included in Appendix C. This relationship justifies the use of the sample TDCR later in the estimation of minimum detectable activities for the samples. The average TDCR_{opt} for runs of background blanks, standards, NTN site samples, and glass vial samples are summarized in Figure 22.

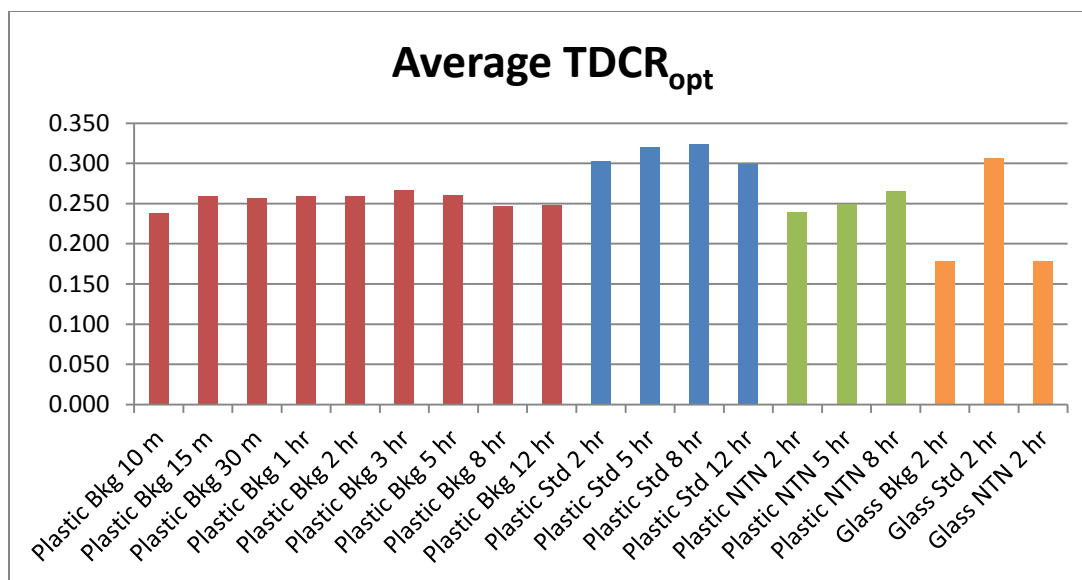


Figure 22: Average efficiency as estimated by TDCR_{opt} for plastic background, standard and sample runs and glass runs, plastic ROI 20-180, glass ROI 16-154

Statistical Considerations of Low Level Counting (Theoretical)

Because the variation in the minimum detectable activity is of critical importance to the motivation of this study, the MDA of the detector was investigated both theoretically and empirically. The MDA of the detector is also dependent on the count time allocation between background and sample counts. A theoretical exploration was conducted to investigate the variation in required count time and procedures necessary to achieve theoretical LLDs and MDAs. One option is to run the background and samples for equal times and run a background sample on intervals between runs of sample water. For example, the CAL or a related laboratory could run one background sample for every 50 rainwater samples. For equal count times, the MDA decreases with increasing count time (see Figure 23), increases with increasing background count/count rate (see Figure 24), and decreases with decreasing efficiency or increasing quench (see Figure 25). The reference equations for the MDA were graphed to estimate the feasibility of counting rainwater samples based on approximate background values.

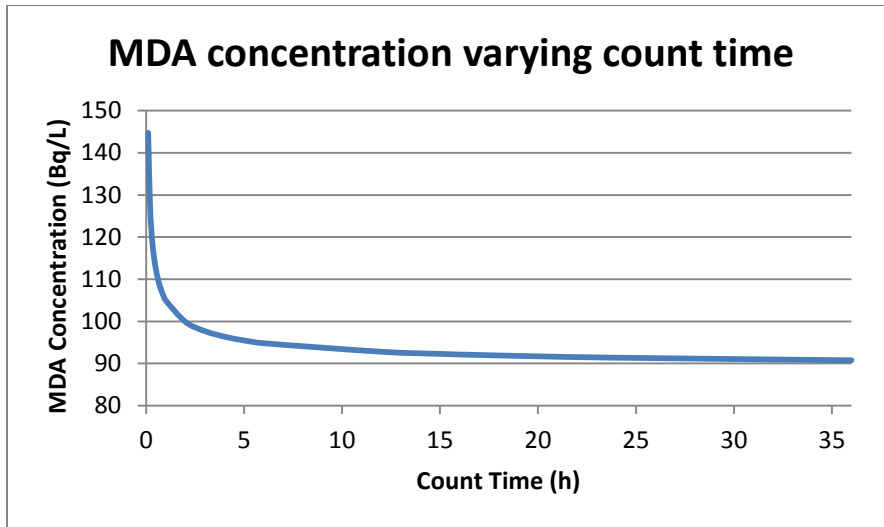


Figure 23: MDA concentration varying count time for constant background count rate (10.3 CPM) and efficiency (24.3%) [21]

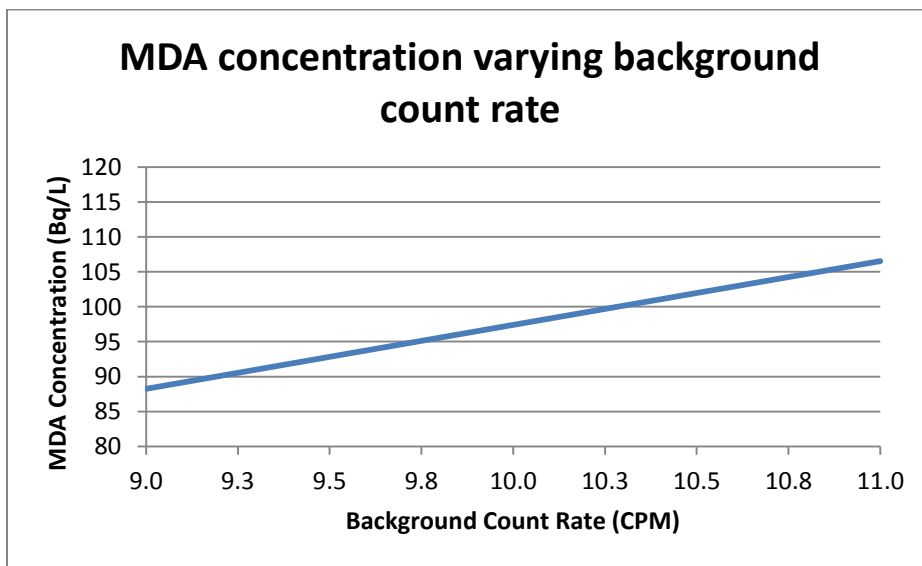


Figure 24: MDA concentration varying background count rate (CPM) for a constant count duration (2 h) and efficiency (24.3%) [21]

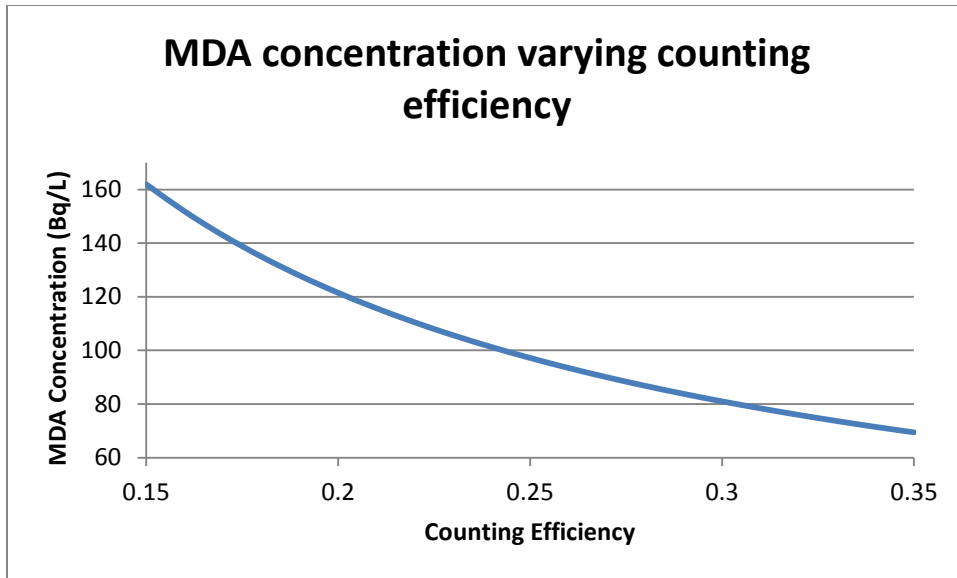


Figure 25: MDA concentration varying counting efficiency for a constant background count rate (10.3 CPM) and count duration (2 h) [21]

An alternative method for calculating the MDA and LLD associated with a low level counting device considers that samples and background counts can be taken for different time periods. It was considered that the CAL or other researchers could count background samples overnight (12 hours) while running the samples during the day. The equation for MDA in Turner [21] does not depend on information about the sample count time. However, one other reference text [23] provides an LLD equation that varies with differing sample and background count times (see Equation 4 in the Introduction):

$$LLD = 3.29 \sqrt{r_b t_g \left(1 + \frac{t_g}{t_b}\right) + 3}$$

For a constant *background* count time, increasing the *sample* count time results in a nearly linear increase in the total counts necessary to detect a radioactive source above background based on this equation (see Figure 26). As the sample count time increases with respect to the

background count time, the ratio $\frac{t_g}{t_b}$ increases, causing the resultant increase in the lower limit of detection.

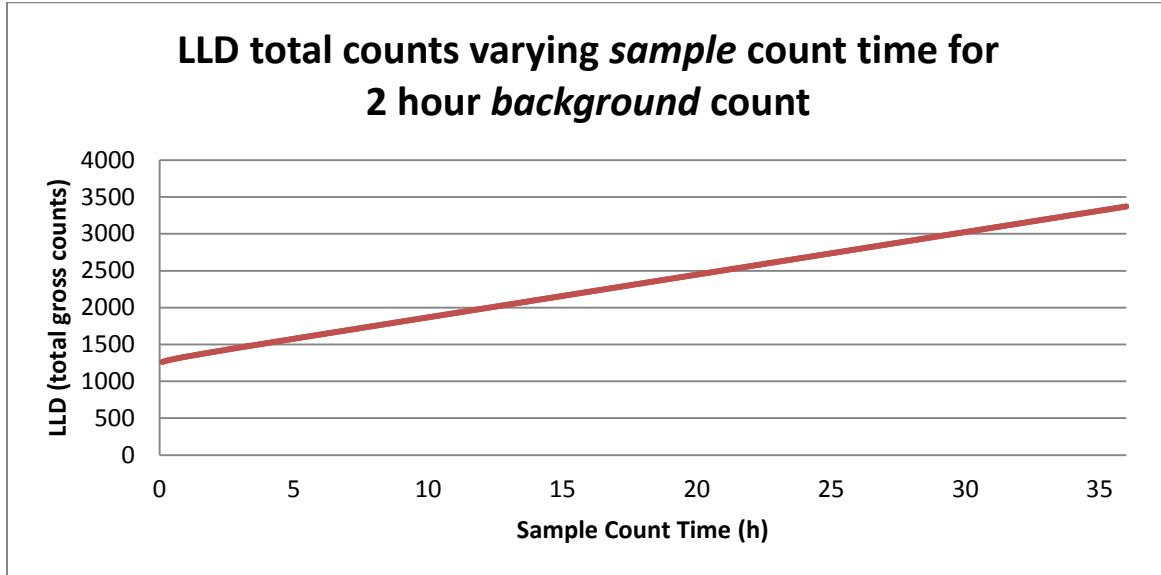


Figure 26: LLD total counts varying sample count time for constant background count time (2 h), background count rate (10.3 CPM), and counting efficiency (24.3%) [23]

However, the minimum detectable activity for the counter depends on the relationship between the LLD and the total sample count time as well as the detection efficiency (ϵ), according to Equation 10.

Equation 10

$$MDA = \frac{3.29 \sqrt{r_b t_g \left(1 + \frac{t_g}{t_b}\right) + 3}}{t_g \times \frac{60 \text{ s}}{\text{min}} \times \epsilon}$$

When division by the sample count time in seconds and the counting efficiency (24.3%) is used to find a minimum detectable activity using this equation, the MDA concentration behaves similarly to the graph for equal background and sample count times. This relationship is shown in Figure 27.

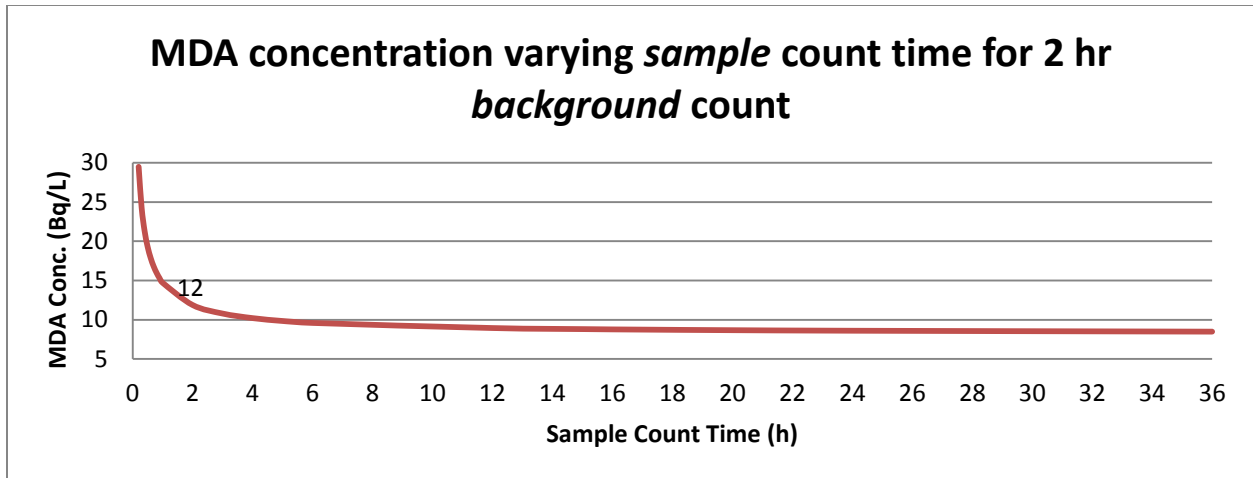


Figure 27: MDA concentration for varying sample count time with respect to a constant (2 h) background count time for background count rate of 10.3 CPM and efficiency of 24.3%

Alternatively, changing the background count time for a constant sample count time of 2 hours (based on Equation 10) results in the net MDA curve featured in Figure 28. The LLD for this curve decreases due to the decreasing ratio $\frac{t_g}{t_b}$, and the sample count time is constant. Thus, the decreasing trend in the LLD is reflected by the net MDA.

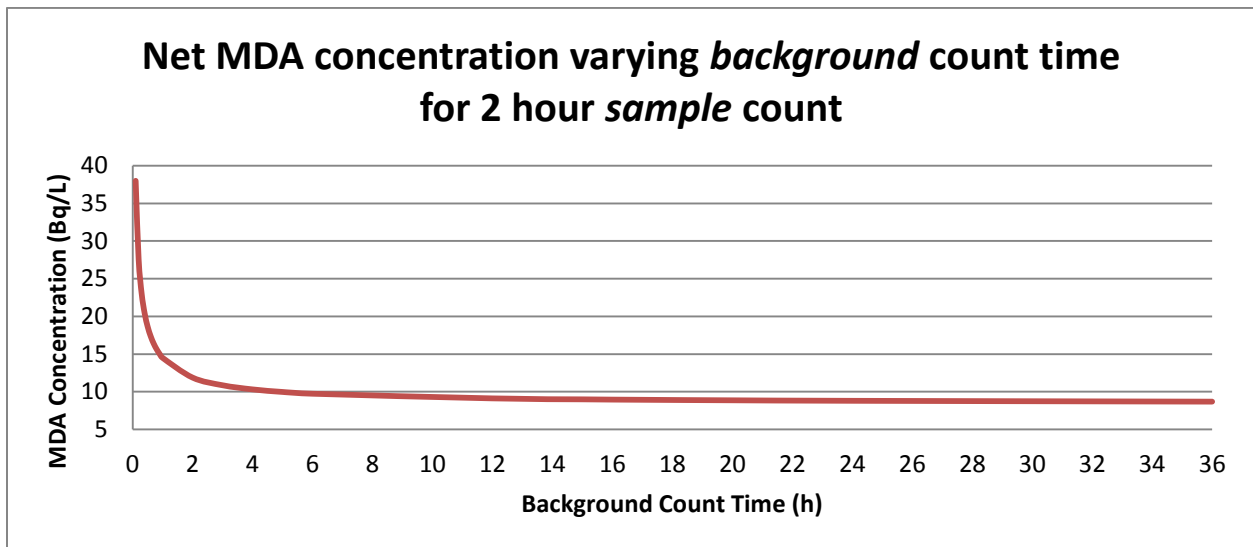


Figure 28: Net MDA concentration for varying background count time with a constant background count rate (10.3 CPM), efficiency (24.3%) and a constant (2 h) sample count time

These theoretical results reflect changes primarily in the derivations of the MDA equation, such that the equation that depends on both sample and background count times fluctuates with changes in multiple variables. For the empirical analyses conducted, equal count times were used for the background blanks and rainwater samples.

Statistical Considerations of Low Level Counting (Empirical)

Counts of background samples for 10 minutes through 12 hours yielded the result in Figure 29. Based on these background counts, the equations in the three reference texts were used to calculate corresponding MDA values for the different count times. The average values obtained for each count time by each of the three methods are included in Figure 30. Due to the higher recorded count rate for the two samples run for 480 minutes, the MDA estimation for this count duration is elevated above those for 300 and 720 minutes in Figure 30. However, the overall results of this comparison indicate that the estimated MDAs differ very little based on the equation used or rounding of the equation terms.

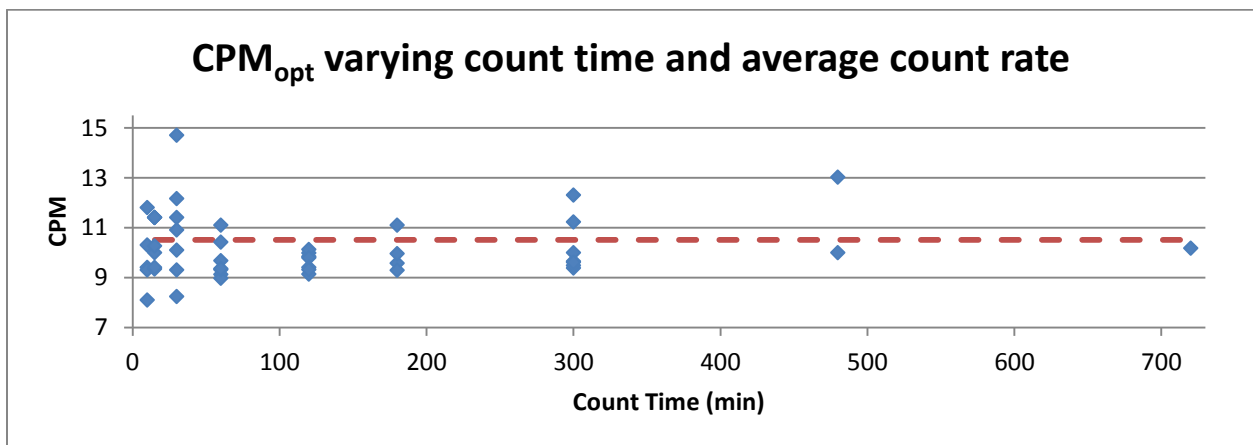


Figure 29: Measurements of CPM_{opt} for background blanks over count durations of 10 m to 12 h (blue) and overall average CPM_{opt} (dashed red line)

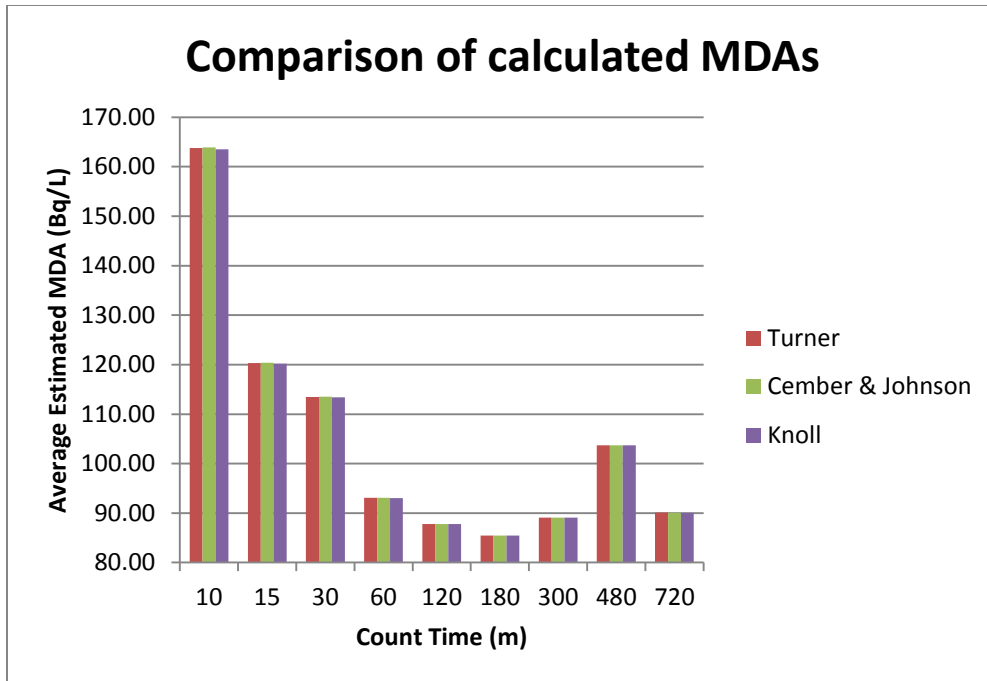


Figure 30: Average MDA calculations for counts of various durations, plastic vials, 8:12 sample to cocktail ratio, Turner [21], Cember and Johnson [23], Knoll [18]. The graph illustrates similarity between the calculation and various simplifications. Note: the high MDA value calculated for 420 minutes reflects the high recorded count rate for the 2 blanks counted for that duration.

After counting the background blanks over count durations between 10 m and 12 h, the average information in Table 12 was obtained.

Table 12: Average values for background counts of various durations, plastic vials, 8:12 sample to cocktail ratio, ROI 20-180

Time	# of samples	CPM _{opt}	TDCR _{opt}	DPM _{opt}	Activity (Bq)	Activity Conc. (Bq/L)
10m	7	12.11	0.239	55.06	0.92	114
15m	7	10.46	0.260	41.87	0.70	87
30m	7	10.97	0.257	43.33	0.72	90
1h	7	9.70	0.260	37.48	0.62	78
2h	7	9.65	0.260	37.21	0.62	77
3h	4	9.98	0.267	37.41	0.62	77
5h	7	10.24	0.260	39.65	0.66	82
8h	2	11.51	0.247	47.23	0.79	98
12h	1	10.18	0.248	40.99	0.68	85
Overall Average		10.51	0.256	42.19	0.70	87

The background measurements and averages were used to investigate the relationship of the NTN site sample counts to the MDAs in a later section. One example of counting the background and sample values for equal times was performed with the 2 hour counts of backgrounds and samples. Using the 2 hour observed average background count rate for plastic vials and the 2 hour observed average $TDCR_{opt}$ for NTN site samples, a curve was created illustrating the effect of varying count time on the MDA concentration (see Figure 31). In this curve, the count over each time interval is extrapolated by assuming an average background of 9.65 CPM for the duration of the counting period, and the efficiency is assumed to be 0.239. From the curve, the MDA for 2 hour counts of the sample is 96 Bq/L above background.

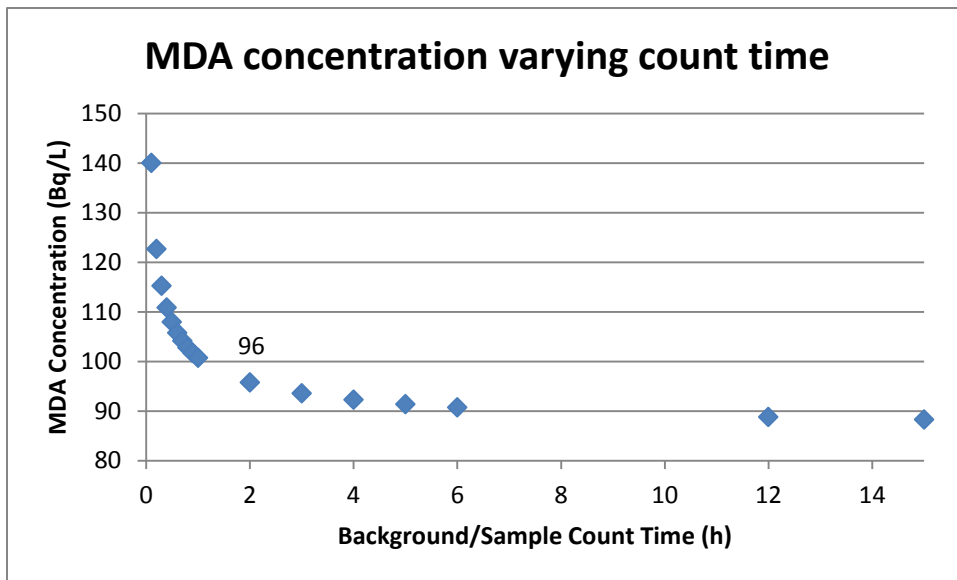


Figure 31: MDA concentration for equal count times of background and sample based on extrapolation of average background count rate (9.65 CPM) and NTN site sample efficiency (23.9%) from 2 hr counts, plastic, 8:12 ratio, ROI 20-180

For comparison, the backgrounds run in glass vials for 2 hours had a higher count rate (averaging 18.6 CPM), and the NTN site samples had an average $TDCR_{opt}$ of 0.179. The calculated MDA for a 2 hour count of backgrounds and samples in glass vials was then 238 Bq/L above background.

Using the background count data, individual calculations were performed to estimate MDAs for various background count durations. These results were plotted against a curve of the MDA generated using the theoretical equation and the overall average background CPM_{opt} (10.5 CPM) and sample overall average $TDCR_{opt}$ (0.243). This plot is included in Figure 32 and simplified in Figure 33.

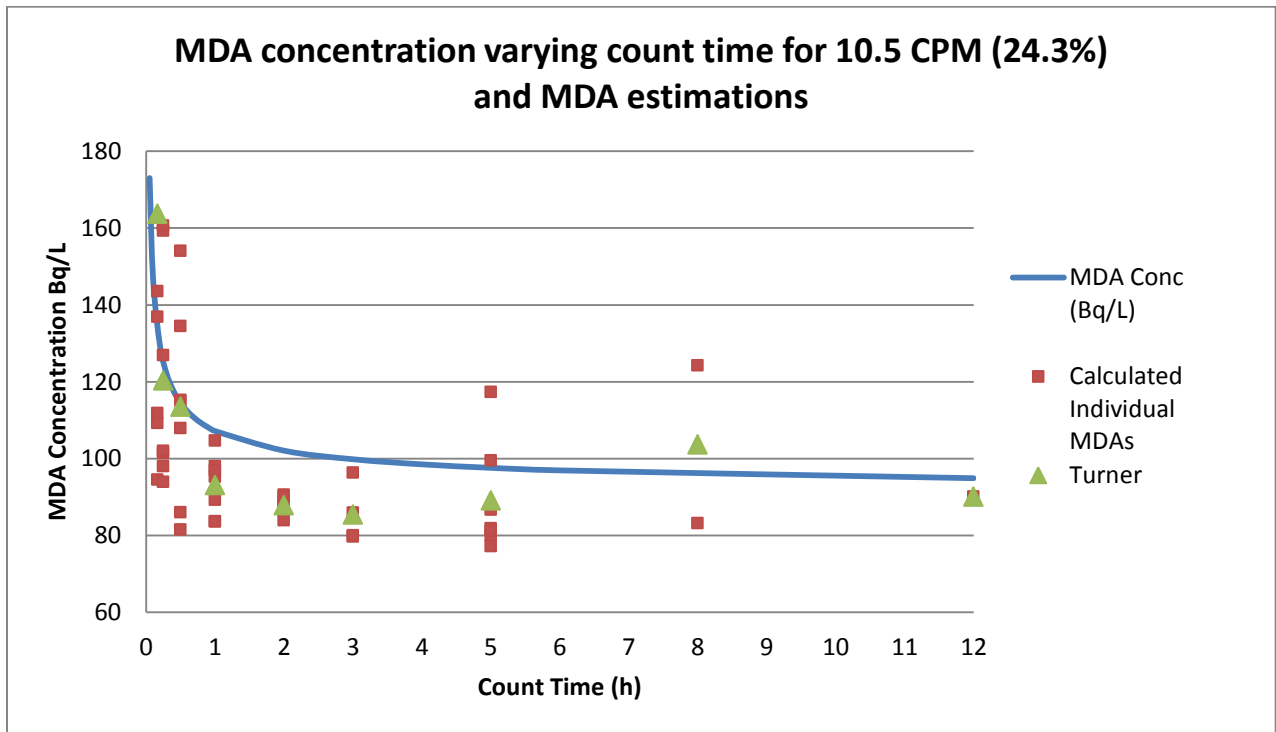


Figure 32: MDA estimations based on individual background counts, average MDA estimations, and theoretical curve of MDA using overall average background of 10.5 CPM and 24.3% efficiency

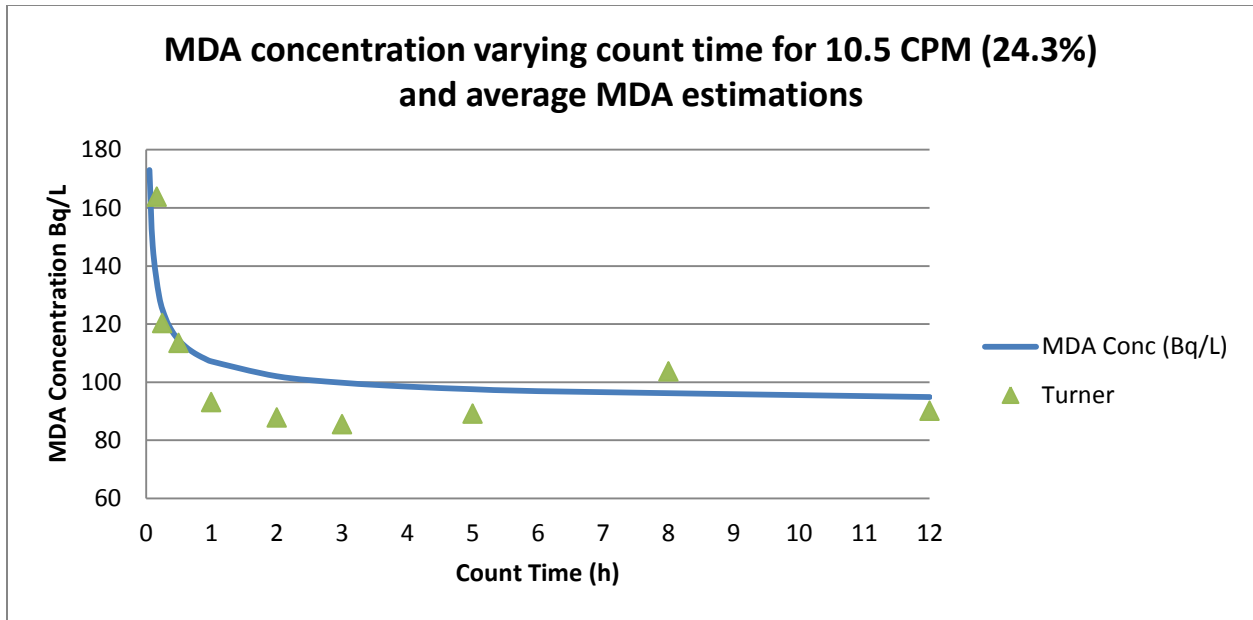


Figure 33: Average MDA estimations and theoretical curve of MDA using overall average background of 10.5 CPM and 24.3% efficiency

Quench Considerations with Rainwater Samples

It was observed that storage of the original Nalgene™ collection bottles resulted in yellowing of the bottles over the duration of storage. While this yellowing did not have a visible effect on the clarity of the rainwater, a comparison of samples based on the coloring of the storage/transportation containers was conducted. Because discoloration of the sample water over time would increase color quench and decrease efficiency of the sample count, the $TDCR_{opt}$ values for 2 hour counts of the samples in plastic vials were compared based on a subjective evaluation of bottle coloring (see Figure 34). The 95% confidence intervals for the means of the three color categories did not diverge enough to indicate a significant contribution to quench from bottle discoloration. Full results of these statistical comparisons are available in Appendix D.

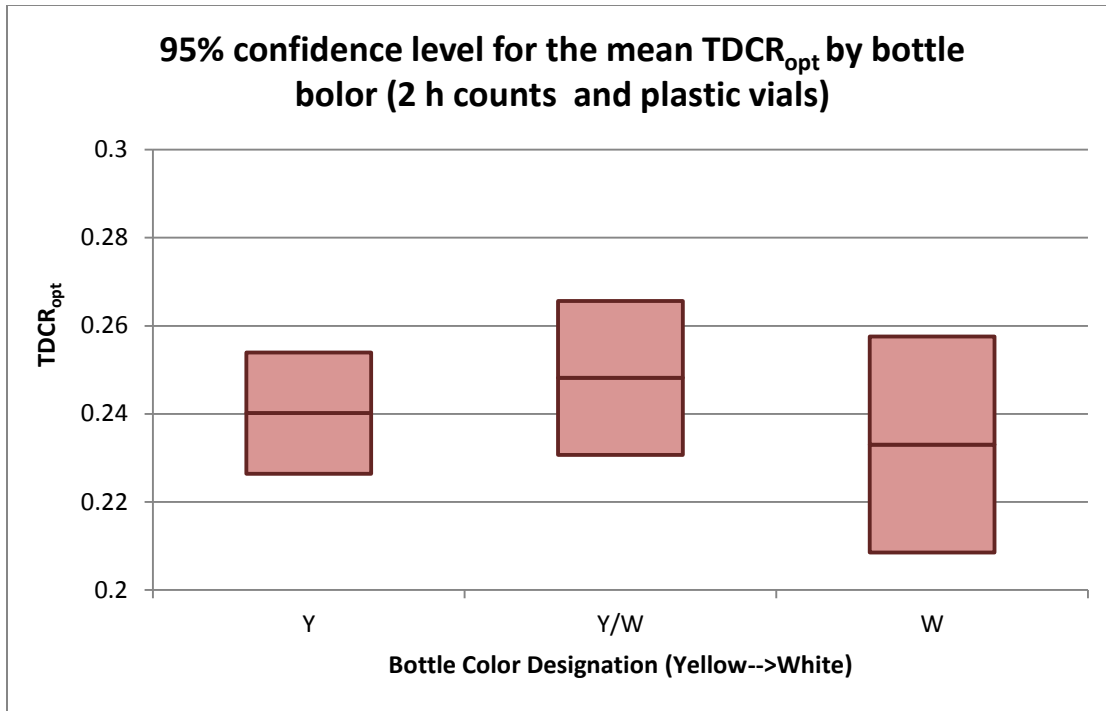


Figure 34: Comparison of efficiency values for NTN site samples in plastic vials based on classification by storage bottle color

Effectiveness of Counting Rainwater Samples for 3H

CSU's LSC allows for an estimation of the absolute radioactivity contained within a water sample regardless of background levels. From this perspective, a graph of the absolute activities returns the result in Figure 35. The 2 hour counts of samples in plastic vials used the average background count rate from the 2 hour counts (9.65 CPM) and the average NTN sample TDCR from the 2 hour counts (0.239) for a 2 hour MDA estimate of 96 Bq/L.

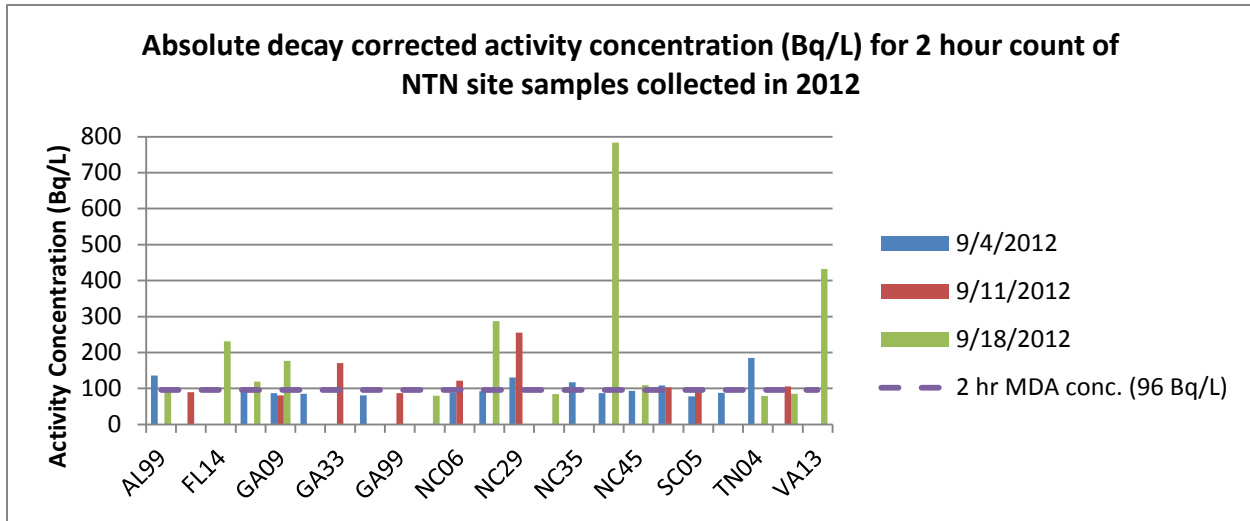


Figure 35: Decay corrected absolute activity concentration measured in NTN site samples (plastic, 2 hour counts, ROI 20-180)

However, subtraction of background values to obtain a net activity concentration and the use of an MDA value based on background counts of deionized water altered the significance of the results dramatically. Because of the high background counts recorded for deionized water blanks and the low expected activity of the NTN site samples, the results of counting the water samples were generally limited in usefulness. Figure 36, Figure 37, and Figure 38 compare the sample counts with the estimated MDA for the sample count parameters for 2 hour counts of plastic vials, 5 hour counts of plastic vials, and 2 hour counts of glass vials, respectively. For net counts of samples counted for 2 hours, the lower limit of detection above background was equivalent to an excess activity of 12 Bq/L. The 5 hour counts of samples in plastic vials used average background count rate from the 5 hour counts (10.24 CPM) and the average NTN sample TDCR from the 5 hour counts (0.249) for a 5 hour net MDA estimate of 12 Bq/L. The 2 hour counts of samples in glass vials used average background count rate of 18.6 CPM for glass and the average NTN sample TDCR for glass (0.179) for a 2 hour glass vial net MDA estimate of 22 Bq/L.

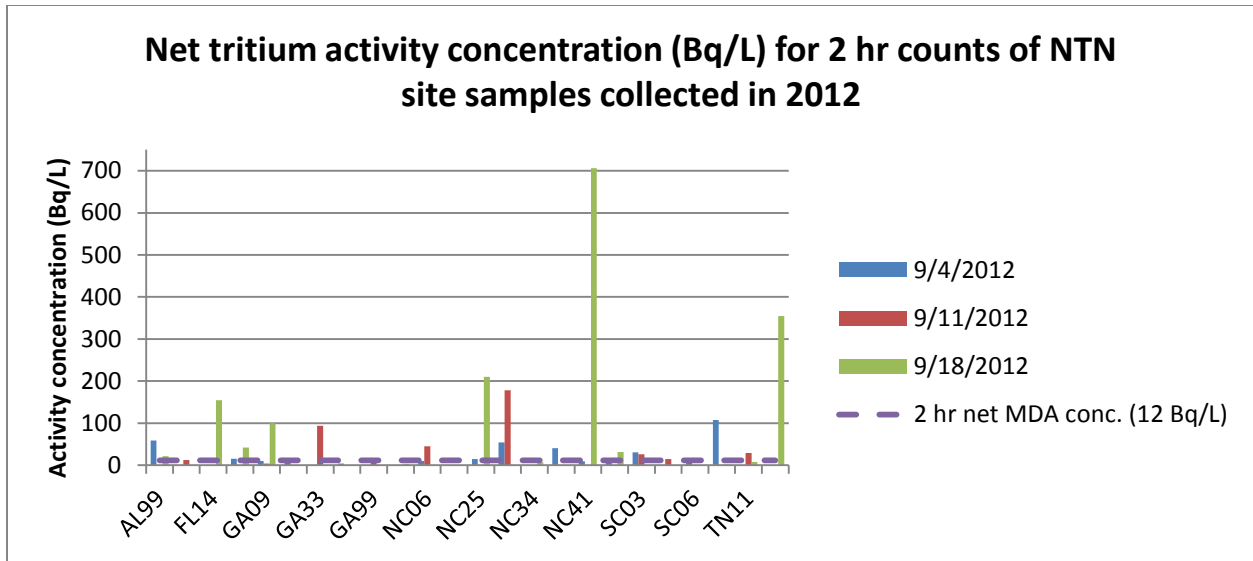


Figure 36: Comparison of NTN site sample net activities and net MDA estimated using 2 hour average background count rate (9.65 CPM) and 2 hour average sample efficiency (23.9%), plastic vials, ROI 20-180

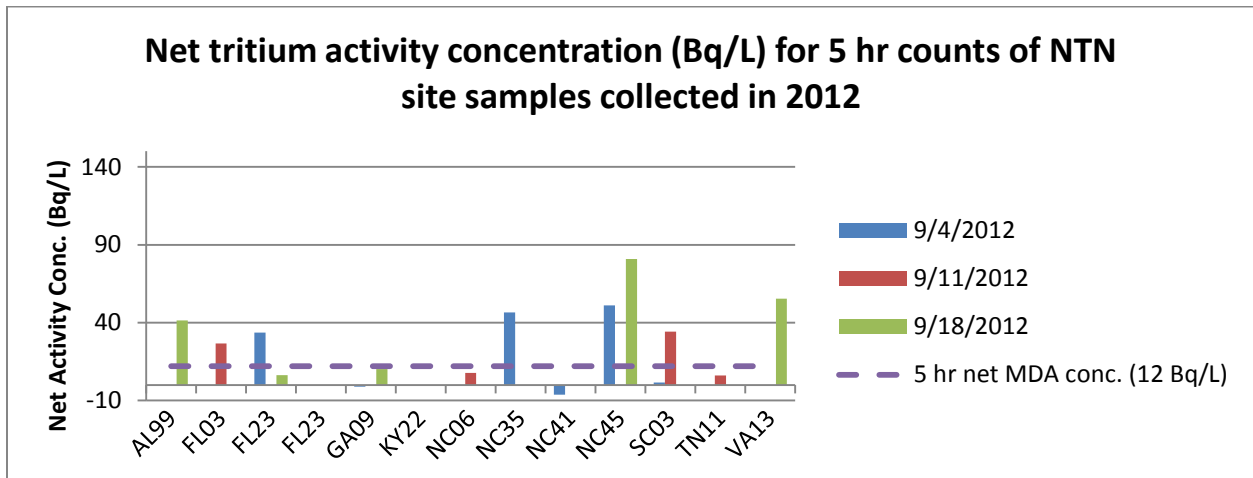


Figure 37: Comparison of NTN site sample net activities and net MDA estimated using 5 hour average background count rate (10.2 CPM) and 5 hour average sample efficiency (24.9%), plastic vials, ROI 20-180

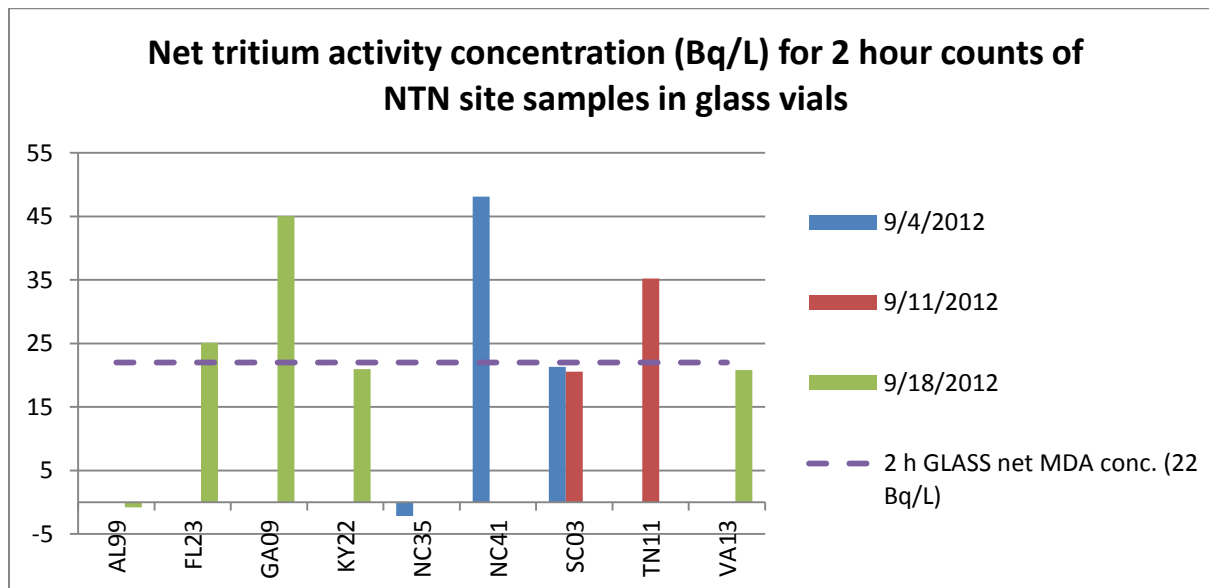


Figure 38: Comparison of NTN site sample net activities and net MDA estimated using 2 hour average background count rate (18.6 CPM) and 2 hour average sample efficiency (17.9%), glass vials, ROI 16-154

Based on the background count levels recorded on CSU's LSC, it would not be possible to count samples with an activity of the levels characterized by other studies as near background (0.6-1.2 Bq/L). The MDA curve levels off for longer count times, so it would not be necessary or practical to count samples for longer than approximately 3 hours, as increases in count duration beyond 3 hours do little to decrease the MDA.

Investigation of Concentration Methods

A large body of research contains information about concentration of samples of tritium for environmental analyses. The primary method used is electrolytic distillation, which can effectively and reproducibly increase the tritium concentration of water samples for analysis in an LSC. This method typically involves distillation of a sample volume of > 100 mL and can

result in a tritium concentration factor of approximately 10. Table 13 includes information about the procedures used and evaluated in the literature.

Concentration of samples on a silica gel column was suggested as a potential concentration method. Collection of tritium on a silica gel is useful for air samples containing water vapor because the gel serves as a desiccant and will take water out of air. The samples can be back-corrected for the total air volume. This procedure is not effective for tritium in water because the process cannot take water out of water. Water samples will saturate the column without increasing the tritium concentration.

Table 13: Literature comparison of tritium concentration methods

Study	Method	Comment
EPA Method 906.0 [7]	100 mL aliquot of sample treated with NaOH and KMnO ₄ , distillation, collection of middle fraction (to limit early/late product interference), LSC Deep well sources for background	Alkaline treatment prevents other radionuclides from being distilled as well, permanganate oxidizes trace organics (reducing quench)
Theodorsson [11]	Electrolytic enrichment based on probability that H ₂ is released at the cathode being 25-35 times higher than for HT, highest separation factor for a cathode of Fe and an anode of stainless steel or Ni	Recommends electrolyzing samples to <10 mL then adding dead water to achieve 10 mL volume desired, recommends continuous/batch filling of cells
Bogen & Welford [10]	Acknowledgements mention electrolytic enrichment	Found in NYC 13 Bq/L: 1971 7.8 Bq/L: 1972 7.4 Bq/L: 1973
Tjahaja & Sukmabuana [6]	Distillation to obtain free water tritium, 13 mL cocktail:2 mL sample, counted 1 hour Distilled at 70°C to near dryness, use KMnO ₄ and activated carbon to decompose and adsorb organic impurities	Air samples: silica gel for water absorption or molecular sieve (aluminosilicate (zeolite))
Jakiel et al [8]	Distillation with 10 mL aliquot of distillate with 10 mL cocktail counted for two 50-min periods, corrected for background 5 CPM, adjusted for detector efficiency 25% determined by counting NIST standards	Detection limit of 7.4 Bq/L (200 pCi/L) with uncertainty of 2σ of 7.4 Bq/L for values below 74 Bq/L
Jakiel et al [8]	Electrolytic distillation – 100 mL sample made basic with 0.8 g sodium peroxide, cell placed in an ice bath until volume is reduced to 13 mL, 10 mL distillate mixed with cocktail and counted for two 500 minute periods	“More sensitive detection” concentration factor of 6.5 detection limit is 0.37 Bq/L (10 pCi/L) with uncertainty 0.37 Bq/L (10 pCi/L)
Muranaka and Shima [28]	Describes 2 categories of tritium enrichment by electrolysis: alkaline electrolyte and solid polymer electrolytic (SPE) film which carries H ⁺ ions from the anode to the cathode (OH ⁻ is moved in alkaline electrolysis)	SPE film removes the need for pH adjustment Volume reduction of 10x results in a tritium enrichment of 7.2x

	Current of 50 A for large volumes (200-800 mL) and 20 A for smaller volumes (80-200 mL)	
Environment Agency [29]	Alkaline distillation: 75 mL sample, 1 g sodium carbonate, reject initial distillate fraction (20 mL), collect 30 mL of distillate, 1 h dark adapt and 500 min count, 10 mL distillate add 10 mL cocktail	
GA Rad Report [30]	Distillation - to remove interferences and ensure constant quench, simple distillations on water samples Electrolytic enrichment to preferentially liberate normal hydrogen, enrichment factor up to 10 Non-distilled - 10 mL of sample with 10 mL LS cocktail (filtering cloudy samples), automatic quench correction, Electrolytic distillation using Fe-Ni electrodes cooled to 2+/-2 degrees C, (electrolysis favors the decomposition of protonated water rather than isotopic water?), 100 g distilled sample and 0.5 g Na ₂ O ₂ as electrolyte, current constant at 4.5 A and gradually decreased to 1.5 A, liquid final volume of water 6 g, 900 min count, counting window 50-150 channels	gives MDCs of 3.7 Bq/L? (table does not specify methodology used)
Garbarino et al [27]	Enrichment in Ostlund-type glass cells (Ostlund and Werner, 1962), says error in measured concentration is about 3-4%	Mean enrichment factor of 13,
Michel [31]	Electrolytic enrichment Distillations carried out before and after the electrolytic enrichment, both distillations made to dryness to avoid isotopic fractionation 330 mL sample water with 2.5 g NaOH, applied voltage of 2.2-2.7 V with max current 10 A and cooling bath 4-8 degrees C Polyethylene vials and 10 mL cocktail with 10 mL sample	Found enrichment factor of 10 based on LSC

DISCUSSION

Characterization of Background or Near-Background Samples

The proposed use of NTN site samples to generate an environmental monitoring program for radionuclides would attempt to characterize very low level tritium concentrations in rainwater. Such a program would require close attention to the type of blanks used to differentiate meaningful tritium concentrations from background. For the purpose of this paper, the NTN site samples were compared to deionized water used in CSU's analytical laboratory. This deionized water is useful as a background in the majority of studies, but it is not controlled or adjusted for the presence of tritium. The high background activity levels recorded and the subsequently high calculated MDAs could be a factor of potentially elevated background tritium rates in CSU's deionized water. In the context of a broad monitoring program, variation in tritium concentrations even in prepared water would interfere with the sensitivity of the results. An alternative to this system of background measurement would be to obtain water samples that are depleted in their tritium content. This extremely low background water can be obtained via collection from an aquifer system unaffected by tritium deposition [24] or by using "old" water that has been stored until the tritium has decayed away. The use of tritium-depleted water for blanks would dramatically alter all of the MDA calculations, and might bring the values down to more reasonable numbers with respect to the concentrations that the program is attempting to measure (on the order of 1 Bq/L). The overall average background count rate was 10.5 CPM, which could be reduced to 1 CPM or less using extremely low background water.

Additionally, the measurement of an elevated count rate for the cocktail-only samples indicates interference from other high background contributors in CSU's lab. This complication

is well illustrated by comparing the average count rates for the deionized water backgrounds and the counts of the cocktail-only background. While the average background count rate for all 49 background counts of plastic vials over various durations was 10.51 CPM, the average background count rate for 4 counts of the cocktail-only vial was 10.54 CPM. Potential contributors to erroneous background signals include the radioactive progeny of naturally occurring radon and the presence of other radioactive materials in the counting room. While it is not appropriate to use cocktail-only measurements to predict the performance of samples that mix cocktail with water, this result is another potential contributor to the high background count rates and the ensuing difficulty distinguishing a true background level and MDA.

Several manipulations of the data and the MDA calculation equation [21] illustrate the potential ways that lower MDA values could be achieved. For example, a reduced background count rate (using tritium-depleted water samples or subtracting out interference observed in the cocktail-only sample) could lower the MDA. The effect of a lower background count rate for varying count times is presented in Figure 39 (1 CPM) and Figure 40 (0.25 CPM). These lower background blank counts would allow for MDA concentrations of 12 Bq/L and 4 Bq/L respectively using 2 hour count times. Similarly, Figure 41 illustrates the required background count rate to achieve low MDA concentrations for a 2 hour count.

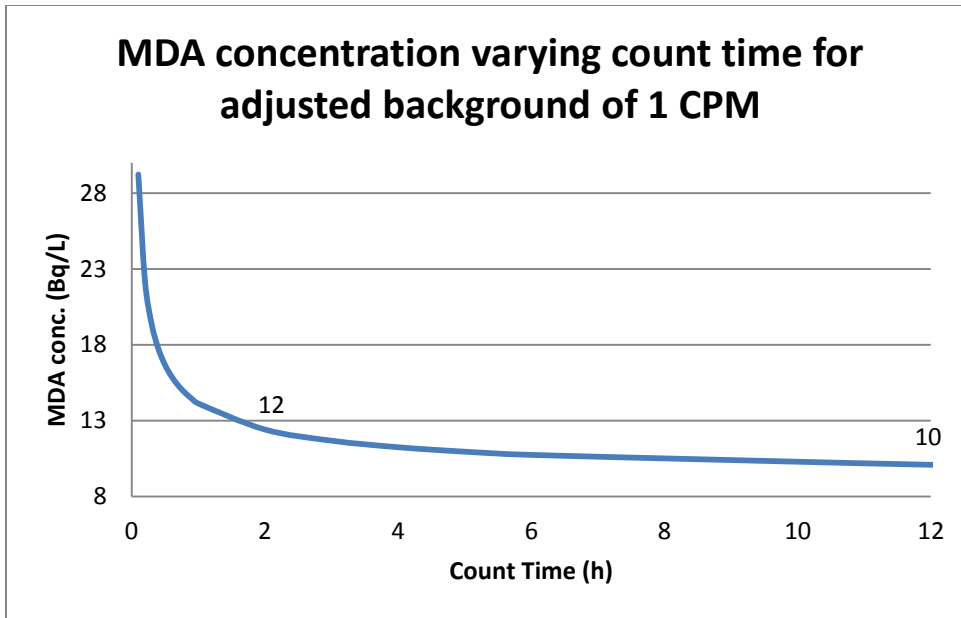


Figure 39: MDA concentrations for varying count time based on a reduced background count rate of 1 CPM and the average NTN site sample TDCR_{opt} of 24.3%

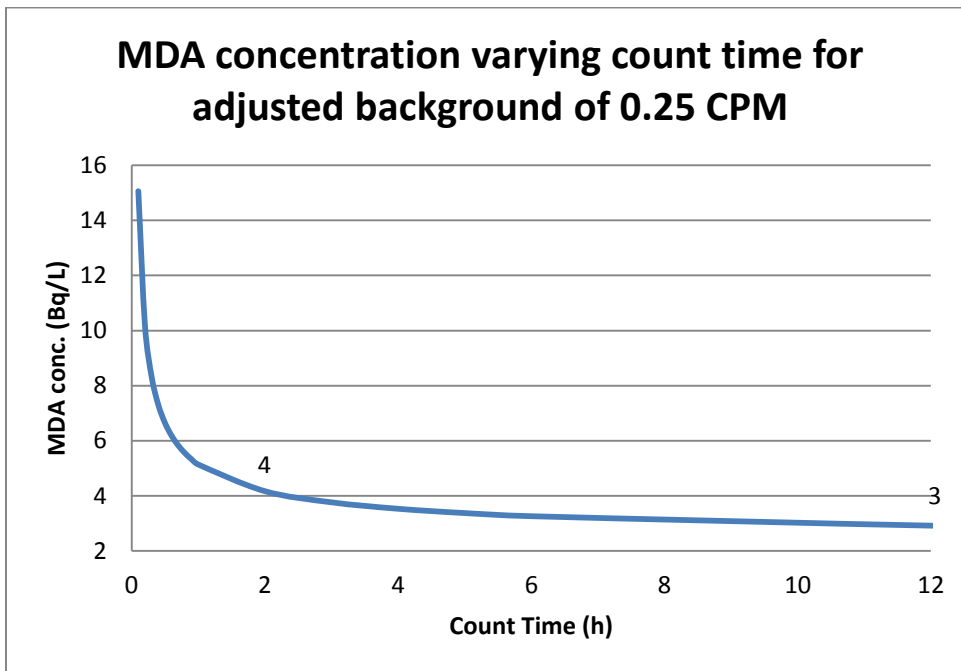


Figure 40: MDA concentrations for varying count time based on a reduced background count rate of 0.25 CPM and the average NTN site sample TDCR_{opt} of 24.3%

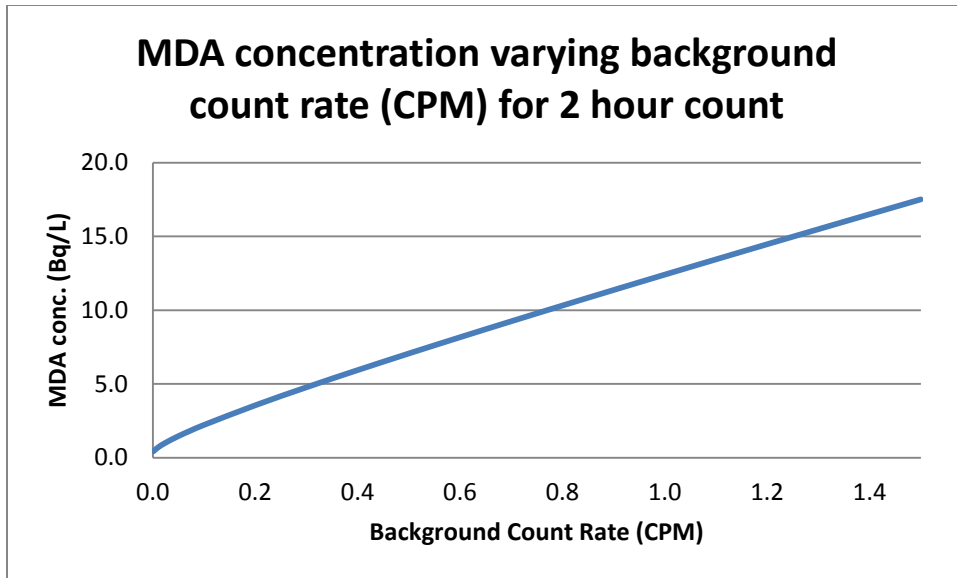


Figure 41: MDA concentrations for varying background count rate based on a count time of 2 hours and the average NTN site sample TDCR_{opt} of 24.3%

Additional LSC Considerations

When using the results of an LSC, it is possible to obtain measurements of samples with an open window, but these results inappropriately estimate the true activity in the samples. Window restriction eliminates unnecessary background signal interference and improves the statistics of the result, which is a critical step especially for very low levels of radioactivity. For example, the average background count rate for the 49 background blank counts was 40.8 CPM for the open window and 10.5 CPM for the restricted ROI of channels 20-180. Similarly, the TDCR for the background blank counts averaged 0.742 for the open window and 0.259 for the 20-180 ROI. The distinct reduction in triple to double coincidence ratio could reflect a decrease in triple incidence or an increase in double incidence counts (or both) within the ROI channels.

An important result observed in this project was the distinct variation in efficiency values (estimated by TDCR_{opt} values) based on the vial type, standard solution activity, and between the deionized water blanks and NTN site water samples. The lower average TDCR_{opt} for glass (for 2

hour counts: 0.179 for glass blanks versus 0.260 for plastic blanks and 0.179 for glass NTN samples versus 0.239 for plastic NTN samples) indicates that glass vials consistently returned lower efficiencies. This was a surprising result given the greater optical clarity of the glass vials, and indicates that plastic vials were the preferable choice for increased efficiency. As mentioned above, the lower TDCR value could result from a decrease in triple incidence or an increase in double incidence. Therefore, it is possible that the glass vials allowed for more erroneous background signals in 2 of the PMTs, potentially from residual radioactivity in the glass.

Regarding the standard spikes, the changing efficiency with respect to activity added is an interesting result. The TDCR value increased over a range of approximately 8% (from 0.26 to 0.34) for increasing added activity concentrations between 0 Bq/L and 440 Bq/L). Possible explanations for the trend in the TDCR have to do with effects occurring between the diluted tritium standard, the deionized water used for dilution, and the scintillation cocktail. For example, the highest activity standard was prepared with approximately 0.2 mL of tritium standard and 7.8 mL of deionized water. A possible explanation for the increasing TDCR is that additions of greater volumes of the prepared tritium standard decreased the quench in the samples.

The comparison between the TDCR efficiency method and the direct counting efficiency estimation method indicated similar performance of these techniques. When the CPM values for the standard solutions were adjusted by subtracting the average background CPM to obtain a net value, the trend in the calculated counting efficiency varied over a range of 11% (0.25 to 0.36) for concentrations greater than 44 Bq/L. This efficiency range is similar to the TDCR estimate for instrument efficiency, which varied over a range of 10% (0.26 to 0.36), indicating that the two methods are comparable for net count rates.

The difference in TDCR values between the deionized water blanks and the NTN site samples justified the use of the NTN site sample TDCR to estimate MDA concentrations. For 2 hour counts a difference of approximately 2% was observed: the mean $TDCR_{opt}$ of the NTN site sample count was 0.239, while the mean $TDCR_{opt}$ of the background blanks was 0.260. This difference can be explained by increased quench in the rainwater samples due to the presence of chemical impurities which were specifically removed from the deionized water. For a large scale monitoring program, accurate estimations of the MDA would require consideration of the quench properties of rainwater samples obtained from each site. A record of rainwater chemistry information is available for the NTN sites based on the evaluations already conducted at the CAL, but it would be necessary to quantify the effect of chemical concentrations on the counting efficiency of the samples in the LSC. Also, concentrations of most rainwater constituents are highly variable even at the same site. Overall, using the sample TDCR for MDA estimates is recommended instead of using background blank TDCR values.

Viable NTN Program Requirements

The original proposals for this project required a rigorous analytical capability of the lab for rainwater samples. The suggested throughput for samples would be 50 samples per week and a detection limit of 0.6 Bq/L to 1.2 Bq/L. Communication with individuals associated with the NADP has indicated that many sites in the NTN store surplus water. After the samples are shipped to the Central Analytical Laboratory, surplus water is preserved and can be made available to interested parties. The relevant contact for more information about surplus water is CAL director Chris Lehman.

For an ideal throughput of 50 samples per week, several count time scenarios are possible assuming that one instrument is used to perform the counts. 50 samples plus 1 blank would be 51 samples in 40 working hours, 120 hours in the 5 day work week, or 144 hours in 6 days (24 hours allowed for manipulation of samples). 16 hours of dark adaptation time are included in these estimations (meaning that the LSC could accommodate half of the samples and would need to be opened twice.)

For a 40 hour work week, this throughput would require approximately 30 minute count times. Using a 24.3% counting efficiency, 30 minute counts could detect 1.9 Bq/L if the background count rate were reduced to 0.01 CPM. At more reasonable background count rates, the MDA would be much higher than the desired analytical range suggested (see Figure 42). Alternatively, if 6 days of the week were reserved for LSC counts, approximately 2 hours and 30 minutes would be available for each sample. In this scenario, an MDA of 0.6 Bq/L could be achieved with background counts of 0.01 CPM, and an MDA of 1.3 Bq/L could be achieved with background counts of 0.1 CPM.

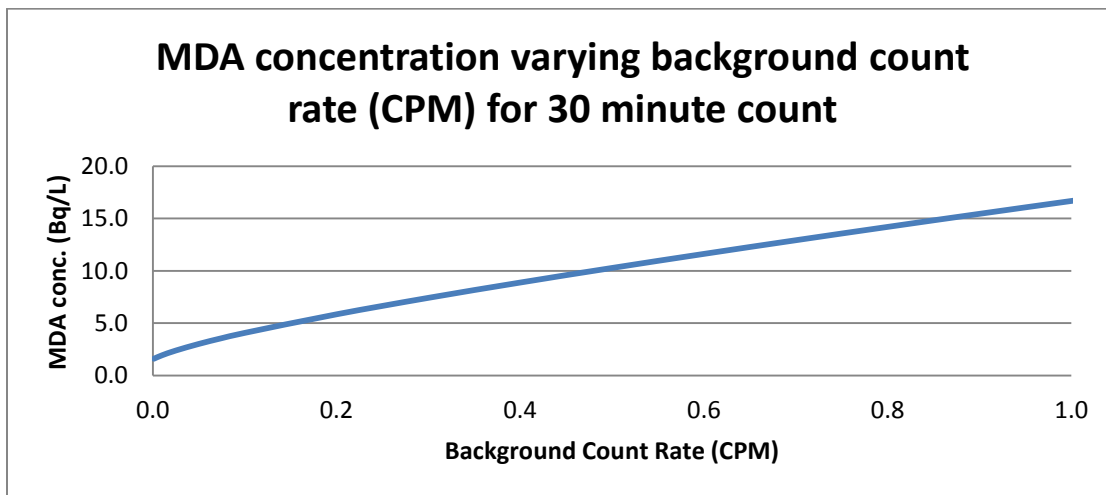


Figure 42: Analytical capability of the lab based on background count rate for rainwater activity estimation based on a counting efficiency of 24.3% and a 30 minute count time

Based on the estimations above, the analytical capability required for a successful monitoring program is technically possible under strict specifications. A very low background count rate is required to achieve the desired MDA for the required counting times, and the lab would need to have a dedicated LSC and a person responsible for ensuring that preparations of the samples and backgrounds were conducted in a timely manner to maintain the throughput. Longer count times (up to 2.5 hours) would be recommended for lower MDA values. These count times and MDAs would be easier to achieve if two or more LSC instruments were used to perform the counts.

Differentiation of Samples by Estimated Activity Level

One important consideration in this program is the very low health impact of tritium, and the difference between the suggested analytical range (0.6-1.2 Bq/L) in relation to the drinking water standard (740 Bq/L). In an effort to improve the practicality of an environmental monitoring program, one option would be to choose a higher level for designation of samples as background. This decision would change the scale on the spatial distribution maps produced by the NADP, and could reflect a level below which the tritium levels are considered to be of limited interest. Even a level of 5% of the EPA standard (37 Bq/L) could be achieved with a 2.5 hour count of a less restrictive background count rate (3.5 CPM for 24.3% efficiency).

With this decision level in mind, another option would be to apply a lower MDA initially in order to decide which NTN sites generate consistently low tritium levels. Counting these samples accurately would require continued use of the very low background information. However, some sites might consistently return higher results, in which case cheaper or more convenient background water and shorter count times could be used. For example, with the

investigated parameters of CSU's LSC, sixteen NTN sites resulted in counts above the MDA concentration of 96 Bq/L for a 2 hour count duration when the results were recorded as a gross sample activity. An important primary investigation would be to count these samples again for reproducibility, especially the high count from NC41, which is close to the EPA drinking water limit. A map of the locations which returned counts higher than background is included in Figure 43. Overall, sites with higher tritium levels would be likely to require less effort from the lab and could potentially be predicted from levels measured over an initial duration (such as one year.)

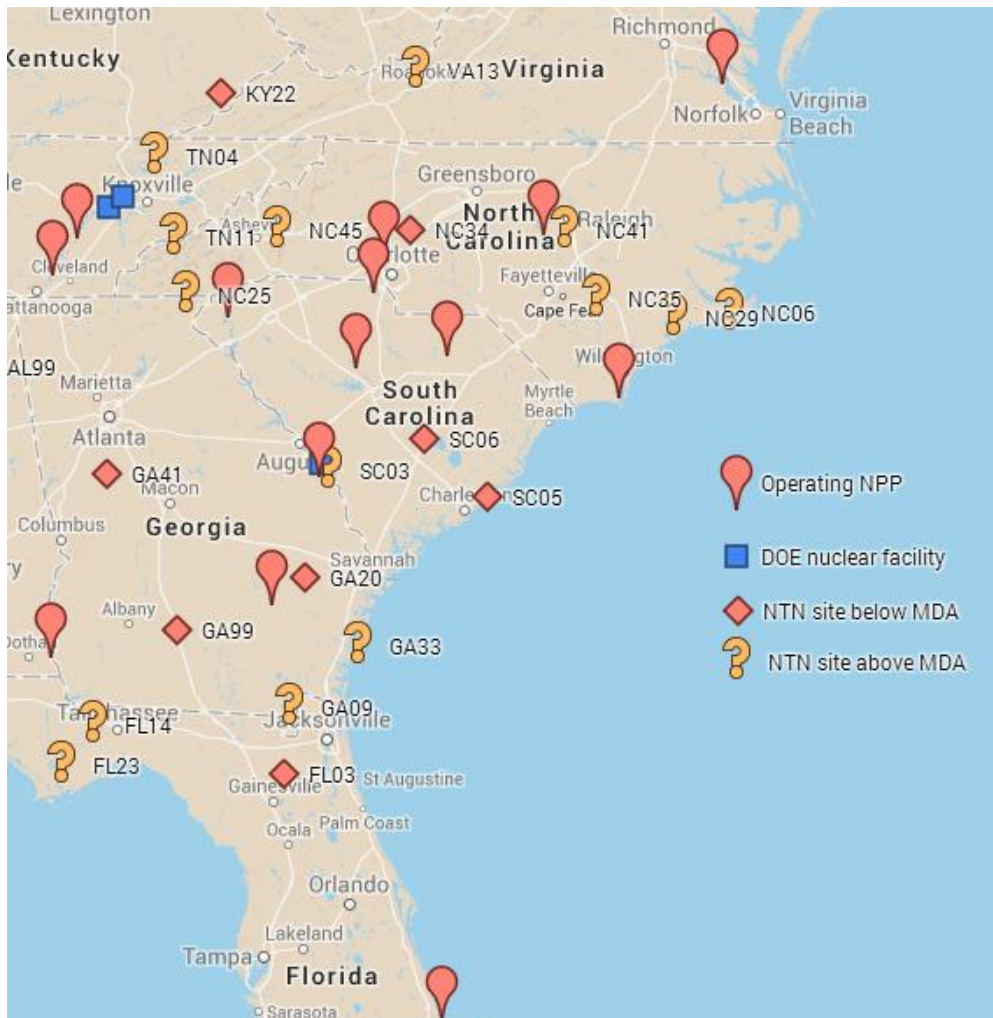


Figure 43: Composite map showing nuclear power reactors (red pins), DOE nuclear sites (blue squares), NTN sites below the MDA (red diamonds), and NTN sites that recorded an absolute activity level above 96 Bq/L in a 2 hour count (question marks), generated using Google maps

Several logical assumptions based on prior research could be used to narrow the focus of this program to sites with potentially higher tritium levels. For example, studies have shown that continental (inland) stations always observe higher deposited tritium levels than coastal and maritime stations, likely due to the dilution of higher tritium content water vapor with lower tritium content evaporated water from the ocean surface [2]. The maximum tritium activity has been observed during late spring and early summer [2]. Additionally, the primary anthropogenic sources of tritium in the atmosphere which contribute to tritium in rainwater are well characterized. Although samples from the NTN site SC03 did not have tritium levels above the MDA for any count duration, this result does not discount the generalization that NTN sites near nuclear facilities will be more likely to contain higher rainwater tritium concentrations.

Figure 44 provides a general depiction of a composite map prepared using information about existing nuclear facilities and the global positioning system (GPS) coordinates associated with each of the 23 NTN sites from which CSU received samples. Maps such as these would allow rapid decisions for which sites to monitor closely after a planned or accidental tritium release.

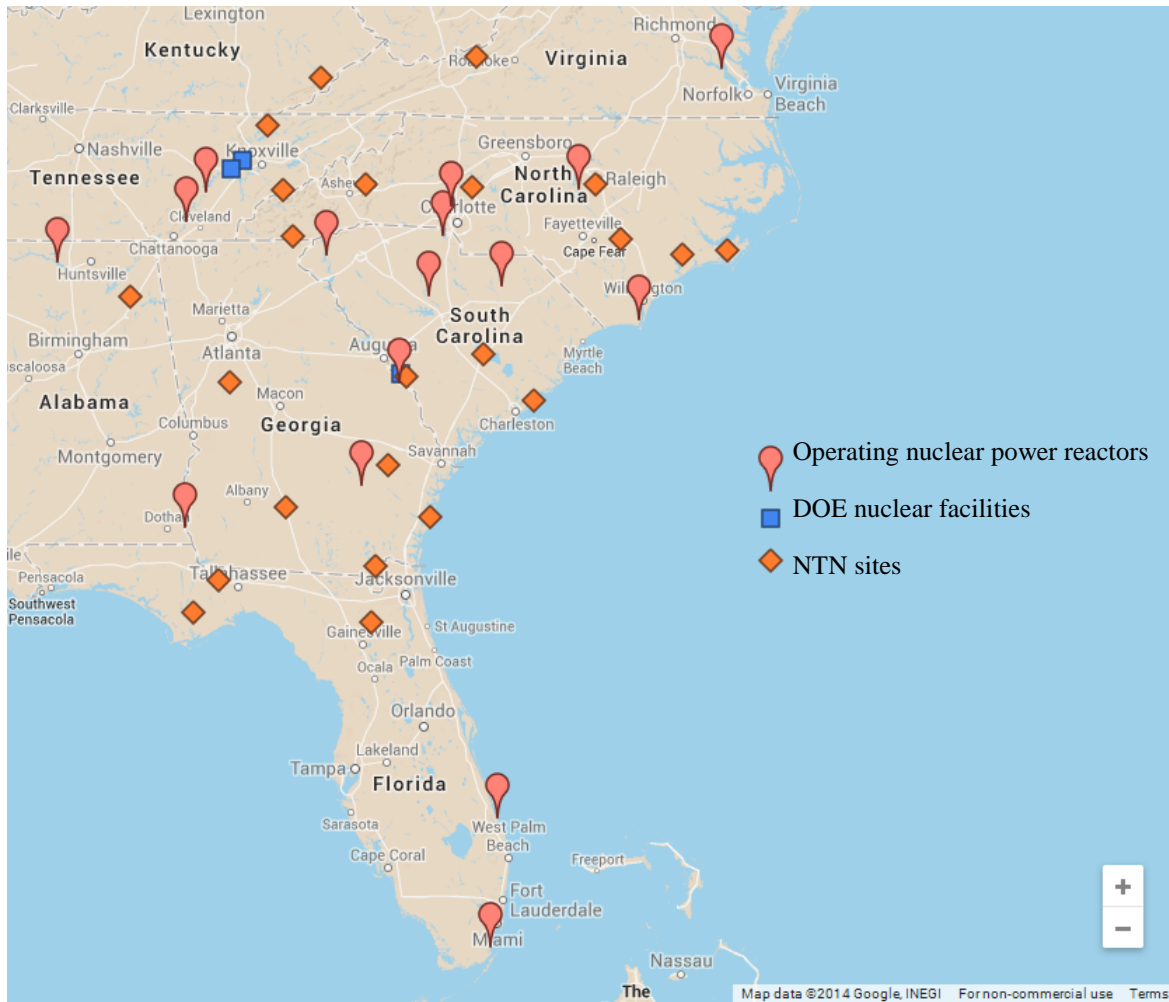


Figure 44: Composite map showing nuclear power reactors (red pins), DOE nuclear sites (blue squares), and NTN sites (orange diamonds), generated using Google maps

Concentration of Samples of Tritium

All of the requirements of a nationwide monitoring program discussed thus far have assumed rainwater samples were unconcentrated for tritium. This assumption simplifies the procedural steps involved in sample preparation and eliminates the uncertainties associated with any concentration procedures. However, the potential for tritium concentration would alleviate much of the concern associated with trying to reduce the MDA to achieve acceptable analytical parameters.

Due to the mass difference between tritiated water (HTO) and normal H₂O, an isotopic effect makes these two solutions separable by distillation. H₂O is composed of 18 nucleons compared to the 20 nucleons that make up HTO, with the higher mass resulting in a lower boiling point and a higher vapor pressure. Additionally, the heavier atomic components will be less likely to move in an electrolytic distillation setup than the lighter ¹H and ²H atoms. The most widely used method for measuring environmental levels of tritium is electrolytic enrichment followed by LSC spectrometry [26]. This method is effective but associated with increased uncertainty, which can be poorly quantified and can lead to erroneous results. Electrolytic enrichment is subject to uncertainty due to the type of cells used, initial volume, enrichment factor, cell design and material components. The original proposed method of tritium concentration on a silica gel column would not be effective for water samples due to saturation of the column.

An original proposal of the project would be to produce a standard operating procedure (SOP) for water sample collection and tritium concentration that would reduce the need to ship large water samples from the CAL to a radionuclide counting lab. Because the measurement volume is limited to the volume of the LSC vial (20 mL) minus the volume of the necessary scintillation cocktail, only approximately 20 mL of water would need to be shipped. If the CAL had the capability to concentrate the water samples from the original surplus volume, a significant reduction of shipping costs could be achieved. Alternatively, if the desired MDA was achieved for unconcentrated samples, the CAL could still prepare small aliquots of the original surplus samples to send.

Alternative Radionuclide Program Options

An alternative option for demonstrating the effectiveness of using NTN samples to monitor radionuclides might be switching to a gamma-emitting radionuclide as a more effective pilot. When the NADP sites were used in the weeks after the nuclear accident at the Fukushima Daiichi site, high purity germanium (HPGe) gamma spectrometry was used to measure three gamma-emitting radionuclides (^{131}I , ^{134}Cs , and ^{137}Cs) on filters and in water samples. For these analyses, the MDA was estimated to range from 0.74 mBq to 6.66 mBq per sample (0.02 pCi – 0.18 pCi) for 40 h and 6 h count times, respectively [14]. Gamma spectrometry has the significant advantage over LSC measurement that the samples are less limited in size and volume. Therefore, measurements could be carried out on large volumes of water to improve statistical likelihood of finding significant results in samples with low activities. While the long count times used in this study would be similarly time-limiting on a large scale, temporal and regional compositing could be used to decrease the sample number.

CONCLUSION

The environmental monitoring program proposed as a collaborative effort between the National Atmospheric Deposition Program (NADP) and Savannah River National Laboratory (SRNL) could be used to characterize the deposition of radionuclides in precipitation to a greater degree than is currently conducted by any other environmental monitoring program in the United States. Sites in the National Trends Network (NTN) frequently produce surplus water after analyses for the various chemical contaminants already monitored by the NADP at their Central Analytical Laboratory (CAL). These surplus water samples could be shipped to a laboratory with radioanalytical capabilities, such as the labs at SRNL or Colorado State University (CSU), for analysis of the tritium content of the rainwater. Information from the analyses conducted could be used to generate maps showing the spatial and temporal distribution of nationwide rainwater tritium levels using the methods already available to the NADP, allowing this program to maximize the usefulness of its extant NTN monitoring network for a new water contaminant of interest.

Several considerations limit the feasibility of a nationwide monitoring program for rainwater tritium. Because background levels of tritium are estimated to be of the order of 1 Bq/L, the analytical requirements of the measurement system are quite stringent. Achieving minimum detectable activity (MDA) concentrations in this range requires that very low background blanks are available for comparison and that the potential interferences with the counting system are well characterized. Long count times (on the order of hours) are also required to improve the counting statistics and lower the MDA values. However, for counting

periods longer than a few hours, the slope of the MDA curve becomes flat. Thus, small increases in count time do little to lower the MDA for periods longer than 3-5 hours.

The raw data produced from CSU's LSC includes counts in an open window (all available channels). Restriction of the region of interest that the LSC uses to estimate activity is important to optimize the statistical differentiation of meaningful signal from the nuclide of interest (tritium in this case) and background interference. Concentration of the tritium content of rainwater samples by electrolytic enrichment is proposed as the preferred means of reducing the complications associated with very low level counting, but this procedure requires higher volumes of water and introduces additional uncertainties into the measurements.

Characterization of the detection efficiency of the LSC system is important because instrument efficiency can dramatically alter the results and change the MDA. Impurities in the rainwater will affect the quench properties of the sample and limit the effectiveness of the LSC in distinguishing a meaningful signal in low activity samples. Therefore, the counting efficiency should be considered in calculating an MDA, as it may vary significantly between background blanks and individual samples. The triple to double coincidence ratio (TDCR) as a measure of efficiency allows for a simple evaluation of this quench effect and eliminates the need for estimating efficiency by direct counts of a calibrated standard solution.

Tritium is a radionuclide with limited associated health effects because of the low energy of its emissions. Therefore, its involvement in a widespread monitoring program is primarily as a pilot nuclide to monitor trends rather than as a subject of environmental health concern. However, the production of tritium by anthropogenic sources increases its relevance to the

environmental monitoring field, and characterization of tritium levels by the NTN could serve to support and expand the local-scale monitoring that takes place at nuclear facilities.

REFERENCES

- [1] Canadian Nuclear Safety Commission, "Investigation of the Environmental Fate of Tritium in the Atmosphere," Canadian Nuclear Safety Commission (CNSC), Ottawa, Ontario, Canada, 2009.
- [2] G. E. Calf, "Tritium activity in rainwater 1962-1986," Australian Nuclear Science and Technology Organisation: Lucas Heights Research Laboratories, 1988.
- [3] Korea Atomic Energy Research Institute (KAERI), "Table of Nuclides," Nuclear Data Center, 2000. [Online]. Available: <http://atom.kaeri.re.kr/>. [Accessed 26 February 2014].
- [4] D. Jackson, T. Jannik, M. LaBone and R. Scheffler, "Radioactivity in Precipitation: Methods & Observations from Savannah River Site," in *Nuclear Energy Institute RETS/REMP Workshop*, Orlando, FL, 2012.
- [5] USNRC, "Operating Nuclear Power Reactors (by Location or Name)," USNRC, 19 March 2014. [Online]. Available: <http://www.nrc.gov/info-finder/reactor/>. [Accessed 28 March 2014].
- [6] P. I. Tjahaja and P. Sukmabuana, "The separation of tritium radionuclide from environmental samples by distillation technique," Nuclear Technology Center for Materials and Radiometry, National Nuclear Energy Agency of Indonesia, Bandung, Indonesia.
- [7] Environmental Protection Agency, "Tritium in Drinking Water Method 906.0," [Online]. Available:

http://www.epa.gov/safewater/radionuclides/training/resources/EPA_Method_906.0.pdf.

- [8] R. Jakiel, M. Weber-Goeke, R. Rosson and B. Kahn, "Tritium concentrations in northeast Georgia rainwater," in *Georgia Water Resources Conference*, Athens, Georgia, 1999.
- [9] W. Plastino, I. Chereji, S. Cuna, L. Kaihola, P. De Felice, N. Lupsa, G. Balas, V. Mirel, P. Berdea and C. Baci, "Tritium in water electrolytic enrichment and liquid scintillation counting," *Radiation Measurements*, vol. 42, pp. 68-73, 2007.
- [10] D. C. Bogen and G. A. Welford, "'Fallout tritium' distribution in the environment," *Health Physics*, vol. 30, no. February, pp. 203-208, 1976.
- [11] P. Theodorsson, "A review of low-level tritium systems and sensitivity requirements," *Applied Radiation and Isotopes*, vol. 50, pp. 311-316, 1999.
- [12] Environmental Protection Agency, "Historical uses of RadNet data," Office of Radiation and Indoor Air Radiation Protection Program, Washington DC, 2008.
- [13] Environmental Protection Agency, "Environmental Radiation Data: Report 145," Office of Radiation and Indoor Air, 2011.
- [14] G. A. Wetherbee, D. A. Gay, T. M. Debey, C. M. Lehmann and M. A. Nilles, "Wet deposition of fission-product isotopes to North America from the Fukushima Dai-ichi Incident, March 2011," *Environmental Science & Technology*, vol. 46, pp. 2574-2582, 2012.
- [15] International Atomic Energy Agency [IAEA], "Environmental isotope data no. 10: world

- survey of isotope concentration in precipitation (1988-1991)," IAEA, Vienna, 1994.
- [16] International Atomic Energy Agency and World Meteorological Organization, "IAEA-WMO Programme on isotopic composition of precipitation: Global network of isotopes in precipitation," Vienna.
- [17] C. Zhilin, X. Shixiong, W. Heyi, C. ruimin, W. guanyin and Z. Yinhang, "The effect of vial type and cocktail quantity on tritium measurement in LSC," Elsevier Ltd., 2010.
- [18] G. F. Knoll, Radiation Detection and Measurement, John Wiley & Sons, Inc., 2010.
- [19] PerkinElmer, "Liquid Scintillation Counting," PerkinElmer, 2014. [Online]. Available: http://www.perkinelmer.com/Resources/TechnicalResources/ApplicationSupportKnowledgebase/radiometric/liquid_scint.xhtml. [Accessed 5 March 2014].
- [20] L. Kaihola, "Liquid scintillation counting performance using glass vials in the Wallac 1220 Quantulus," in *Liquid Scintillation Counting and Organic Scintillators*, Chelsea, Michigan, Lewis Publishers, 1991, pp. 495-500.
- [21] J. E. Turner, Atoms, Radiation, and Radiation Protection, 3rd ed., Oak Ridge, TN: Wiley-VCH, 2007.
- [22] G. F. Knoll, Radiation Detection and Measurement, Castleton-on-Hudson, NY: John Wiley & Sons, Inc., 2010.
- [23] H. Cember and T. E. Johnson, Introduction to Health Physics, Fourth Edition ed., New York: McGraw Hill, 2009.

- [24] M. Groning, M. Dargie and H. Tatzber, "Seventh IAEA intercomparison of low-level tritium measurements in water (TRIC2004)," International Atomic Energy Agency, Isotope Hydrology Laboratory, Vienna, 2007.
- [25] Schafer, D. Hebert and U. Zeiske, "On low-level tritium measurements with LSC Quantulus," *Applied Radiation and Isotopes*, vol. 53, pp. 309-315, 2000.
- [26] M. Groning and K. Rozanski, "Uncertainty assessment of environmental tritium measurements in water," *Accred Qual Assur*, vol. 8, pp. 359-366, 2003.
- [27] G. Gabarino, M. Magnoni, S. Bertino and M. C. Losana, "Development of an electrolysis system for tritium enrichment in superficial water samples," *Radiation Protection Dosimetry*, vol. 137, no. 3-4, pp. 329-331, 2009.
- [28] G. Muranaka and N. Shima, "Electrolytic enrichment of tritium in water using SPE film," InTech, 2012.
- [29] Environment Agency, "The determination of tritium (tritiated water) activity concentration by alkaline distillation and liquid scintillation counting," Environment Agency, Lancaster LA1, 1999.
- [30] Georgia Department of Natural Resources Environmental Protection Division, "Environmental Radiation Surveillance Report 2000-2002," 2004.
- [31] R. L. Michel, "Tritium deposition in the continental United States, 1953-83," U.S. Geological Survey Water Resources Investigations, Reston, Virginia, 1989.

- [32] M. Schurch, R. Kozel, U. Schotterer and J.-P. Tripet, "Observation of isotopes in the water cycle - the Swiss National Network (NISOT)," *Environmental Geology*, vol. 45, pp. 1-11, 2003.
- [33] E. Everett and W. Nestel, "Use of collective radiological effluents as a performance indicator in the commercial U.S. nuclear power industry," in *21st Annual RETS/REMP Workshop*, Oakbrook, Illinois, 2011.
- [34] N. Daugherty and R. Conaster, "Radioactive effluents from nuclear power plants: Annual Report," Nuclear Regulatory Commission, Washington DC, 2007.
- [35] A. Brown, "2008 Results of Radiological Environmental Monitoring Programs," Ontario Power Generation, 2008.
- [36] G. W. Patton, A. T. Cooper and M. R. Tinker, "Ambient air sampling for tritium - determination of breakthrough volumes and collection efficiencies for silica gel adsorbent," *Health Physics*, vol. 72, no. March, pp. 397-407, 1997.
- [37] EcoMetrix, "Investigation of the environmental fate of tritium in the atmosphere," Canadian Nuclear Safety Commission, 2009.
- [38] J. Doroski, "Tritium - the "real" background - & other items of interest," 2011.
- [39] Environmental Protection Agency, "Tutorial 5.1 - Tritium analysis by liquid scintillation counting," 11 March 2011. [Online]. Available:
http://www.epa.gov/safewater/radionuclides/training/module5/tutorial_5.1.html.

- [40] Georgia Department of Natural Resources Environmental Protection Division, "Environmental Radiation Surveillance Report 1997 - Mid 1999," 1999.
- [41] S. Kaufmann and W. F. Libby, "The natural distribution of tritium," *Physical Review*, vol. 93, no. 6, pp. 1337-1344, 1954.
- [42] L. S. Lau and T. Hailu, "Tritium measurements in natural Hawaiian waters: instrumentation," Board of Water Supply, City and County, Honolulu, 1968.
- [43] W. F. Libby, "Radioactive fallout," United States Atomic Energy Commission, 1958.
- [44] A. S. Mason and H. G. Ostlund, "Atmospheric HT and HTO: V. distribution and large-scale circulation," in *International Symposium on the Behaviour of Tritium in the Environment*, San Francisco, 1978.
- [45] G. Mazur and P. Mazur, "Influence of coal-fired power stations on the concentration of radioisotopes in the environment," *Nukleonika*, vol. 55, no. 2, pp. 243-246, 2010.
- [46] T. K. Reji, P. M. Ravi, T. L. Ajith, B. N. Dileep, A. G. Hegde and P. K. Sarkar, "Environmental transportation of tritium and estimation of site-specific model parameters for Kaiga site, India," *Radiation Protection Dosimetry*, pp. 1-5, 2011.
- [47] S. L. Simon, A. Bouville and H. L. Beck, "The geographic distribution of radionuclide deposition across the continental US from atmospheric nuclear testing," *Journal of Environmental Radioactivity*, vol. 74, pp. 91-105, 2004.
- [48] G. L. Stewart and C. M. Hoffman, "Tritium rainout over the United States in 1962 and

- 1963," Geological Survey Circular, Washington, 1966.
- [49] L. L. Thatcher, "The distribution of tritium fallout in precipitation over North America," *International Association of Scientific Hydrology, Bulletin*, vol. 7, no. 2, pp. 48-58, 2009.
- [50] R. W. Vachon, J. W. C. White, E. Gutmann and J. M. Welker, "Amount-weighted annual isotopic (δ -18-O) values are affected by the seasonality of precipitation: A sensitivity study," *Geophysical Research Letters*, vol. 34, 2007.
- [51] W. Whicker, "Radionuclide behavior: classic observations in various ecosystems (Presentation IV)," Colorado State University, Fort Collins, 2009.
- [52] L. A. Volk, "2012 Annual Meeting and Scientific Symposium: Proceedings," in *National Atmospheric Deposition Program (NADP) 2012 Technical Committee Meeting*, Portland, ME, 2012.
- [53] Institute for Radiological Protection and Nuclear Safety [IRSN], "Assessment on the 66th day of projected external doses from the nuclear accident in Fukushima," IRSN Directorate of Radiological Protection and Human Health, Paris, 2011.
- [54] R. Atkinson, *Tritium uncertainty analysis for surface water samples at the Savannah River Site*, Fort Collins, CO: Colorado State University, 2012.

APPENDIX A: NTN SITE SAMPLE PREPARATIONS

NTN site sample preparations for 42 original samples from 23 site locations and samples selected for count times of 2, 5, and 8 hours

		TK4900SW	FL03	
TK4829SW	AL99	TK5076SW	FL14	
TK5301SW	AL99	TK5062SW	FL23	
TK5520SW	FL03	TK5435SW	GA41	
TK5318SW	FL14	TK5037SW	KY22	
TK4756SW	FL23	TK5084SW	VA13	
TK5304SW	FL23			
TK4839SW	GA09	TK5301SW	AL99	Standard 8:12 Plastic 2 hr counts
TK5089SW	GA09	TK5304SW	FL23	
TK5320SW	GA09	TK5320SW	GA09	2012 Prep 7:14 Plastic (not reported)
TK4827SW	GA20	TK5302SW	KY22	
TK5164SW	GA33	TK4758SW	NC35	8:12 Prep Glass
TK4893SW	GA41	TK4823SW	NC41	
TK5034SW	GA99	TK4749SW	SC03	Duplicate 8:12 5 hr counts
TK5302SW	KY22	TK5041SW	SC03	
TK4765SW	NC06	TK5104SW	TN11	Duplicate 8:12 8 hr counts
TK5081SW	NC06	TK5314SW	VA13	
TK4834SW	NC25			
TK5431SW	NC25	TK5301SW	AL99	
TK4822SW	NC29	TK5520SW	FL03	
TK5079SW	NC29	TK4756SW	FL23	
TK5294SW	NC34	TK5304SW	FL23	
TK4758SW	NC35	TK4839SW	GA09	
TK4823SW	NC41	TK5320SW	GA09	
TK5344SW	NC41	TK5302SW	KY22	
TK4833SW	NC45	TK5081SW	NC06	
TK5311SW	NC45	TK4758SW	NC35	
TK4749SW	SC03	TK4823SW	NC41	
TK5041SW	SC03	TK4833SW	NC45	
TK4826SW	SC05	TK5311SW	NC45	
TK5075SW	SC05	TK4749SW	SC03	
TK5055SW	SC06	TK5041SW	SC03	
TK4840SW	TN04	TK5104SW	TN11	
TK5306SW	TN04	TK5314SW	VA13	
TK5104SW	TN11			
TK5324SW	TN11	TK4749SW	SC03	
TK5314SW	VA13	TK5041SW	SC03	

APPENDIX B: T-TESTS COMPARING BACKGROUND AND SAMPLE COUNTS

T-tests for sample counts versus background counts illustrating the significance of a statistical difference in the means of the background and rainwater counts

ROI beta double incidence 20-180

2 Hr Bkg 2 Hr Sample

1096	1604	1126
1197	1243	2683
1181	1180	1628
1215	2369	2916
1174	1276	1208
1129	1461	1346
1117	1156	1247
	1173	6326
	2249	1286
	1158	1428
	1851	1427
	1081	1558
	1199	1118
	1156	1194
	1278	1203
	1483	2125
	1178	1122
	4041	1234

t-Test: Two-Sample Assuming Unequal Variances

	<i>2 Hr Sample</i>	<i>2 Hr Bkg</i>
Mean	1675.305556	1158.429
Variance	1026183.247	1986.619
Observations	36	7
Hypothesized Mean Difference	0	
df	36	
t Stat	3.046314319	
P(T<=t) one-tail	0.002159216	
t Critical one-tail	1.688297714	
P(T<=t) two-tail	0.004318431	
t Critical two-tail	2.028094001	

ROI beta double incidence 20-180

5 Hr Bkg 5 Hr Sample

2895	3983
2813	3412
3692	3495
2844	2890
3000	2858
2883	3143
3368	2888
	2965
	4022
	2791
	5021
	3814
	4364

t-Test: Two-Sample Assuming Unequal Variances

	<i>5 Hr Sample</i>	<i>5 Hr Bkg</i>
Mean	3487.8125	3070.714286
Variance	451460.6958	110550.5714
Observations	16	7
Hypothesized Mean Difference	0	
df	20	
t Stat	1.988229138	
P(T<=t) one-tail	0.030323586	
t Critical one-tail	1.724718243	
P(T<=t) two-tail	0.060647171	
t Critical two-tail	2.085963447	

2974
 2987
 4198

ROI beta double incidence 20-180

8 Hr

Bkg 8 Hr Sample

6251 5511

t-Test: Two-Sample Assuming Unequal Variances

4799 6623

	<i>8 Hr Sample</i>	<i>8 Hr Bkg</i>
Mean	6067	5525
Variance	618272	1054152
Observations	2	2
Hypothesized Mean Difference	0	
df	2	
t Stat	0.592708409	
P(T<=t) one-tail	0.306733416	
t Critical one-tail	2.91998558	
P(T<=t) two-tail	0.613466832	
t Critical two-tail	4.30265273	

APPENDIX C: TDCR COMPARISON – 2 HOUR COUNTS

Results of TDCR comparison for plastic NTN site samples and blanks counted for 2 hours

Plastic NTN 2 hr	Plastic Bkg 2 hr	2 Hour Count Comparisons		
0.219451	0.248175	F-Test Two-Sample for Variances		
0.236525	0.281537	<hr/>		
0.251695	0.252329		<i>Bkg</i>	<i>NTN Sites</i>
0.192064	0.262551	Mean	0.239367	0.259628
0.257837	0.25724	Variance	0.000933	0.000115
0.231348	0.259522	Observations	36	7
0.24654	0.256043	df	35	6
0.262575		F	8.094609	
0.238773		P(F<=f) one-tail	0.007262	
0.25734		F Critical one-tail	3.788879	
0.203674		<hr/>		
0.252544		F stat is greater than F critical, reject the null hypothesis, the		
0.258549		variances of the two populations are unequal		
0.273356		t-Test: Two-Sample Assuming Unequal Variances		
0.276213		<hr/>		
0.228591			<i>Bkg</i>	<i>NTN Sites</i>
0.236234		Mean	0.239367	0.259628
0.178531		Variance	0.000933	0.000115
0.238329		Observations	36	7
0.212277		Hypothesized Mean Difference	0	
0.266556		df	28	
0.219911		t Stat	-3.11225	
0.268645		P(T<=t) one-tail	0.002124	
0.150648		t Critical one-tail	1.701131	
0.263608		P(T<=t) two-tail	0.004247	
0.243697		t Critical two-tail	2.048407	
0.252278		t stat is less than t critical so we reject the null hypothesis,		
0.27792		the means of the two populations are unequal		
0.273703				
0.246231				
0.256027				
0.217882				
0.268271				
0.221232				
0.26146				
0.176689				

APPENDIX D: TDCR COMPARISONS BY BOTTLE COLOR

Results of descriptive statistics and TDCR comparison t-tests based on bottle discoloration

ID	Site	Color	TDCR _{opt}
TK4829SW	AL99	Y	0.219
TK5301SW	AL99	Y	0.237
TK5520SW	FL03	Y	0.252
TK5318SW	FL14	Y	0.192
TK4756SW	FL23	Y	0.258
TK5320SW	GA09	Y	0.239
TK4827SW	GA20	Y	0.257
TK5164SW	GA33	Y	0.204
TK4893SW	GA41	Y	0.253
TK5302SW	KY22	Y	0.273
TK5041SW	SC03	Y	0.278
TK5075SW	SC05	Y	0.246
TK5055SW	SC06	Y	0.256
TK4840SW	TN04	Y	0.218
TK5104SW	TN11	Y	0.221

Yellow TDCRopt

Mean	0.24017
Standard Error	0.006419
Median	0.246231
Mode	#N/A
Standard Deviation	0.024862
Sample Variance	0.000618
Range	0.085856
Minimum	0.192064
Maximum	0.27792
Sum	3.602551
Count	15
Confidence Level(95.0%)	0.013768

ID	Site	Color	TDCR _{opt}
TK5304SW	FL23	Y/W	0.231
TK5034SW	GA99	Y/W	0.259
TK5081SW	NC06	Y/W	0.229
TK4822SW	NC29	Y/W	0.238
TK5294SW	NC34	Y/W	0.267
TK4758SW	NC35	Y/W	0.220
TK4826SW	SC05	Y/W	0.274
TK5306SW	TN04	Y/W	0.268

Y/W TDCRopt

Mean	0.248157
Standard Error	0.007396
Median	0.248439
Mode	#N/A
Standard Deviation	0.02092
Sample Variance	0.000438
Range	0.053792
Minimum	0.219911
Maximum	0.273703
Sum	1.985258
Count	8
Confidence Level(95.0%)	0.017489

ID	Site	Color	TDCR _{opt}
TK4839SW	GA09	W	0.247
TK5089SW	GA09	W	0.263
TK4765SW	NC06	W	0.276
TK4834SW	NC25	W	0.236
TK5431SW	NC25	W	0.179
TK5079SW	NC29	W	0.212

White TDCRopt

Mean	0.23303
Standard Error	0.011263
Median	0.24654
Mode	#N/A
Standard Deviation	0.040608

TK4823SW	NC41	W	0.269	Sample Variance	0.001649
TK5344SW	NC41	W	0.151	Range	0.125565
TK4833SW	NC45	W	0.264	Minimum	0.150648
TK5311SW	NC45	W	0.244	Maximum	0.276213
TK4749SW	SC03	W	0.252	Sum	3.029395
TK5324SW	TN11	W	0.261	Count	13
TK5314SW	VA13	W	0.177	Confidence Level(95.0%)	0.024539

t-Test: Two-Sample Assuming Unequal Variances

	<i>Yellow</i>	<i>Yellow/White</i>
Mean	0.240170088	0.24815728
Variance	0.000618109	0.000437642
Observations	15	8
Hypothesized Mean Difference	0	
df	17	
t Stat	-0.81556095	
P(T<=t) one-tail	0.213015498	
t Critical one-tail	1.739606726	
P(T<=t) two-tail	0.426030997	
t Critical two-tail	2.109815578	

t-Test: Two-Sample Assuming Unequal Variances

	<i>Yellow/White</i>	<i>White</i>
Mean	0.24815728	0.233030403
Variance	0.000437642	0.00164902
Observations	8	13
Hypothesized Mean Difference	0	
df	19	
t Stat	1.122658279	
P(T<=t) one-tail	0.137784742	
t Critical one-tail	1.729132812	
P(T<=t) two-tail	0.275569484	
t Critical two-tail	2.093024054	

t-Test: Two-Sample Assuming Unequal Variances

	<i>Yellow</i>	<i>White</i>
Mean	0.240170088	0.233030403
Variance	0.000618109	0.00164902
Observations	15	13
Hypothesized Mean Difference	0	
df	19	
t Stat	0.550748506	
P(T<=t) one-tail	0.294112026	
t Critical one-tail	1.729132812	
P(T<=t) two-tail	0.588224053	
t Critical two-tail	2.093024054	
